

AN ABSTRACT OF THE THESIS OF

Kelia E. Axler for the degree of Master of Science in Integrative Biology presented on June 11, 2019.

Title: Influence of River Plumes on Larval Fish Distributions, Predator-Prey Relationships, and Fitness in the Northern Gulf of Mexico

Abstract approved: _____

(Su Sponaugle)

River plumes discharging into continental shelf waters have the potential to influence patchiness of larval fishes, prey, and gelatinous predators. Using a high-resolution plankton imaging system, we sampled larval fishes, copepods, and planktonic predators (ctenophores, hydromedusae, and siphonophores) across multiple freshwater pulses exiting the mouth of Mobile Bay (Alabama, USA) into the northern Gulf of Mexico in April before, during, and immediately after the largest flood event of 2016. Water column profiles were used to quantify changes in the vertical and horizontal structure of planktonic distributions, enabling a fine-scale examination of the predator and prey fields across distinct plume regimes. Before the peak flood event, the water column was highly stratified and high-density concentrations of fish larvae and zooplankton were observed in nearby regions of hydrodynamic convergence. This situation potentially provided a rich feeding environment for larvae but also subjected them to increased predation pressure. As the plume flow strengthened and the water column became more turbulent, fish larvae were advected offshore by strong currents and subjected to highly turbulent conditions of wind-forcing and mixing processes of the plume. The plume outflow was sampled with a multinet system to measure the effects of entrainment within a plume at the scale of an individual fish larva. Each net tow was classified as having sampled one of two distinct water masses based on known salinity values: either plume (salinity <25) or shelf (salinity >32). Size frequency distributions of larval striped anchovy (*Anchoa hepsetus*) and sand

seatrout (*Cynoscion arenarius*) indicated that larger individuals were present in shelf waters but absent from plumes. Sagittal otolith microstructure analysis revealed that recent growth of both focal species was significantly lower for plume-residents during the last few days prior to capture. Furthermore, plume-residents were in poorer morphometric condition (e.g., skinnier at length) than their shelf counterparts. Additionally, diet analyses suggested that plume-residents may have been feeding on a poorer quality diet (comprised substantially of small phytoplankton as opposed to more nutritious copepods) than those captured from shelf waters. Taken together, these results suggest that larval survival is negatively affected by river plume physical processes and that there are biological consequences for marine fish larvae that encounter high-magnitude plume regimes.

©Copyright by Kelia E. Axler
June 11, 2019
All Rights Reserved

Influence of River Plumes on Larval Fish Distributions, Predator-Prey Relationships, and Fitness
in the Northern Gulf of Mexico

by

Kelia E. Axler

A THESIS

submitted to

Oregon State University

in partial fulfillment of
the requirements for the
degree of

Master of Science

Presented June 11, 2019
Commencement June 2019

Master of Science thesis of Kelia E. Axler presented on June 11, 2019

APPROVED:

Dr. Su Sponaugle, Major Professor, representing Integrative Biology

Dr. Virginia Weis, Head of the Department of Integrative Biology

Dr. Philip Mote, Dean of the Graduate School

I understand that my thesis will become part of the permanent collection of Oregon State University libraries. My signature below authorizes release of my thesis to any reader upon request.

Kelia E. Axler, Author

ACKNOWLEDGEMENTS

First and foremost, I would like to acknowledge Dr. Su Sponaugle for her support and guidance throughout this process. Her expertise and mentorship throughout the past three years has shaped my science career and pushed me to become a much stronger researcher. Additionally, I would like to thank Dr. Robert Cowen for his encouragement, advice, and serving as a role model for strong leadership (and lots of patience with breaking equipment!) in the field while at sea. I would also like to thank Dr. Frank Hernandez, for serving on my committee and offering me (a recent college graduate with little marine science experience at the time) a position in his lab back in 2014 and jumpstarting my career in fisheries oceanography. Finally, I would like to thank Dr. Sarah Henkel for her support as a member of my committee.

Furthermore, I would like to acknowledge all past and present members of the Oregon State University's Plankton Ecology Lab that have helped me with this research, especially Christian Briseño-Avena, Moritz Schmid, Kelsey Swieca, Miram Gleiber, Will Fennie, Jami Ivory, Megan Wilson, Daniel Ottmann, Katie Shulzitski, and Esther Goldstein, for a combination of teaching, mentorship, insightful conversations, and probably most importantly: loads of laughs. I would also like to acknowledge all the help I received from past and present members of the University of Southern Mississippi's Fisheries Oceanography and Ecology Lab and CONCORDE project, especially, Carla Culpepper, Olivia Lestrade, Ali Deary, Adam Greer, Angie Hoover, Eric Haffey, Meghan Angelina, Luciano Chiaverano, Cindy Gavins, Lanora Vasquez del Mercado, Kristin Heidenreich, Carley Zapfe, Sarah Muffelman, Jana Herrmann, Adam Boyette, Kevin Martin, Inia Soto Ramos, Brooke Jones, Sabrina Parra, Steven Dykstra, and Brian Dzwonkowski.

A Gulf of Mexico Research Initiative grant sponsored me throughout my first year of the program, granting me the financial opportunity to pursue this degree. I received additional funding from the Hatfield Marine Science Center Mamie L. Markham Research Award, the College of Earth, Ocean, and Atmospheric Sciences Ocean Ecology of Marine Nekton Award, multiple Hatfield Student Organization travel and research awards, Integrative Biology teaching assistantships and Zoology Research Funds.

CONTRIBUTION OF AUTHORS

Chapters 2 & 3: Kelia Axler, Christian Briseño-Avena, Su Sponaugle, and Robert Cowen conceived and designed the study. GOMRI supplied resources while Kelia Axler, Christian Briseño-Avena, and other CONCORDE personnel acquired the data. Kelia Axler conducted the statistical analyses and wrote both chapters with the guidance and editorial assistance of Su Sponaugle.

TABLE OF CONTENTS

| | <u>Page</u> |
|--|-------------|
| CHAPTER 1 – General Introduction..... | 1 |
| References..... | 6 |
| CHAPTER 2 – Variability in the fine-scale distributions and predator-prey relationships of larval fishes associated with the Mobile Bay river plume during flood conditions..... | 9 |
| Introduction..... | 9 |
| Methods..... | 12 |
| Results..... | 17 |
| Discussion..... | 22 |
| References..... | 27 |
| CHAPTER 3 – Impact of river plumes and coastal processes on larval fish fitness and survival in the northern Gulf of Mexico..... | 48 |
| Introduction..... | 48 |
| Methods..... | 51 |
| Results..... | 58 |
| Discussion..... | 63 |
| References..... | 74 |
| CHAPTER 4 – General Conclusions..... | 96 |
| APPENDICES..... | 98 |

LIST OF FIGURES

| <u>Figure</u> | <u>Page</u> |
|--|-------------|
| 2.1 Study region and sampling transects and stations | 34 |
| 2.2 Collaborative sampling effort schematic | 35 |
| 2.3 Physical properties of stratified Mobile Bay plume regime | 36 |
| 2.4 Physical properties of slightly-mixed Mobile Bay plume regime..... | 37 |
| 2.5 Physical properties of well-mixed Mobile Bay plume regime | 38 |
| 2.6 Larval fish and zooplankton ISIS compilation | 39 |
| 2.7 Mean larval fish concentration across plume regimes | 40 |
| 2.8 Current velocities and turbulence structure of water column | 41 |
| 2.9 Fine-scale vertical distributions of larval fish and zooplankton..... | 42 |
| 2.10 Fine-scale horizontal distributions of larval fish and zooplankton | 43 |
| 2.11 Spearman correlation matrices for larval fish and zooplankton concentrations | 46 |
| 3.1 Study region and sampling transects and stations | 87 |
| 3.2 Larval fish concentrations and community composition between water masses | 88 |
| 3.3 Zooplankton concentrations and community composition between water masses | 89 |
| 3.4 Size and age distributions of fish larvae between plume and shelf waters | 90 |
| 3.5 Detrended recent growth of larval striped anchovy and sand seatrout | 91 |
| 3.6 Mean daily growth for larval striped anchovy and sand seatrout by water mass | 92 |
| 3.7 NMS ordination of larval fish body morphometrics by water mass | 93 |
| 3.8 Numerical proportions of ingested prey by water mass of larval striped anchovy | 94 |
| 3.9 Numerical proportions of ingested prey by water mass of larval sand seatrout | 95 |

LIST OF TABLES

| <u>Table</u> | <u>Page</u> |
|---|-------------|
| 2.1 Mobile River/Bay daily freshwater discharge rates | 33 |
| 3.1 Correlations between NMS axes and morphometric residuals for striped anchovy and sand seatrout..... | 83 |
| 3.2 Gut content analysis (%N, FO, %FO) of striped anchovy..... | 84 |
| 3.3 Gut content analysis (%N, FO, %FO) of sand seatrout..... | 85 |
| 3.4 Prey selectivity analysis of plume-collected sand seatrout..... | 86 |

LIST OF APPENDICES

| <u>Appendix</u> | <u>Page</u> |
|---|-------------|
| APPENDIX A – CHAPTER 3 SUPPLEMENTARY TABLES AND FIGURES | 98 |
| Table S.3.1 Summary of collected plankton samples | 98 |
| Table S.3.2 Number of focal larval fish specimens | 99 |
| Table S.3.3 Summary of biotic and abiotic variables for each larval fish species..... | 100 |

CHAPTER 1: GENERAL INTRODUCTION

Most marine fishes have a planktonic larval phase characterized by high mortality rates that heavily influence recruitment to the adult population (Hjort 1914) and physical oceanographic features are primary determinants of the survival of these early life stages (Houde 2009). Factors that regulate survival of the pelagic larval stages, such as prey supply, feeding success, growth rate, and predation pressure are all influenced by oceanographic and environmental processes (e.g., river plumes, mesoscale fronts, water column stratification, currents, and eddies) that drive larval fish distributions as well as their zooplankton prey and predator interactions (Grimes & Finucane 1991; Houde 2008). Therefore, survival of the early life stages is tightly linked to the oceanographic conditions encountered during the larval phase. This is especially true in hydrographically complex coastal systems that serve as nurseries for a variety of fish species and are heavily impacted by anthropogenic activities.

The northern Gulf of Mexico (nGOM) is one such region and is thus well suited for examining the influence of physical features on larval fish ecology. For instance, coastal river plumes are seasonal oceanographic features that strongly influence biological distributions in the nGOM (Grimes & Finucane 1991) yet are poorly characterized at the resolution necessary to describe their impacts on the planktonic larval stages of marine fishes. Furthermore, on April 20th, 2010, the Deepwater Horizon (DWH) oil rig exploded and resulted in the largest oil spill in U.S. waters, releasing over 200 million gallons of crude oil while an additional 2 million gallons of toxic dispersants were released into the nGOM to attempt to limit the damages of the spill (Ramseur 2010). Due to the complex regional hydrography and scarce baseline data available on this river-dominated coastal ecosystem, the extent of damage to exposed planktonic communities remains poorly understood.

The northern Gulf of Mexico (nGOM)

The Mississippi-Alabama coastal ecosystem is a shallow, productive region that receives a steady but seasonally variable supply of nutrients from multiple freshwater inputs including the Mississippi River and the Mobile River/Bay system in a highly productive region termed the “Fertile Fisheries Crescent” (Gunter 1963). The numerous freshwater discharges across the

Mississippi Bight drive a large influx of nutrient and sediment-laden waters that promote high levels of primary and secondary production (Lohrenz et al. 1997), which in turn support the larval and juvenile stages of many marine fish species (Grimes 2001). Additionally, the productive waters of the nGOM sustain many valuable commercial and recreational marine species, all of which contribute to the region's billion-dollar commercial and recreational fishing industry (McCrea-Strub et al. 2011). Depending on the spatial distributions of marine fishes at the time of the DWH oil spill, species may have been directly exposed to contaminants or indirectly affected via the destruction of critical spawning and nursery habitats as well as the bioaccumulation of polycyclic aromatic hydrocarbons (PAHs) in the food web (Jackson et al. 1989; Peterson et al. 2003; Almeda et al. 2013). Additionally, due to the timing of spawning and pelagic nature of the larval stages, certain marine fish larvae experienced high spatial and temporal overlap with the DWH oil spill and were deemed vulnerable to direct toxin exposure, including the larvae of such economically important fishes as bluefin tuna (*Thunnus thynnus*) and red snapper (*Lutjanus campechanus*) (Hazen et al. 2016; Hernandez et al. 2016). However, a lack of historical data on the spatial and temporal distributions of ichthyoplankton limited predictions of the impact of oil and dispersants on the recruitment and population dynamics of exploited species. In addition to the lack of distributional data, there are few growth and diet data for many regional fish species and the rapid advancement of larval individual-based models (IBMs) has outpaced basic research on the ecology and growth of the species and life stages being modelled (Peck et al. 2012). Therefore, the DWH oil spill also highlighted the need to gather data and further develop ecosystem-based fisheries management (EBFM) in the nGOM (Sagarese et al. 2016). Ecosystem models, which are critical part of EBFM, require a comprehensive understanding of the trophic interactions of all modeled species (Ainsworth et al. 2010). Further research into the basic ecology and predator-prey dynamics of the early life stages of coastal fishes is needed to support these models and increase our ability to manage these nearshore ecosystems (Fodrie et al. 2014). Additionally, rising global temperatures are expected to drive shifts in the distributions of marine communities and documenting changes in fish assemblages is a critical first step toward understanding how future climate scenarios will affect fisheries production in the nGOM.

CONCORDE

The CONsortium for oil spill pathways in COastal River-Dominated Ecosystems (CONCORDE) was formed in response to the DWH oil spill and aims to improve understanding of the ecological impacts of environmental disturbances on the nGOM by providing high-resolution, seasonal descriptions of the nearshore biophysical environment (Greer et al. 2018). The CONCORDE study primarily focused on the area inshore of the 50 m isobath and east of the Mississippi River outflow to include the Mississippi Sound, Mobile Bay, and Mississippi-Alabama barrier islands in a very productive region known as the Mississippi Bight (Fig. 2.1). The Mississippi Bight is a highly energetic environment, with circulation controlled by the buoyancy-driven flow of the fresher, surface water offshore, resulting onshore movement of deeper, more saline waters. These movements likely had a strong influence on the shoreward transport of oil during the DWH oil spill and planktonic organisms (including larval fishes) entrained within these coastal water masses may have suffered increased exposure to oil and dispersant toxins. The primary objective of CONCORDE was to develop a synthesis model to assess and predict the effects of future oil spills entering the Mississippi Bight (Greer et al. 2018).

Freshwater input from rivers promotes density stratification of the water column and introduces nutrients, which stimulates the production of new organic matter by algae, thus altering potential exposure pathways for oil and dispersants. Therefore, river plumes are physical processes of particular interest to CONCORDE because these features act to structure ichthyoplankton and zooplankton communities in a way that potentially makes them more vulnerable to oil spills. In the absence of anthropogenic disturbance, these features influence biological processes that regulate recruitment such as spatial distributions, feeding, growth, and predation of larval fishes (Grimes 2001). The April 2016 CONCORDE field and modeling efforts focused on the influence of seasonal freshwater plumes and coastal physics as potential transport pathways of oil and dispersants.

Larval fish and zooplankton assessment tools

Planktonic distributions and food webs are inherently complex and difficult to study. Traditional net sampling methods are unable to resolve the fine-scale horizontal and vertical

distributions of organisms due to the inability to identify when organisms were captured during a tow. In addition, due to clogging, traditional nets cannot be towed continuously over long distances to characterize fine-scale, regional distributions of organisms. Higher-resolution baseline data on larval fish distributions throughout the nGOM are needed to expand the abilities of fisheries scientists to track changes, estimate the impacts of future environmental disturbances, and better inform management and recovery efforts. Additionally, these data will make it more feasible to understand the effects of different plume regimes on the habitat use, growth, and survival of marine fish larvae residing in a river-dominated region of the nGOM. Recent developments in plankton imaging technology allow for measurements at this fine-scale (i.e., centimeters to meters) resolution, revealing novel information on larval fish distributions and trophic interactions in response to environmental drivers.

In this study, we used high-resolution imaging technology, the *In Situ* Ichthyoplankton Imaging System (ISIS; Cowen & Guigand 2008) to simultaneously sample fine-scale distributions, predator-prey spatial relationships, and the surrounding environmental conditions. The large sample volume and rapid tow speeds of the ISIS make it a practical tool for studying rare organisms such as larval fishes. ISIS image sampling was combined with depth-discrete net tows using a Bedford Institute of Oceanography Net Environmental Sampling System (BIONESS; Open Seas Instrumentation, Inc., Musquodoboit Harbor, Nova Scotia) to sample larval fishes and enable a spatial analysis of size and daily growth.

Objectives

Within the CONCORDE framework, my thesis research explores how river plumes can structure assemblages and influence trophic dynamics and fitness of larval fishes in the Mississippi Bight. Chapter 2 examines how river plumes affect the distributions and predator-prey relationships of larval fishes across different plume regimes. Chapter 3 examines the biological consequences of these altered distributions (e.g., growth, condition, and diet). These baseline data fit into CONCORDE's primary objective of examining the impacts of variable environmental conditions and provide insights into the potential ecosystem impacts of oil reaching the shelf and nearshore waters. Furthermore, characterizing larval fish distributions

and fitness at high spatial and temporal resolution advances our understanding of the processes that influence recruitment to adult populations.

References

- Ainsworth CH, Kaplan IC, Levin PS & Mangel M (2010) A statistical approach for estimating fish diet compositions from multiple data sources: Gulf of California case study. *Ecol Appl* 20:2188–2202.
- Almeda R, Wambaugh Z, Chai C, Wang Z, Liu Z & Buskey EJ (2013) Effects of crude oil exposure on bioaccumulation of polycyclic aromatic hydrocarbons and survival of adult and larval stages of gelatinous zooplankton. *PLoS One* 8:20–21.
- Cowen RK & Guigand CM (2008) In situ ichthyoplankton imaging system (ISIIS): System design and preliminary results. *Limnol Oceanogr Methods* 6:126–132.
- Fodrie FJ, Able KW, Galvez F, Heck KL, Jensen OP, López-Duarte PC, Martin CW, Turner RE & Whitehead A (2014) Integrating organismal and population responses of estuarine fishes in Macondo spill research. *Bioscience* 64:778–788.
- Greer C, Shiller A, Hofmann E, Wiggert J, Warner S, Parra S, Pan C, Book J, Joung D, Dykstra S, Krause J, Dzwonkowski B, Soto I, Cambazoglu M, Deary A, Briseño-Avena C, Boyette A, Kastler J, Sanial V, Hode L, Nwankwo U, Chiaverano L, Fitzpatrick P, Lau Y, Dinniman M, Martin K, Ho P, Mojzis A, Howden S, Hernandez F, Church I, Miles T, Sponaugle S, Moum J, Arnone R, Cowen R, Jacobs G, Schofield O & Graham W (2018) Functioning of coastal river-dominated ecosystems and implications for oil spill response. *Oceanography* 31:90–103.
- Grimes CB (2001) Fishery production and the Mississippi River discharge. *Fisheries* 26:17–26.
- Grimes CB & Finucane JH (1991) Spatial distribution and abundance of larval and juvenile fish, chlorophyll and macrozooplankton around the Mississippi River discharge plume, and the role of the plume in fish recruitment. *Mar Ecol Prog Ser* 75:109–119.
- Gunter G (1963) The fertile fisheries crescent. *J Mississippi Acad Sci* 9:286–290.
- Hazen EL, Carlisle AB, Wilson SG, Ganong JE, Castleton MR, Schallert RJ, Stokesbury MJ, Bograd SJ & Block BA (2016) Quantifying overlap between the Deepwater Horizon oil spill and predicted bluefin tuna spawning habitat in the Gulf of Mexico. *Sci Rep* 6:33824.

- Hernandez FJ, Filbrun JE, Fang J & Ransom JT (2016) Condition of larval red snapper (*Lutjanus campechanus*) relative to environmental variability and the Deepwater Horizon oil spill. *Environ Res Lett* 11.
- Hjort J (1914) Fluctuations in the great fisheries of northern Europe viewed in the light of biological research. *Rapp Process Réunions Cons Perm Intern Explor Mer* 20:1–228.
- Houde ED (2008) Emerging from Hjort's shadow. *J Northwest Atl Fish Sci* 41:53–70.
- Houde ED (2009) Recruitment variability. In: T. Jakobsen, B.A. Fogarty, B.A. Megrey & E. Moksness (eds). *Fish Reproductive Biology: Implications for assessment and management*. Wiley-Blackwell: West Sussex, UK. pp. 91–171.
- Jackson JBC, Cubitt JD, Keller BD, Batista V, Burns K, Caffey HM, Caldwell RL, Garrity SD, Getter CD, Gonzalez C, Guzman HM, Kaufmann KW, Knap AH, Levings SC, Marshall MJ, Steger R, Thompson RC & Weil E (1989) Ecological effects of a major oil spill on Panamanian coastal marine communities. *Science* (80-) 243:37–44.
- Lohrenz SE, Fahnenstiel GL, Redalje DG, Lang GA, Chen X & Dagg MJ (1997) Variations in primary production of northern Gulf of Mexico continental shelf waters linked to nutrient inputs from the Mississippi river. *Mar Ecol Prog Ser* 155:45–54.
- McCrea-Strub A, Kleisner K, Swartz Student W, Watson R & Zeller D (2011) Potential impact of the Deepwater Horizon oil spill on commercial fisheries in the Gulf of Mexico. *Fisheries* 36:332–336.
- Peck MA, Huebert KB & Llopiz JK (2012) Intrinsic and extrinsic factors driving match-mismatch dynamics during the early life history of marine fishes. *Adv Ecol Res* 47:177–302.
- Peterson CH, Rice SD, Short JW, Esler D, Bodkin JL, Ballachey BE & Irons DB (2003) Long-term ecosystem response to the Exxon Valdez oil spill. *Science* (80)302:2082–2086.
- Ramseur JL (2010) Deepwater Horizon oil spill: the fate of the oil. *Cong Res Serv* 1–20:R41531.
- Sagarese SR, Nuttall MA, Geers TM, Laretta M V., Walter III JF & Serafy JE (2016) Quantifying the trophic importance of Gulf menhaden within the northern Gulf of Mexico ecosystem. *Mar Coast Fish* 8:23–45.

Shulzitski K, Sponaugle S, Hauff M, Walter K, D'Alessandro EK & Cowen RK (2015) Close encounters with eddies: oceanographic features increase growth of larval reef fishes during their journey to the reef. *Biol Lett* 11:20140746.

CHAPTER 2: VARIABILITY IN THE FINE-SCALE DISTRIBUTIONS AND PREDATOR-PREY RELATIONSHIPS OF LARVAL FISHES ASSOCIATED WITH THE MOBILE BAY RIVER PLUME DURING FLOOD CONDITIONS

2.1 Introduction

River plumes discharging into nearshore environments have been shown to be important biophysical drivers of the distributions, transport, and survival of the early life stages of coastal and estuarine fish assemblages (Govoni et al. 1989; Grimes & Finucane 1991; Le Pape et al. 2003; Carassou et al. 2012). While often only a few meters thick, these features are one of the most influential hydrological processes affecting ecosystem structure and function in coastal regions around the world. River plumes have a characteristic hydrographic structure that results from the seaward projection of a turbid, low salinity water mass. As buoyant plume waters move offshore, they overlay the higher salinity (denser), more oligotrophic (clearer) coastal shelf waters and are frequently accompanied by turbulent mixing as surface plume and shelf waters converge at a well-defined frontal interface, known as the plume front (Garvine & Monk 1974). Ephemeral in nature, plumes frequently flood, ebb, meander, and dissipate on hourly, daily, and seasonal time scales because they are strongly influenced by tides, winds, and the magnitude of river discharge from upstream sources (Stumpf et al. 1993; Govoni 1997). Buoyant and surface-seeking planktonic organisms can be swept up and passively carried by these converging water masses (Bowman & Iverson 1978; Olson & Backus 1985; Le Fèvre 1987). This results in both a retention and transport mechanism that aggregates particulates, including zooplankton and ichthyoplankton, in high concentrations near the surface of the frontal zone of a plume as it moves horizontally offshore (e.g., Govoni et al. 1989; Grimes & Finucane 1991; Govoni & Grimes 1992; Sánchez-Velasco et al. 2014). Therefore, the timing of encounter with a plume greatly influences a larval fish's feeding environment and survival, as such regions of convergence accumulate buoyant particles such as larval prey or potential predators over time.

As surface plumes spread horizontally, planktonic organisms from deeper waters below the plume can also be entrained (Dagg et al. 2004). In this way, river plumes have been shown to structure certain ichthyoplankton distributions on horizontal (cross-shore) and vertical

(depth) spatial scales, due to the strong salinity and density gradients between inshore and offshore water masses (Govoni 1997; Grimes 2001; Carassou et al. 2012). The degree to which river plumes influence the plankton community at both vertical and horizontal scales has several important implications for larval fish population dynamics. Salinity, temperature, dissolved oxygen concentration, food availability, and predation all vary substantially with the passage of a freshwater river plume through a coastal ecosystem on temporal scales commensurate with larval fish feeding, growth, and development. High concentrations of prey should lead to better feeding opportunities, faster growth, and higher condition of fish larvae, and thus potentially higher recruitment. In addition, the same physical processes that can concentrate fish larvae and their zooplanktonic prey within near-surface frontal zones can also increase encounter rates with known larval fish predators, such as gelatinous zooplankton (e.g., ctenophores, hydromedusae, and siphonophores (Purcell & Arai 2001), which are known to actively seek out and aggregate along hydrodynamic fronts (MacGregor & Houde 1996; Graham et al. 2001; Bakun 2006; McClatchie et al. 2012; Luo et al. 2014). Thus, entrainment within a river plume could lead to increased spatial overlap and heightened predation risk for fish larvae.

Although the feeding environment in and around eutrophic estuaries may be rich (e.g., high concentrations of copepods and other known larval fish prey), it can also be highly variable due to changes in the magnitude of river discharge and the physical gradients (salinity, density, temperature, thin layers) and hydrodynamic processes (convergent fronts, stratification) associated with the passage of a freshwater plume through the region. For instance, the impacts of physical processes, especially wind-stress and associated mixing (micro-turbulence), are considered to be critical for larval survival in the “stable ocean”, “plankton contact” and “optimal environmental window” hypotheses, respectively (Lasker 1978b; Rothschild & Osborn 1988; Cury & Roy 1989). These hypotheses incorporate the idea that such physical processes can disperse aggregations of prey that normally persist under non-turbulent conditions, affecting the larval environment at smaller scales than typically considered and thus potentially render highly turbulent, well-mixed discharge plumes unfavorable feeding environments for fish larvae. Furthermore, losses due to variable flushing and turbulence-induced dispersal of

populations offshore and away from estuarine nurseries where food may be unsuitable or in low supply could be a significant source of mortality for fish larvae. In regions heavily influenced by riverine and estuarine discharge, these buoyant coastal currents are expected to have a prominent role in driving variability in fisheries production and recruitment (Grimes 2001). In short, it is well understood that river plumes strongly influence biological distributions (Grimes & Finucane 1991). However, despite the many studies that have attempted to determine the impact of coastal river plumes on larval fish recruitment, the mechanisms remain poorly understood due to the difficulty inherent in studying these ephemeral and dynamic features at the resolution necessary to fully characterize their impacts at scales relevant to fish larvae. Furthermore, the vast majority of studies of river plume dynamics have used traditional net-based sampling that integrates over broad vertical and spatial domains.

The northern Gulf of Mexico (nGOM) is a river-dominated coastal region that receives freshwater input from multiple sources. The inner shelf environment off of coastal Alabama, for instance, is a particularly productive region due to the unique geographic boundaries of the Mississippi River Delta to the west and the Mobile River/Bay system to the north, both of which have large sediment and nutrient loadings that drive high primary and secondary productivity, especially within plume frontal waters (Turner & Rabalais 1991; Cowan et al. 1996; Lohrenz et al. 1997). Although it drains the fourth largest watershed in the United States (Schroeder & Lysinger 1979), Mobile Bay's connections to the nGOM are relatively small such that large volumes of freshwater exit through narrow and shallow passes, regularly creating large seasonal plumes in the eastern Mississippi Bight (Dinnel et al. 1990; Dzwonkowski et al. 2015). The inner shelf region immediately south of Mobile Bay and the Alabama coast supports a highly diverse larval fish assemblage and serves as an important nursery area for nearshore and estuarine-dependent fishes (Hernandez et al. 2010a,b). The physical oceanography and shelf circulation of the region are well-described (Schroeder & Lysinger 1979; Dinnel et al. 1990; Gelfenbaum & Stumpf 1993; Dzwonkowski et al. 2011; Dzwonkowski et al. 2014; Coogan & Dzwonkowski 2018), making the Mobile Bay outflow a prime location to investigate fundamental questions regarding the effect of river plumes on larval fish ecology. This study was designed to examine how river plumes affect fine-scale distributions of larval fishes and

their potential prey and predators. Understanding more about the fine-scale distributions of larval fishes and zooplankton should provide insights into trophic relationships, larval transport, and population variability in the context of river discharge and associated hydrodynamic processes. We investigated the impact of different Mobile Bay plume regimes on larval fish and zooplankton assemblages by sampling three distinct plume regimes throughout the peak flood event of 2016: 1) A shallow, highly-stratified water column during persistent upwelling-favorable conditions, 2) a deeper, slightly-mixed plume, and 3) a deep, well-mixed and highly turbulent plume.

2.2 Methods

2.2.1 Study region

Mobile Bay is a wide yet shallow estuary in the northern Gulf of Mexico that receives freshwater from the combined discharge of the Alabama and Tombigbee river systems. The Mobile Bay plume has a long-term (1976-2011) daily mean discharge of $2,656 \text{ m}^3 \text{ s}^{-1}$ (Dzwonkowski et al. 2014), yet the flow is seasonally variable, ranging from $\sim 500 \text{ m}^3 \text{ s}^{-1}$ during the low-flow summer season to $>7,000 \text{ m}^3 \text{ s}^{-1}$ during winter and spring rainfalls (Schroeder & Lysinger 1979). While the extent of the plume varies in response to this flow (Dinnel et al. 1990), Mobile Bay discharges enough freshwater to produce a buoyant, turbid plume that extends tens of kilometers onto the continental shelf for much of the year (Schroeder & Lysinger 1979), with large plumes occurring when river discharge exceeds $4,500 \text{ m}^3 \text{ s}^{-1}$ (Dinnel et al. 1990). Approximately 85% of the Mobile River discharge passes through a tidal inlet (Main Pass) into the Gulf of Mexico, while Pass aux Herons transmits the remainder westward to the Mississippi Sound (Ryan 1969). Like most of the estuaries in this region, the bay has a predominantly diurnal microtidal range ($\sim 0.5 \text{ m}$ at Dauphin Island; Gelfenbaum & Stumpf 1993). Water column structure (e.g., stratification and mixing) in this shallow estuary is largely driven by wind stress and river discharge (Park, Kim & Schroeder 2007; Kim & Park 2012). Wind stress can stimulate a nearly complete mixing of the water column and a downward advection of surface waters, resulting in weak, if any, stratification. However, at other times (i.e., lighter wind conditions) the water column may be highly stratified, leading to well-defined density

fronts along the plume boundaries that increase the complexity of their interaction with shelf waters (Gelfenbaum & Stumpf 1993).

2.2.2 River plume sampling

To examine the influence of river plumes on the spatial distributions of larval fishes and zooplankton, and as part of a larger field campaign for the interdisciplinary CONsortium for oil exposure pathways in COastal River-Dominated Ecosystems (CONCORDE) program (see Greer et al. 2018), we collected both *in situ* plankton imagery and biological samples during one 2-week cruise in the Mississippi Bight aboard the *R/V Point Sur* from March 30 – April 11, 2016 (Fig. 2.2). Larval fishes and zooplankton were sampled across multiple freshwater pulses exiting the mouth of Mobile Bay (Alabama, USA) using a high-resolution plankton imaging system throughout the largest freshwater discharge event of 2016. The ISIIS was towed behind the *R/V Point Sur* to sample three zonal transects approximately 20 km in length that arced from east to west around the mouth of Mobile Bay ~10 km due south of the Main Pass at the farthest point and ~5 km close to shore on either end of the transect (Fig. 2.1). All three transects were similar in length and sampled inside of the 20 m isobath. The first transect was sampled during daylight hours, beginning at ~10:00 and ending at ~14:00 CDT on April 9, 2016. The other two transects began at ~21:00 and ended ~02:00 CDT on the nights of April 9-10 and April 10-11, 2016.

Imagery data collected throughout the cruise were used to train and test the sparse Convolutional Neural Network (sCNN; see below) to automate the classification of the images. Images of fish larvae and zooplankton were captured using the In Situ Ichthyoplankton Imaging System (ISIIS; Cowen & Guigand 2008), a towed shadowgraph imager that uses a line-scan camera to sample large volumes of water (150-185 L⁻¹) (Cowen et al. 2013). The ISIIS undulates from within ~1 m of the surface to within 2 m of the bottom using motor-actuated wings at a horizontal speed through the water of ~2.5 ms⁻¹ and vertical speed of 0.2–0.3 ms⁻¹. Two cameras imaged zooplankton between approximately 500 μm and 12 cm in length while simultaneously measuring salinity, temperature, and depth (Sea-Bird Electronics 49 FastCAT), dissolved oxygen (SBE 43), fluorescence, Chl-a fluorescence (Wet Labs FLRT), and photosynthetically active radiation (PAR; Biospherical QCP-2300). The images and

oceanographic data are linked by a common timestamp, which enables description of the fine-scale physical environment for each individual organism. Full water column profiles were used to quantify changes in the vertical and horizontal structure of planktonic distributions enabling a fine-scale examination of larval fish distributions and associated predator and prey fields across each plume regime.

2.2.3 River plume characterization

At the same time ISIS measured the distribution of planktonic organisms in an arc around the Mobile Bay outflow, the *R/V Pelican* towed a Chameleon microstructure profiler (Moum et al. 1995) to measure microscale turbulence, temperature, conductivity, optical backscatter (800 nm), and fluorescence throughout the water column in a parallel arc ~ 3 km inshore (Fig. 2.1). River plumes were identified by their unique physiochemical signatures using a combination of plume-tracking drifters, ISIS-mounted environmental sensors (Sea-Bird SBE 49 FastCAT, Sea-Bird 43, Wet Labs FLRT, and Biospherical QCP-2300), shipboard ADCP data (Teledyne RD Instruments; 600 kHz Workhorse Mariner and 75 kHz Ocean Surveyor), and Chameleon microstructure profiler data (Fig. 2.2). From this suite of oceanographic data, we were able to delineate the geographic position, movement, depth, and boundaries of the plume for each day of sampling, yielding a detailed view of estuarine-shelf processes and corresponding oceanographic and biological responses.

2.2.4 Mean river discharge

Daily freshwater discharge data were obtained from two USGS gauging stations, the Claiborne Lock & Dam in the Alabama River (USGS 2016a) and the Coffeerville Lock & Dam in the Tombigbee River (USGS 2016b). Their summed discharge was extrapolated for the entire delta watershed (Q_2) following the method of Schroeder (1979) and Dykstra and Dzwonkowski (*in prep*):

$$Q_2 = \frac{A_2}{A_1} * Q_1$$

where Q_1 is the summed discharge, A_1 is the station watershed area, and A_2 is the delta watershed area (Table 2.1). River discharge was lagged six days to account for travel time from

the upriver gauging stations to the mouth of the bay (Dinnel et al. 1990; Dysktra & Dzwonkowski *in prep*).

2.2.5 Plankton image processing and automated classification pipeline

All collected ISIS images were segmented into single frames and the frames were automatically processed using a “flat-fielding” technique that removed image artifacts (e.g., the small vertical black lines that are found on images created with a line scan camera). To identify regions of interest (e.g., single planktonic organisms and hereafter referred to as vignettes), a k-harmonic means clustering algorithm was used on the flat-fielded frames and the vignettes were saved in preparation for the classification pipeline. A total of 89 different categories of plankton taxa were identifiable in the CONCORDE data set.

A sparse Convolutional Neural Networks (sCNN) was used to automate identification of imaged taxa following Luo et al. (2018). The *SparseConvNets with Fractional Max-Pooling* (Graham 2015) configuration was used to train the sCNN until an error rate of $\leq 5\%$ was achieved closely following the methodology of Luo et al. (2018). The sCNN was trained and tested by randomly extracting and manually identifying 45,594 image segments, originating from all CONCORDE transects (three total field surveys) as well as all three seasons (fall, spring, summer) to capture the diversity of organisms (and image quality due to variable turbidity) in a variety of water conditions (e.g., mixing, river plume regimes, thermal stratification). The images were each identified using the trained sCNN to generate a probability that each image belonged to any of the 89 taxa classes, where the class with the highest probability was ultimately selected as the correct automatically identified one. Probability filtering was applied to remove images of low classification confidence, which still allowed for the prediction of true spatial distributions (Faillettaz et al. 2016) using a Loess model to determine at which probability threshold a cutoff should be made to reach 90% classification precision at the broader group level (Luo et al. 2018). Vignettes were re-classified as unknown if their maximum assigned probability was less than or equal to the determined thresholds.

To evaluate the final automated classification pipeline performance, a confusion matrix was generated for another randomly selected number of images. After the filtering thresholds

were applied, F1-scores (harmonic mean of precision and recall, $F1 = \frac{2*P*R}{(P+R)}$) were calculated using the number of true positives (TP), false positives (FP), false negatives (FN), precision ($P = \frac{TP}{(TP+FP)}$), and recall ($R = \frac{TP}{(TP+FN)}$). Application of the filtering thresholds to the classified images removed images with a low confidence classification.

Timestamps were then used to merge the imagery data with the physical data (salinity, temperature, depth, etc) collected by ISIS and these were binned into 1-m vertical strata along the sampling path through the water. The resulting data were then used to estimate concentrations of organisms (ind. m⁻³) based on the volume of water filtered, calculated average tow speed, and time spent by ISIS in each 1-m vertical stratum. Finally, a correction factor based on the results of the confusion matrix was applied to these concentrations where

$$\text{Correction factor}(\text{taxon}) = \frac{\text{Precision}(\text{taxon})}{\text{Recall}(\text{taxon})}.$$

Images of larval fishes from each transect were extracted by the sCNN using the same automated methodology as the zooplankton imagery. However, automatically classified larval fishes were manually reviewed by a human expert to verify correct identifications and to take the classifications to lower taxonomic levels than the sCNN was trained to do for the larger data set.

2.2.6 Data analysis

Vertical distributions of larval fishes and zooplankton were calculated by taking the number of individuals found in each 1-m vertical bin divided by the volume sampled by ISIS in that bin. Kruskal-Wallis tests were used to compare larval fish concentrations among the three transects because this analysis makes no assumptions about the distribution of the data. Data analysis was performed in R (v3.4.1, R Core Team, 2017) using packages “dplyr” (Wickham et al. 2018) and “ggplot2” (Wickham 2016) for data analysis and visualization, respectively.

Correlation matrices were constructed to compare predator and prey relationships among different plankton groups and to examine whether high abundances of organisms were correlated with environmental variables across the different plume regimes. Non-parametric Spearman rank correlation coefficients make no assumptions about the normality or variability

in the data and were therefore used on organism concentrations sampled and average environmental variables across in each m^3 bin. The significance levels of these correlations were assessed using an approximation of the Student's t distribution in the 'Hmisc' package of R (Harrell et al. 2016), with a conservative p-value significance threshold of 0.01.

2.3 Results

2.3.1 Physical environment and river discharge

In early to mid-April of 2016, the Mobile Bay river plume was advected along the coast, but its position and physical structure varied in response to other environmental conditions such as wind-forcing and ambient circulation. Three distinct plume regimes were sampled during our study period (April 9, 9-10, and 10-11) that varied in both magnitude of river discharge, level of turbulence, and degree of water column stratification or mixing processes. Average freshwater input ($\leq 2000 \text{ m}^3\text{s}^{-1}$) and light westerly winds (≤ 9 knots on average) prevailed during the week preceding our sampling efforts, setting up a stratified water column with a shallow lens of low-salinity plume water that overlaid higher-salinity shelf water for our first day of sampling.

On April 9, upwelling conditions (westerly winds) forced the plume offshore where it was pushed eastward by shelf currents (Fig. 2.3). A distinct halocline with a salinity difference of ~ 10 was observed at ~ 2 m depth throughout the entire transect that separated the relatively fresh and turbid water from the saltier, clearer water. Strong stratification between layers limited the vertical exchange of suspended sediments and chlorophyll a (as observed in optical backscatter and fluorescence plots, Fig. 2.3). Plume-tracking drifters released on the afternoon of April 9 from the eastern and central side of Main Pass moved offshore and to the east, consistent with the movement of a buoyancy-driven plume forced south by strong upwelling conditions (westerly winds) and east by shelf currents. However, drifters released from the west side of Main Pass were retained for nearly 7 hrs in a localized region ~ 5 km south of the coast and 15 km west of Main Pass, likely due to the strong hydrodynamic convergence caused by the intersection of the alongshore current with surface waters forced backwards toward shore by the southwesterly winds. Eventually the drifters were released from the region of

convergence and continued moving west toward the Mississippi Sound. During these low wind conditions, turbulent kinetic energy dissipation rate was $\epsilon=10^{-7} \text{ W kg}^{-1}$ throughout the majority of the water column with a mid-layer water mass below the plume at $\epsilon=10^{-8} \text{ W kg}^{-1}$. The plume was observed to be directly influencing the middle portion of our transect and moving east at 0.3 ms^{-1} ; however, there was less water movement observed on either the west or east end of the transect but some shoreward (northern) movement of bottom water below the surface plume.

Overnight on April 9-10, winds remained calm, averaging 6.9 kts from the southwest. However, the halocline and chlorophyll layer deepened to $\sim 6 \text{ m}$ as spring rains led to increased river discharge from Mobile Bay (Table 2.1), directly subjecting the majority of our transect to the pull of strong eastward currents ($\geq 0.5 \text{ ms}^{-1}$) and producing a large vertical salinity gradient of 10-20 at the surface and 36 at depth. Turbulence increased with the higher river input to $\epsilon \sim 10^{-6} \text{ W kg}^{-1}$ in the plume water but remained approximately $\epsilon=10^{-7} \text{ W kg}^{-1}$ in the shelf waters below, which continued their slow ($\sim 0.1\text{-}0.2 \text{ ms}^{-1}$) but steady shoreward movement (Fig. 2.4).

A very different regime of wind, stratification, and mixing was observed the following night of April 10-11 as the winds shifted direction and started blowing 19.2 kts from the southeast. These strong downwelling winds pushed the surface waters even deeper, eroding the stratification and homogenizing the water column salinity to a uniform 25 in the upper 10 m. Meanwhile, the Mobile Bay outflow continued to increase and reached the highest discharge rate of the entire year on April 10, 2016 (Table 2.1). Current velocities within the plume remained high ($\sim 0.4 \text{ ms}^{-1}$) and continued to flow strongly offshore and eastward as turbulence values increased ten-fold to $\epsilon=10^{-5} \text{ W kg}^{-1}$ throughout the majority of the water column. It is important to note that the plume shifted even farther east on this day and so the strongest turbulence and eastward currents were observed on the eastern half of the transect (Fig. 2.5). A commonality among the three different plume regimes was that surface water within the plume generally showed a net seaward transport (as visualized by U current velocities); however, the V current velocities displayed a net shoreward movement of dense, saline, coastal water beneath the outflowing river water (Figs. 2.3-5). This could have important

implications for retention and dispersal of larval fishes and zooplankton within the nearshore system.

2.3.2 Larval fish and zooplankton distributions and plume discharge

Fish larvae and zooplankton exhibited large spatial and temporal variability in both their overall abundances and vertical and horizontal distributions over the three different plume regimes. A total of 941 fish larvae were identified in the automatically-classified images. The most abundant families were Engraulidae (28.7%), Sciaenidae (19.3%), Microdesmidae (12.0%), and Gobiidae (4.3%) (Fig. 2.6). Approximately 33% of larval fish found were not identifiable to the family level due to poor image quality, fish orientation into the camera, or a lack of visible meristics. The abundance of larval fishes in the ISIS images was highly variable across plume regimes and taxa (Fig. 2.7) and peak larval fish concentrations differed significantly between the three transects (independent-samples Kruskal-Wallis test, $p < 0.001$). Larval fish concentrations were negatively related to the magnitude of Mobile Bay plume discharge, current velocity, turbulence, and mixing processes (Fig. 2.8). The maximum transect-average larval fish concentration was $0.321 \text{ ind. m}^{-3}$, which occurred during the day on April 9 when the water column was highly stratified by a shallow plume ($\sim 12.5\%$ of the water column). As the plume strengthened on the night of April 9-10 and encompassed more of the water column both vertically ($\sim 40\%$) and horizontally, this biological feature dispersed and fish larvae were less abundant overall ($0.164 \text{ ind. m}^{-3}$). The lowest concentration of larval fishes ($0.0595 \text{ ind. m}^{-3}$) was recorded the following night of April 10-11 as the Mobile Bay plume rose to its highest discharge rate of the entire year ($\sim 6,000 \text{ m}^3\text{s}^{-1}$) and the plume flooded $\sim 80\%$ of the water column with highly turbulent, low salinity water.

Fine-scale vertical (Fig. 2.9) and horizontal (Fig. 2.10) larval fish and zooplankton concentrations were also examined. Similar to fish larvae, zooplankton concentrations differed significantly across the three plume regimes, beginning as a dense aggregation during the stratified regime and becoming more dispersed and less abundant overall as plume flow, turbulence, and mixing processes increased over time (independent-samples Kruskal-Wallis tests, $p < 0.05$). The aggregation occurred on the western end of the transect in the

approximate spatio-temporal vicinity of the region of elevated hydrodynamic convergence indicated by the movements of entrained plume-tracking drifters (Fig. 2.10a). Prevailing westerly winds the week prior to sample collection suggests that this region of convergence may have been present for at least a few days, aggregating plankton and potentially creating a rich feeding environment. The eastward and continued offshore movement of the plume led to limited freshwater influence on this western end of the transect. The middle portion of this transect, however, was subjected to the direct flow and eastward currents ($\sim 0.3 \text{ ms}^{-1}$) of the plume. In response, relatively few fish larvae and gelatinous zooplankton were observed in these regions. Calanoid copepods were densely clustered at both east and west ends of the transect, but less concentrated in the middle of the transect where the plume currents were strongest. Interestingly, fish larvae were found to co-occur with their copepod prey on the western end of the transect but not the eastern end, where a similar aggregation of calanoid copepods was recorded.

Though stratification remained, the Mobile Bay plume discharge increased during the night of April 9-10, deepening the halocline to 6 m and encompassing approximately 40% of the water column in low salinity (≤ 25 salinity), high levels of turbulence ($\epsilon = 10^{-6}$ to $10^{-7} \text{ W kg}^{-1}$), and very strong eastward currents ($\geq 0.5 \text{ ms}^{-1}$). All taxa decreased in overall abundance and became patchier in distribution as this pulse of nutrient-rich plume water flooded the sample region (except for hydromedusae, which became more abundant and appeared to aggregate along the halocline with the chlorophyll layer, Fig. 2.10b). A patch of fish larvae remained concentrated on the western edge of the transect suggesting that the region of convergence was still present, yet plume currents were strong enough to disperse most of the fish larvae and zooplankton eastward and offshore.

The winds reversed overnight on April 10-11 and began blowing strongly from the southeast, mixing the chlorophyll layer and homogenizing the upper 10 m of the water column to a uniform salinity of 25. As the Mobile Bay plume peaked to its highest discharge rate of 2016, the entire water column was taken over by strong turbulence ($\epsilon = 10^{-5} \text{ W kg}^{-1}$) and fast currents ($\sim 0.4 \text{ ms}^{-1}$) that continued advecting water offshore and to the east. As intense downwelling processes took over the system, larval fishes and zooplankton became even more

dispersed in their distributions, consistent with being flushed offshore by the plume (Fig. 2.10c). Ctenophores were entirely absent from this transect. The strongest currents were observed in the eastern half of the transect with much less water movement in the western half. It is possible that the same region of convergence was still present to the west of Mobile Bay as calanoid copepods and hydromedusae were detected aggregating on the western end of the transect as previously observed.

2.3.3 Physical and biological correlations

Correlation coefficients indicated that the fine-scale physical environment inhabited by our focus plankton groups varied widely across different plume regimes. In stratified conditions (April 9), fish larvae, ctenophores, hydromedusae, and siphonophores were more negatively correlated with salinity and temperature, reflecting their association with low salinity, though cooler, plume waters (Fig. 2.11a). Calanoid copepods were positively correlated with all physical variables except for salinity, suggesting an association with slightly warmer plume waters. The warmer waters inhabited by copepods could be due to their residency in shallower surface waters than the other plankton groups. Unlike hydromedusae or siphonophores, fish larvae, calanoid copepods, and ctenophores were found in higher oxygen waters.

On April 9-10, plume discharge increased and deepened the halocline to 6 m but did not erode water column stratification. Fish larvae and siphonophores were not correlated with any of the physical variables measured, and hydromedusae was only associated with high oxygen waters (Fig. 2.11b). However, copepods and ctenophores remained associated with warm, highly oxygenated plume waters. As the plume strengthened and the majority of the water column became inundated and mixed with turbulent plume waters (April 10-11), organism abundances were less consistently related to physical variables (Fig. 2.11c). For example, fish larvae were more abundant in high salinity, low oxygen, and low fluorescence waters, potentially due either to physical advection offshore or to ontogenetic migration away from the plume. Calanoid copepods were not correlated with salinity and were found in cooler, low oxygen and low fluorescence waters. Hydromedusae were positively correlated with low salinity and high temperature, fluorescence, and oxygen plume waters. In contrast,

siphonophores were found in low temperature and fluorescence waters, with no correlation with salinity or oxygen. It appears that while hydromedusae may have tracked the plume's movements, larval fishes and copepods were more abundant outside of the plume due either to avoidance behaviors or physical advection away from the advancing water mass.

2.3.4 Predator-prey relationships

Spearman correlation coefficients were used to calculate the overlap of different prey and predator groups with fish larvae in varying plume regimes using concentrations calculated from 1 m³ depth bins. During the April 9 plume regime, the coastal Mississippi-Alabama shelf was characterized by water column stratification with a thin, near-surface plume layer. During these conditions, all taxa were found to be strongly and significantly correlated with each other: fish larvae showed a high correlation with ctenophores, hydromedusae, and siphonophores and a lower, though still significant, correlation with calanoid copepods (Fig. 2.11a). Despite the plume strengthening and deepening to encompass nearly half of the water column during the night of April 9-10, fish larvae remained highly correlated with their copepod prey, becoming slightly less correlated with ctenophores and siphonophores, and uncorrelated with hydromedusae (Fig. 2.11b). As the plume continued to strengthen on the night of April 10-11 and downwelling and turbulent mixing processes spread through 80% of the water column, fish larvae became uncorrelated with both their prey and predators (Fig. 2.11c). Increasing Mobile Bay discharge rates of ~6,000 m³s⁻¹ and associated mixing processes appeared to have an inverse relationship with the spatial overlap of fish larvae and their zooplankton prey and predators.

2.4 Discussion

While it is well-established that mesoscale frontal features such as those inherent in river plumes cause major variations in physical oceanography and biological distributions (e.g., Kiørboe et al. 1988; Govoni et al. 1989; Munk et al. 2002; Lee et al. 2005), the use of *in situ* imagery allowed for a substantially higher resolution investigation of these processes. Like convergent fronts and gyres associated with oceanic circulation systems, plumes are often

spatially and temporally variable in nature and can be heavily influenced by ocean currents, wind, and upwelling regime (Epifaniot et al. 1989). Analyses of the fine-scale vertical and horizontal distributions of larval fishes and their zooplankton prey and predators enabled a comprehensive examination of the changes in overall abundances and correlations among organisms across different regimes of wind-stress, stratification, mixing, and river discharge just offshore of Mobile Bay.

River plumes and associated water column stratification and mixing processes were observed to facilitate the formation and dissipation of multi-taxa planktonic aggregations. The highest abundances of fish larvae, copepods, ctenophores, hydromedusae, and siphonophores of the study period occurred during the highly stratified plume regime approximately 15 km west of Main Pass. Concentrations of biota within river plume frontal regions have been attributed to high levels of physical convergence on both sides of the front, typically higher on the high density (shelf water) side than the low density (plume water) side (Govoni et al. 1989; Grimes & Finucane 1991). Similarly, our findings are likely driven by a localized region of hydrodynamic convergence, where the surface plume and alongshore, current-driven shelf waters met, causing a retention of the drifters, fish larvae, and zooplankton. Importantly, the eastward and continued offshore movement of the plume led to limited mixing on this western end of the transect. Significantly fewer larval fishes and zooplankton were observed in the middle portion of the transect, which was under direct plume influence and subjected to the main flow and thus the highest current velocities. This observation underscores the extreme spatio-temporal variability in the physical (currents and turbulence profiles) and biological (predator-prey spatial overlap) environment that are relevant at the scale of the individual fish larva and inherent of river-dominated ecosystems.

Greater river discharge resulted in an expansive plume that subjected the majority of the water column to high levels of turbulence and mixing processes as the convergent front moved through our sampling area. Larval fishes and zooplankton became less abundant and more dispersed in their distributions, either due to active migration out of the unfavorable plume environment or transport offshore by strong southeasterly currents. Convergent fronts have been observed to concentrate larval fishes and zooplankton, but once a plume front

passes through an area and the physical convergence dissipates, it can leave behind a patchy distribution of plankton that varies in size. Patches may maintain their integrity (from minutes to hours) before they disperse (Grimes & Kingsford 1996; Kingsford & Suthers 1996). As a result, substantial plankton patchiness has been observed in the broad plume frontal region (Govoni & Grimes 1992). Such variable convergent processes have the potential to alter larval fish and zooplankton distributions on a regular basis, especially during the high seasonal flows of spring, with major implications for the growth and survival of early life stages of nearshore fishes.

Plumes can also affect recruitment by transporting fish larvae to areas of favorable or less favorable prey and predator encounters (Lambert & Ware 1984; Leggett et al. 1984). Throughout their pelagic life, fish larvae must balance foraging for prey (e.g., copepods) with avoiding predators (e.g., ctenophores, hydromedusae, siphonophores) (Houde 2002). Predator-prey dynamics during this study varied by plume regime and depended strongly on the prevailing physical oceanographic conditions. A biological aggregation, undisturbed by low wind conditions and located outside of the direct flow of the Mobile Bay plume, contained high abundances of copepod prey and gelatinous predators. As the river plume discharge increased but the water column remained stratified, fish larvae remained correlated with their prey but co-occurred with fewer predators (no longer correlated with hydromedusae). Strong currents and turbulence filled the water column, amplified by the highest freshwater flow of the year, dispersed the biological feature and reduced the probability of both prey and predator contact, creating a very poor feeding environment but a potential refuge from predators. There may be an ecological “sweet spot” here wherein a stratified water column under enough plume-influence and microturbulence to facilitate larval encounter with prey (e.g., Plankton Contact Hypothesis; Rothschild & Osborn 1988; MacKenzie & Kiørboe 1995; MacKenzie 2000) is combined with high enough turbulence and fast-flowing currents to reduce predation by poorly-swimming, tactile gelatinous predators. Thorough testing of this hypothesis would require more *in situ* studies under similar conditions. Ultimately, however, the environmental variability inherent in a river-dominated region such as the northern Gulf of Mexico exemplifies how rapidly the feeding and predation environment can shift from favorable to poor (abundant

to scant prey supply; low to high predator contact) over relatively small vertical scales of ~10 m and short temporal scales (hours to days) depending on the ensuing regimes of wind-stress, turbulent mixing, hydrographic convergence, and advective processes.

River plumes also inherently impact fish recruitment by transporting young stages into or away from estuarine nursery areas (Nelson 1977; Shaw et al. 1985) or areas of recruitment to adult stocks (Power 1986). Circulation patterns are important in the transport of eggs and early larvae from spawning grounds to nursery grounds, and in some systems, survival may be more transport-constrained than food-limited (Parrish et al. 1981). Mapping the flow patterns of plume and shelf water and examining the fine-scale distributions of fish larvae across them improves our understanding of physical processes that are critically linked to the dispersal and retention of fish larvae in and around these nursery areas. Many fishes in the northern Gulf of Mexico are estuarine-dependent, wherein they utilize the estuary during some portion of their life. This generally occurs during the early life stages, as estuaries are commonly enriched by nutrients from freshwater runoff and the resultant primary and secondary production is widely assumed to provide a favorable feeding environment and an important nursery habitat for fish larvae and juveniles. Striped anchovy (*Anchoa hepsetus*), an engraulid, and sand seatrout (*Cynoscion arenarius*), a sciaenid, are two such examples of fishes that utilize the Mobile Bay estuary and inshore coastal environment for some parts of their early life stages. Both species frequently spawn nearshore or in estuaries in the northern Gulf of Mexico, primarily peaking in spawning activity during the high-flow months of March and April. Marley (1983) surveyed planktonic fish eggs in lower Mobile Bay and estimated striped anchovy and sciaenids to be spawning either immediately outside the Mobile Bay estuary or within the high-salinity intrusions into the bay. Variability in the distribution of eggs was determined to be driven by the magnitude of river discharge into the estuary, ambient circulation patterns in the region, and spawning location of the adults. Therefore, transport of larvae away from these favorable nursery habitats by high magnitude plume flows before larvae have fully developed may negatively impact recruitment. However, the net landward movement of denser, coastal water beneath the outflowing river water suggests that fish eggs spawned in and around the tidal passes of Mobile Bay are more likely to enter the estuary or be retained nearby than to be

transported offshore (Marley 1983). Upon hatching, larvae may use behavioral responses (e.g., vertical or horizontal swimming; Rijnsdorp et al. 1985; Epifanio 1988; Paris & Cowen 2004) to take advantage of favorable currents at different depths (e.g., tidal actions, shoreward currents underlying seaward plume discharge) as a retention mechanism to stay within suitable nursery habitats and reduce dispersive losses away from highly productive nearshore regions.

Fine-scale (1-m) spatial relationships provide insights into how river plumes structure larval fish distributions and their predator-prey relationships, either by physical forcing mechanisms or avoidance behaviors. Using high-resolution *in situ* imaging, we found fewer organisms in the well-mixed, high-flow plume regime as compared to the stratified regime. A concentrated biomass of larval fishes and zooplankton was found in a highly stratified region outside of the plume and its associated currents and turbulence. Such plume regimes that increase larval fish spatial overlap with their copepod prey may offer conditions that promote enhanced feeding and growth, potentially resulting in higher survival of larvae in those locations relative to larvae within the central turbulent plume (Chapter 3). This mechanism could lead to increased production of recruits in the Mobile Bay estuary region. However, it remains to be demonstrated whether such faster growth, potentially leading to enhanced survival, is not offset by higher mortality due to predation, or where such conditions do produce more recruits, whether these recruits contribute significantly to the adult stock or fishery (Grimes & Finucane 1991). Measuring the success of such cohorts would entail sustained high-resolution *in situ* sampling combined with individual growth analyses and cohort tracking, together a substantial research endeavor. Short of such an extensive collaborative study, results of the present study are a first step towards improving our understanding of larval fish habitat use and predator-prey relationships under differing plume regimes. Coupling *in situ* biophysical observations with detailed physical descriptions enabled a comprehensive examination of the different mechanisms underlying the impacts of river plume processes on ecology and survival of the early life stages of marine fish larvae. These data can be applied to river-influenced coastal regions to better understand population variability in marine fish communities in river-influenced coastal regions throughout the world.

References

- Bakun A (2006) Fronts and eddies as key structures in the habitat of marine fish larvae: opportunity, adaptive response and competitive advantage. *Sci Mar* 70S2:105–122.
- Bowman MJ & Iverson RL (1978) Estuarine and plume fronts. In: M.J. Bowman & W.E. Esaias (eds). *Oceanic Fronts in Coastal Processes*. Springer-Verlag, New York. pp. 87–104.
- Carassou L, Hernandez FJ, Powers SP & Graham WM (2012) Cross-shore, seasonal, and depth-related structure of ichthyoplankton assemblages in coastal Alabama. *Trans Am Fish Soc* 141:1137–1150.
- Coogan J & Dzwonkowski B (2018) Observations of wind forcing effects on estuary length and salinity flux in a river-dominated, microtidal estuary, Mobile Bay, Alabama. *J Phys Oceanogr* 48:1787–1802.
- Cowan JLW, Pennock JR & Boynton WR (1996) Seasonal and interannual patterns of sediment-water nutrient and oxygen fluxes in Mobile Bay, Alabama (USA): regulating factors and ecological significance. *Mar Ecol Prog Ser* 141:229–245.
- Cowen RK, Greer AT, Guigand CM, Hare JA, Richardson DE & Walsh HJ (2013) Evaluation of the In Situ Ichthyoplankton Imaging System (ISIIS): Comparison with the traditional (bongo net) sampler. *Fish Bull* 111:1–12.
- Cowen RK & Guigand CM (2008) In situ ichthyoplankton imaging system (ISIIS): System design and preliminary results. *Limnol Oceanogr Methods* 6:126–132.
- Cury P & Roy C (1989) Optimal environmental window and pelagic fish recruitment success in upwelling areas. *Can J Fish Aquat Sci* 46:670–680.
- Dagg M, Benner R, Lohrenz S & Lawrence D (2004) Transformation of dissolved and particulate materials on continental shelves influenced by large rivers: plume processes. *Cont Shelf Res* 24:833–858.
- Dinnel SP, Schroeder WW & Wiseman Jr. WJ (1990) Estuarine-shelf exchange using Landsat images of discharge plumes. *J Coast Res* 6:789–799.
- Dzwonkowski B, Park K & Collini R (2015) The coupled estuarine-shelf response of a river-dominated system during the transition from low to high discharge. *J Geophys Res Ocean* 120:6145–6163.

- Dzwonkowski B, Park K, Ha HK, Graham WM, Hernandez FJ & Powers SP (2011) Hydrographic variability on a coastal shelf directly influenced by estuarine outflow. *Cont Shelf Res* 31:939–950.
- Dzwonkowski B, Park K, Lee J, Webb BM & Valle-Levinson A (2014) Spatial variability of flow over a river-influenced inner shelf in coastal Alabama during spring. *Cont Shelf Res* 74:25–34.
- Epifanio CE (1988) Transport of crab larvae between estuaries and the continental shelf. In: *Coastal-Offshore Ecosystem Interactions*. Springer, Berlin, Heidelberg. pp. 291–305.
- Epifanio CE, Masse AK & Garvine RW (1989) Transport of blue crab larvae by surface currents off Delaware Bay, USA. *Mar Ecol Prog Ser* 54:35–41.
- Faillietaz R, Picheral M, Luo JY, Guigand C, Cowen RK & Irisson JO (2016) Imperfect automatic image classification successfully describes plankton distribution patterns. *Methods Oceanogr* 15–16.
- Le Fèvre J (1987) Aspects of the biology of frontal systems. *Adv Mar Biol* 23:163–299.
- Garvine RW & Monk JD (1974) Frontal structure of a river plume. *Ocean Atmos* 79:2251–2259.
- Gelfenbaum G & Stumpf RP (1993) Observations of currents and structure across a buoyant plume front density. *Estuaries* 16:40–52.
- Govoni JJ (1997) The association of the population recruitment of gulf menhaden, *Brevoortia patronus*, with Mississippi River discharge. *J Mar Syst* 12:101–108.
- Govoni JJ & Grimes CB (1992) The surface accumulation of larval fishes by hydrodynamic convergence within the Mississippi River plume front. *Cont Shelf Res* 12:1265–1276.
- Govoni JJ, Hoss DE & Colby DR (1989) The spatial distribution of larval fishes about the Mississippi River plume. *Limnol Oceanogr* 34:178–187.
- Graham WM, Pagès F & Hamner WM (2001) A physical context for gelatinous zooplankton aggregations: A review. *Hydrobiologia* 155:199–212.
- Greer C, Shiller A, Hofmann E, Wiggert J, Warner S, Parra S, Pan C, Book J, Joung D, Dykstra S, Krause J, Dzwonkowski B, Soto I, Cambazoglu M, Deary A, Briseño-Avena C, Boyette A, Kastler J, Sanial V, Hode L, Nwankwo U, Chiaverano L, Fitzpatrick P, Lau Y, Dinniman M, Martin K, Ho P, Mojziz A, Howden S & Hernandez F, Church I, Miles TN, Sponaugle S,

- Moum JN, Arnone RA, Cowen RK, Jacobs GA, Schofield O, & Graham WM (2018) Functioning of coastal river-dominated ecosystems and implications for oil spill response. *Oceanography* 31:90–103.
- Grimes CB (2001) Fishery production and the Mississippi River discharge. *Fisheries* 26:17–26.
- Grimes CB & Finucane JH (1991) Spatial distribution and abundance of larval and juvenile fish, chlorophyll and macrozooplankton around the Mississippi River discharge plume, and the role of the plume in fish recruitment. *Mar Ecol Prog Ser* 75:109–119.
- Grimes CB & Kingsford MJ (1996) How do riverine plumes of different sizes influence fish larvae: Do they enhance recruitment? *Mar Freshw Res* 47:191–208.
- Harrell, Jr, FE, with contributions from C. Dupont and many others. 2016. Hmisc: Harrell Miscellaneous. R package version 3.17-4. <http://CRAN.R-project.org/package=Hmisc>.
- Hernandez FJ, Powers SP & Graham WM (2010a) Detailed examination of ichthyoplankton seasonality from a high-resolution time series in the northern Gulf of Mexico during 2004–2006. *Trans Am Fish Soc* 139:1511–1525.
- Hernandez FJ, Powers SP & Graham WM (2010b) Seasonal variability in ichthyoplankton abundance and assemblage composition in the northern Gulf of Mexico off Alabama. *Fish Bull* 108:193–207.
- Houde ED (2002) Mortality. In: Fuiman LA, Werner RG (eds). *Fishery science. The unique contributions of early life stages*. Blackwell, Oxford. pp. 64–87.
- Kim CK & Park K (2012) A modeling study of water and salt exchange for a micro-tidal, stratified northern Gulf of Mexico estuary. *Artic J Mar Syst* 96–97:103–115.
- Kingsford MJ & Suthers IM (1996) The influence of tidal phase on patterns of ichthyoplankton abundance in the vicinity of an estuarine front, Botany Bay, Australia. *Estuar Coast Shelf Sci* 43:33–54.
- Kjørboe T, Munk P, Richardson K, Christensen V & Paulsen H (1988) Plankton dynamics and larval herring growth, drift and survival in a frontal area. *Mar Ecol Prog Ser* 44:205–219.
- Lambert TC & Ware DM (1984) Reproductive strategies of demersal and pelagic spawning fish. *Can J Fish Aquat Sci* 41:1565–1569.
- Lasker R (1978) The relationship between oceanographic conditions and larval anchovy food in

- the California Current: Identification of factors contributing to recruitment failure. *Rapp Procs-Verbaux des Reunions du Cons Int pour l'Exploration la Mer* 173:212–230.
- Lee O, Nash RDM & Danilowicz BS (2005) Small-scale spatio-temporal variability in ichthyoplankton and zooplankton distribution in relation to a tidal-mixing front in the Irish Sea. *ICES J Mar Sci* 62:1021–1036.
- Leggett WC, Frank KT & Carscadden JE (1984) Meteorological and hydrographic regulation of year-class strength in capelin (*Mallotus villosus*). *Can J Fish Aquat Sci* 41:1193–1201.
- Le Pape O, Chauvet F, Désaunay Y & Guérault D (2003) Relationship between interannual variations of the river plume and the extent of nursery grounds for the common sole (*Solea solea*, L.) in Vilaine Bay. Effects on recruitment variability. *J Sea Res* 50:177–185.
- Lohrenz SE, Fahnenstiel GL, Redalje DG, Lang GA, Chen X & Dagg MJ (1997) Variations in primary production of northern Gulf of Mexico continental shelf waters linked to nutrient inputs from the Mississippi river. *Mar Ecol Prog Ser* 155:45–54.
- Luo JY, Grassian B, Tang D, Irisson JO, Greer AT, Guigand CM, McClatchie S & Cowen RK (2014) Environmental drivers of the fine-scale distribution of a gelatinous zooplankton community across a mesoscale front. *Mar Ecol Prog Ser* 510:129–149.
- Luo JY, Irisson JO, Graham B, Guigand C, Sarafraz A, Mader C & Cowen RK (2018) Automated plankton image analysis using convolutional neural networks. *Limnol Oceanogr Methods* 16.
- MacGregor J & Houde E (1996) Onshore-offshore pattern and variability in distribution and abundance of bay anchovy *Anchoa mitchilli* eggs and larvae in Chesapeake Bay. *Mar Ecol Prog Ser* 138:15–25.
- MacKenzie BR (2000) Turbulence, larval fish ecology and fisheries recruitment: A review of field studies. *Oceanol Acta* 23:357–375.
- MacKenzie BR & Kiørboe T (1995) Encounter rates and swimming behavior of pause-travel and cruise larval fish predators in calm and turbulent laboratory environments. *Limnol Oceanogr* 40:1278–1289.
- Marley RD (1983) Spatial distribution patterns of planktonic fish eggs in lower Mobile Bay, Alabama. *Trans Am Fish Soc* 112:257–266.

- McClatchie S, Cowen R, Nieto K, Greer A, Luo JY, Guigand C, Demer D, Griffith D & Rudnick D (2012) Resolution of fine biological structure including small narcomedusae across a front in the Southern California Bight. *J Geophys Res* 117:C04020.
- Moum JN, Gregg MC, Lien RC & Carr ME (1995) Comparison of turbulence kinetic energy dissipation rate estimates from two ocean microstructure profilers. *J Atmos Ocean Technol* 12:346–366.
- Munk P, Wright PJ & Pihl NJ (2002) Distribution of the early larval stages of cod, plaice and lesser sandeel across haline fronts in the North Sea. *Estuar Coast Shelf Sci* 55:139–49.
- Nelson WR (1977) Larval transport and year-class strength of Atlantic menhaden, *Brevoortia tyrannus*. *Fish Bull US* 75:23–41.
- Olson DB & Backus RH (1985) The concentrating of organisms at fronts: a cold-water fish and a warm-core Gulf Stream ring. *J Mar Res* 43:113–137.
- Paris CB & Cowen RK (2004) Direct evidence of a biophysical retention mechanism for coral reef fish larvae. *Limnol Oceanogr* 49:1964–1979.
- Park K, Kim CK & Schroeder WW (2007) Temporal variability in summertime bottom hypoxia in shallow areas of Mobile Bay, Alabama. *Estuaries and Coasts* 30:54–65.
- Parrish RH, Nelson CS & Bakun A (1981) Biological oceanography transport mechanisms and reproductive success of fishes in the California Current. *Biol Oceanogr* 1:175–203.
- Power JH (1986) A model of the drift of northern anchovy, *Engraulis mordax*, larvae in the California Current. *Fish Bull* 84:585–603.
- Purcell JE & Arai MN (2001) Interactions of pelagic cnidarians and ctenophores with fish: A review. *Hydrobiologia* 451:27–44.
- Rijnsdorp AD, Van Stralen M & Van Der Veer HW (1985) Selective tidal transport of North Sea plaice larvae *Pleuronectes platessa* in coastal nursery areas. *Trans Am Fish Soc* 114:461–470.
- Rothschild BJ & Osborn TR (1988) Small-scale turbulence and plankton contact rates. *J Plankton Res* 10:465–474.
- Ryan JJ (1969) A sedimentology study of Mobile Bay, Alabama. Dep Geol Florida State Univ Tallahassee, Florida.

- Sánchez-Velasco L, Lavín MF, Jiménez-Rosenberg SPA & Godínez VM (2014) Preferred larval fish habitat in a frontal zone of the northern Gulf of California during the early cyclonic phase of the seasonal circulation (June 2008). *J Mar Syst* 129:368–380.
- Schroeder WW (1979) The dispersion and impact of Mobile River system waters in Mobile Bay, Alabama, Bull. 37, 48 p., Water Resour. Res. Inst., Auburn Univ., Auburn, Alabama.
- Schroeder WW & Lysinger WR (1979) Hydrography and circulation in Mobile Bay. H.A. Loyacano & J.P. Smith (eds). In: *Symposium on the Natural Resources of the Mobile Bay Estuary*. U.S. Army Corps of Eng.: Mobile, AL. pp. 75–94.
- Shaw RF, Wiseman WJ, Turner RE, Rouse LJ, Condrey RE & Kelly FJ (1985) Transport of larval gulf menhaden (*Brevoortia patronus*) in continental shelf waters of western Louisiana: A hypothesis. *Trans Am Fish Soc* 114:452–460.
- Stumpf RP, Gelfenbaum G & Pennock JR (1993) Wind and tidal forcing of a buoyant plume, Mobile Bay, Alabama. *Cont Shelf Res* 13:1281–1301.
- Turner RE & Rabalais NN (1991) Changes in Mississippi River water quality this century. *Bioscience* 41:140–147.
- Wickham H (2016) *Ggplot2: Elegant Graphics for Data Analysis*. Springer-Verlag New York.
- Wickham H, François R, Henry L & Müller K (2018) *Dplyr: A Grammar of Data Manipulation*. R package version 0.7.6. <https://CRAN.R-project.org/package=dplyr>.

Table 2.1. Daily freshwater discharge rates of the Mobile Bay plume before, during, and after the April 2016 sampling period. Total freshwater discharge was estimated by summing daily river discharge data collected at two gauging stations at the head of Mobile Bay. River discharge was lagged six days to account for travel time from the upriver gauging stations to the bay. Bolded numbers correspond to the BIONESS and ISIIS plume study sampling period. Asterisk (*) shows the peak discharge of the whole year (April 10, 2016).

| Discharge Date | Collection Date | Average Daily Mobile Bay Discharge Rate (m^3s^{-1}) |
|----------------|-----------------|---|
| 3/28/16 | 4/3/16 | 1857.33 |
| 3/29/16 | 4/4/16 | 2081.543 |
| 3/30/16 | 4/5/16 | 1724.015 |
| 3/31/16 | 4/6/16 | 1951.257 |
| 4/1/16 | 4/7/16 | 3620.734 |
| 4/2/16 | 4/8/16 | 5108.416 |
| 4/3/16 | 4/9/16 | 5765.905 |
| 4/4/16 | 4/10/16 | 5944.669* |
| 4/5/16 | 4/11/16 | 5532.602 |
| 4/6/16 | 4/12/16 | 4517.585 |
| 4/7/16 | 4/13/16 | 3317.743 |
| 4/8/16 | 4/14/16 | 2123.962 |
| 4/9/16 | 4/15/16 | 1848.241 |
| 4/10/16 | 4/16/16 | 1687.656 |
| 4/11/16 | 4/17/16 | 1521.011 |

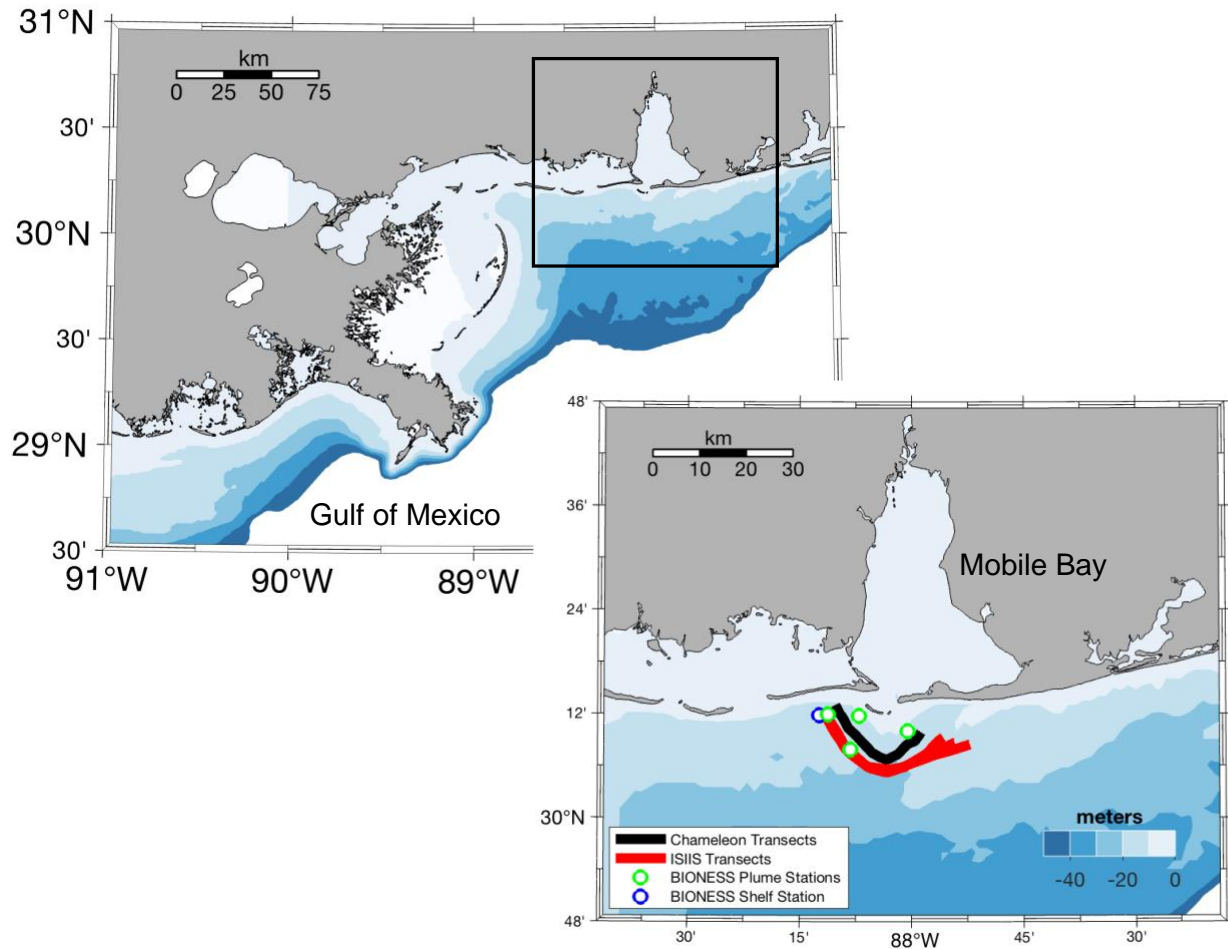


Fig. 2.1. The Mobile Bay plume outflow in the northern Gulf of Mexico was sampled for larval fishes and zooplankton during the peak flood event on April 8-11, 2016. Ichthyoplankton and zooplankton were sampled using a Chameleon microstructure profiler, an In Situ Ichthyoplankton Imaging System (ISiIS) and a Bedford Institute of Oceanography Net Environmental Sampling System (BIONESS). The ISiIS was towed in three, 20-km long arcs (red lines) through the Mobile Bay plume outflow to sample the fine-scale distributions of larval fishes and zooplankton across varying plume regimes, while the Chameleon was towed in a parallel arc ~3 km inshore to characterize the *in situ* physical properties of each plume (black lines). The BIONESS was deployed to capture fish larvae from plume (green circles; n=10 nets at 4 stations) and shelf (blue circle; n=9 nets at 1 station) water masses.

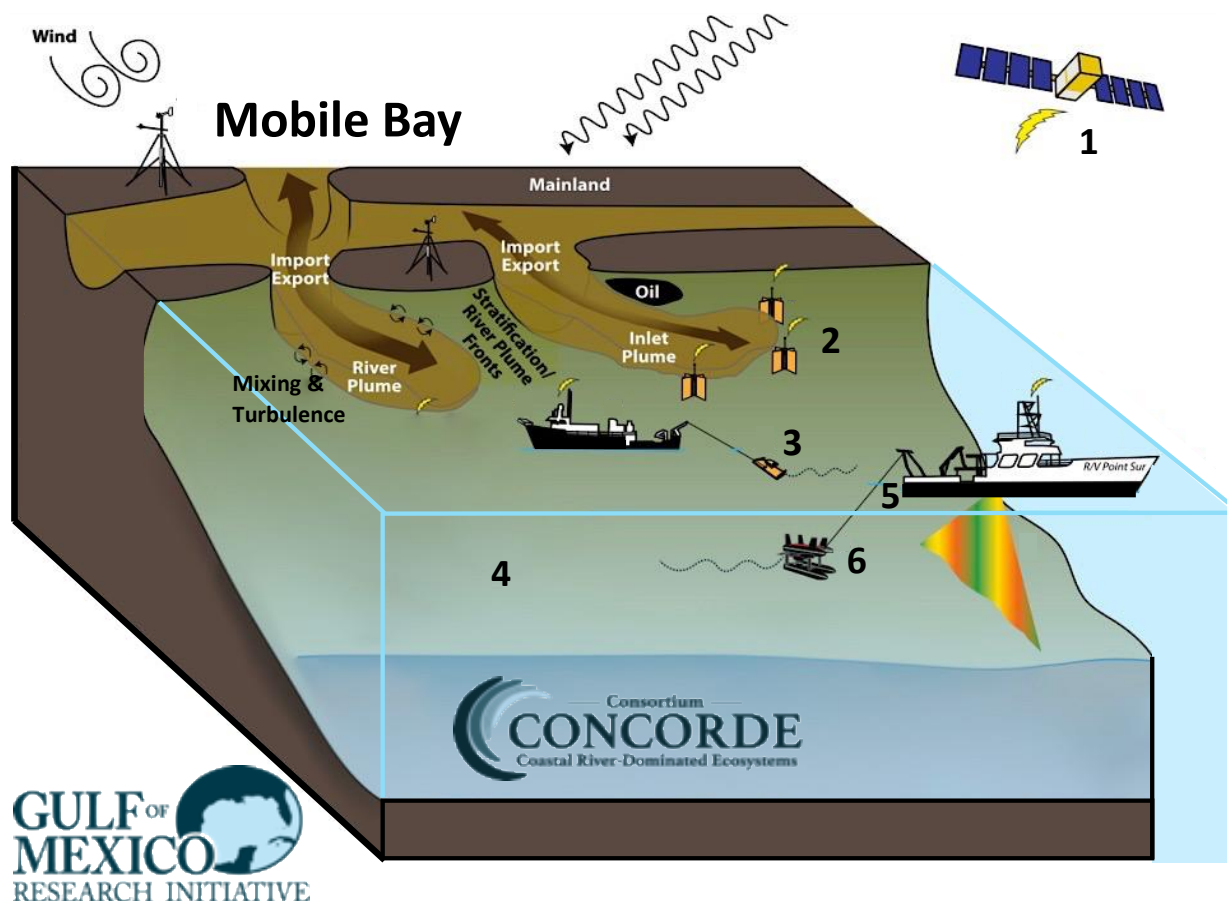


Fig. 2.2. As part of a large-scale, collaborative effort, the Mobile Bay river plume was sampled on April 8-11, 2016 using a variety of oceanographic equipment (Greer et al. 2018). To track and measure such processes as plume location, movement, physical properties, and larval fish and zooplankton spatial distributions, we used data collected from (1) the Suomi National Polar-Orbiting Partnership satellite equipped with a Visible Infrared Imaging Radiometer Suite; (2) surface drifters; (3) R/V Pelican, which is equipped with a CTD, a Chameleon microstructure profiler; (4) shipboard ADCP and (5) R/V Point Sur equipped with a CTD rosette, a BIONESS multi-net system sampling at different depths, as well as (6) an In Situ Ichthyoplankton Imaging System (ISIS).

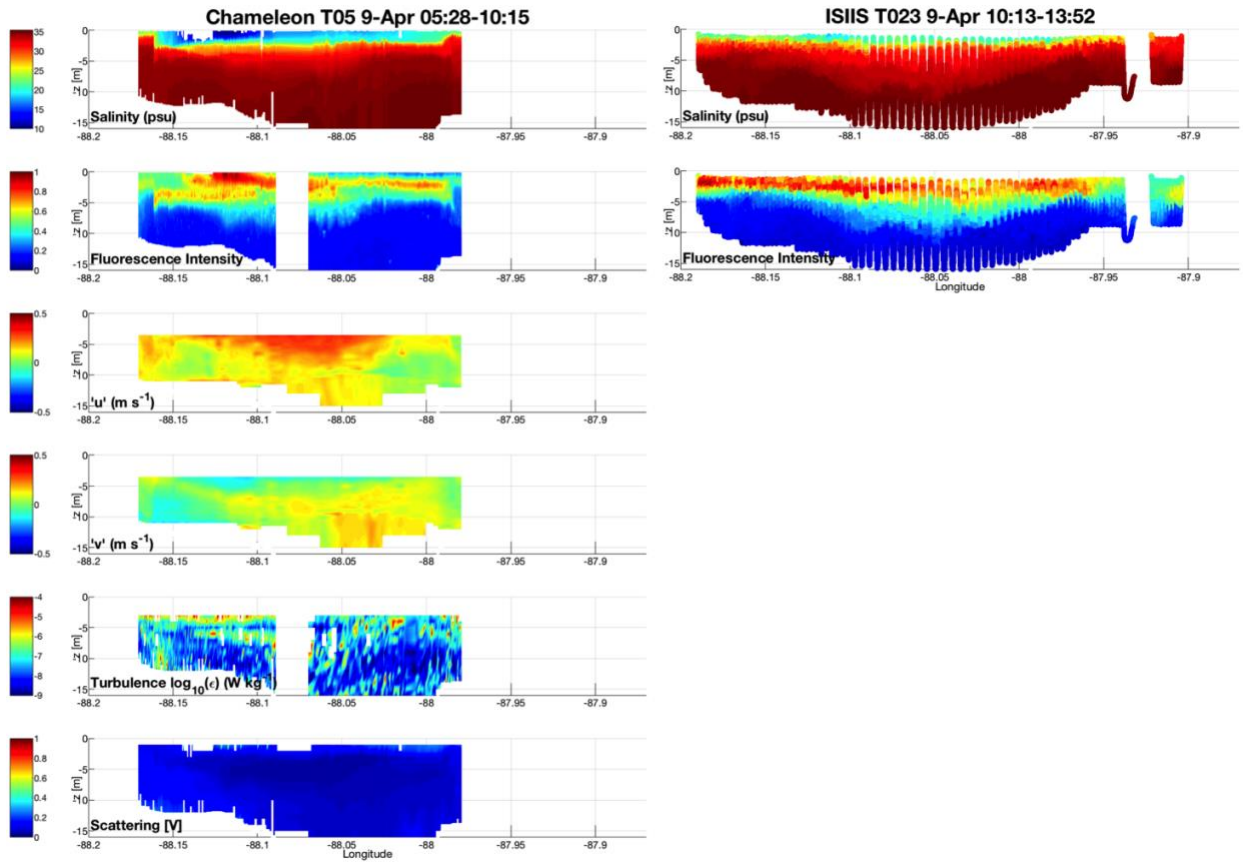


Fig. 2.3. Physical properties of the stratified Mobile Bay plume regime on April 9, 2016 from spatiotemporally similar Chameleon microstructure profiler (left panels) and In Situ Ichthyoplankton Imaging System (ISIIS) transects (right panels).

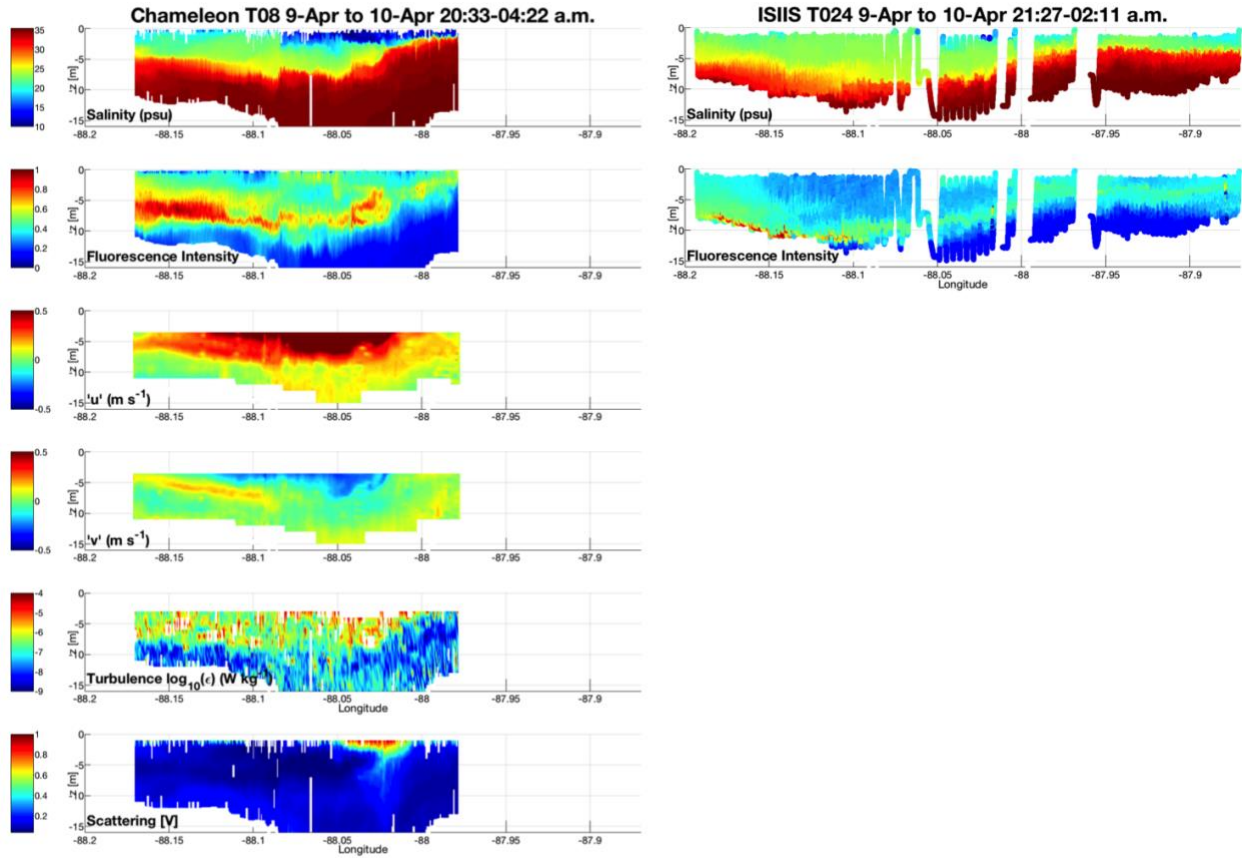


Fig. 2.4. Physical properties of the slightly-mixed Mobile Bay plume regime on April 9-10, 2016 from spatiotemporally similar Chameleon microstructure profiler (left panels) and In Situ Ichthyoplankton Imaging System (ISIIS) transects (right panels).

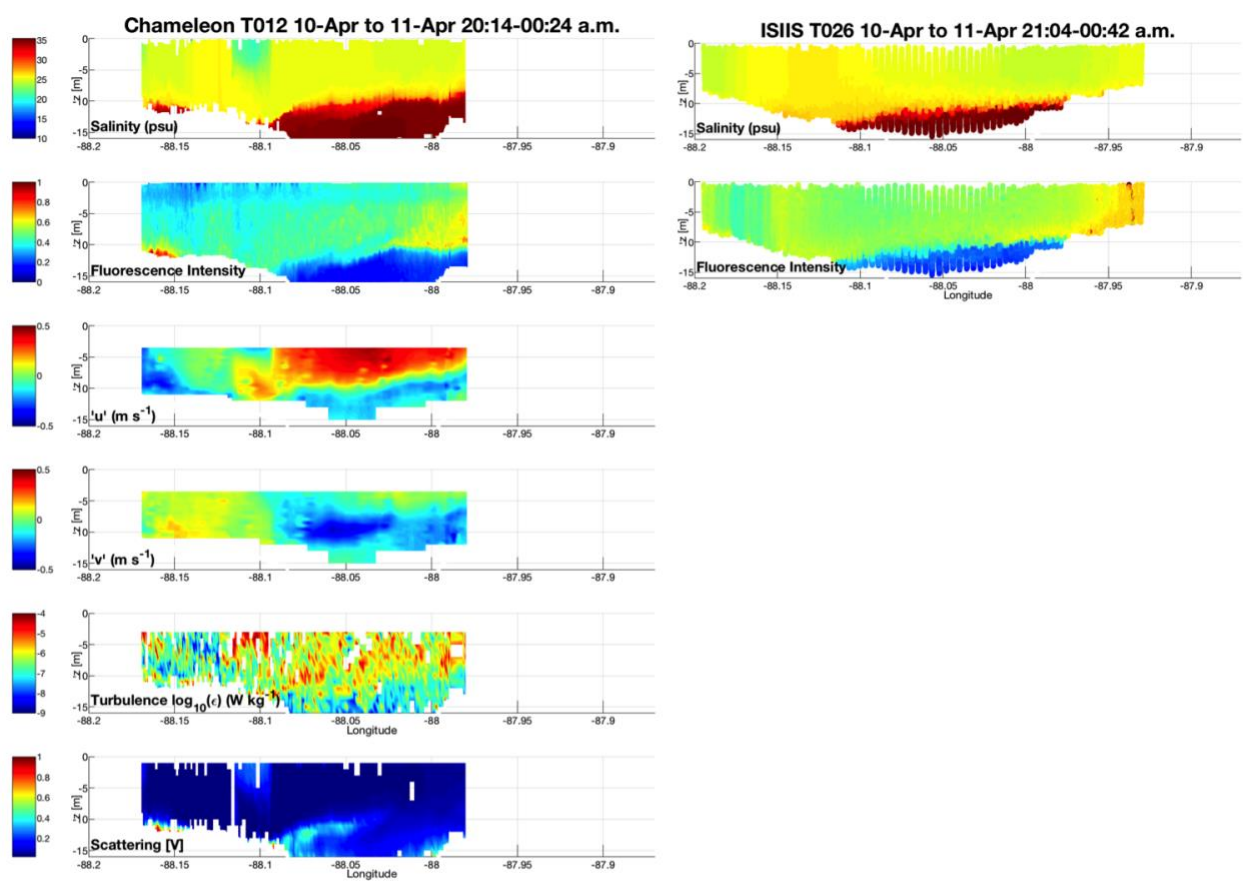


Fig. 2.5. Physical properties of the well-mixed Mobile Bay plume regime on April 10-11, 2016 from spatiotemporally similar Chameleon microstructure profiler (left panels) and In Situ Ichthyoplankton Imaging System (ISIS) transects (right panels).

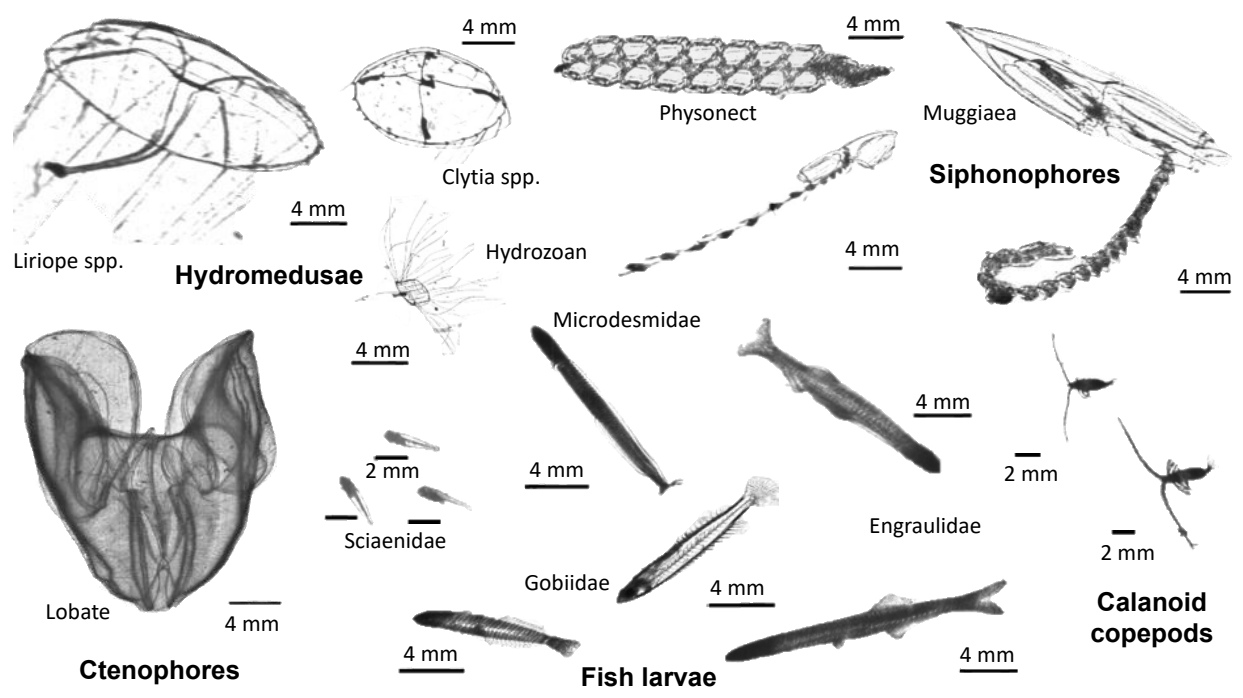


Fig. 2.6. Larval fishes and zooplankton prey and predators imaged by the In Situ Ichthyoplankton Imaging System (ISiIS) around Mobile Bay April 9-11, 2016.

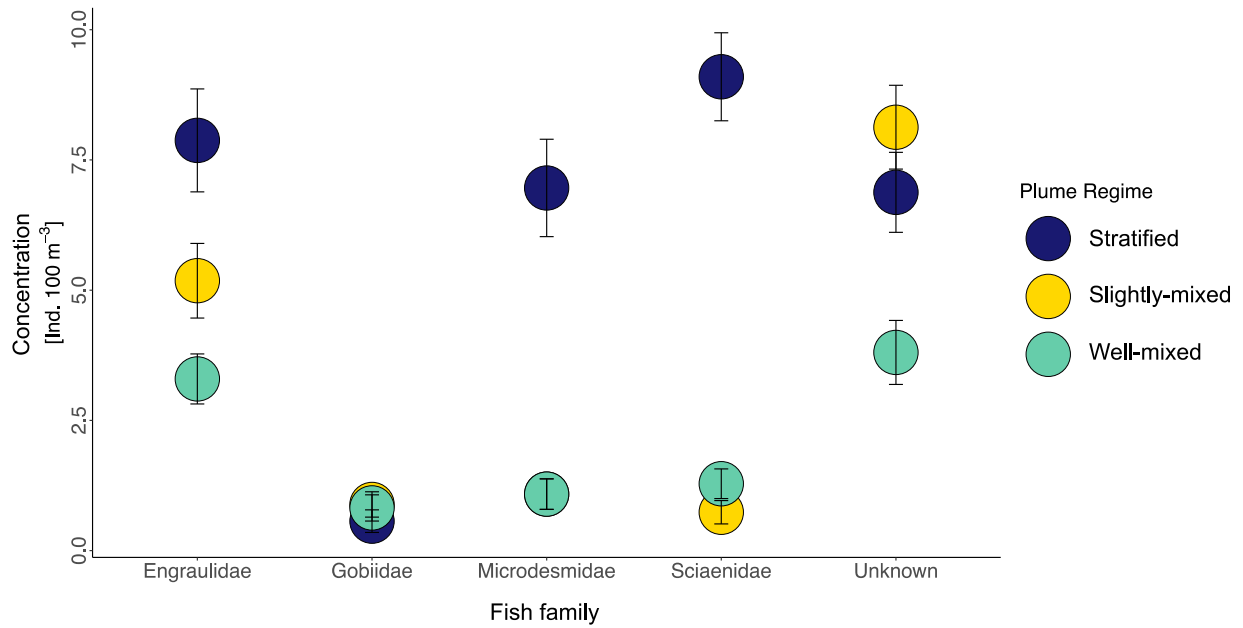


Fig. 2.7. Mean (\pm SE) concentration of the five most abundant larval fish taxa sampled by ISIIS across different Mobile Bay plume regimes: Stratified (April 9), slightly-mixed (April 9-10), and well-mixed (April 10-11).

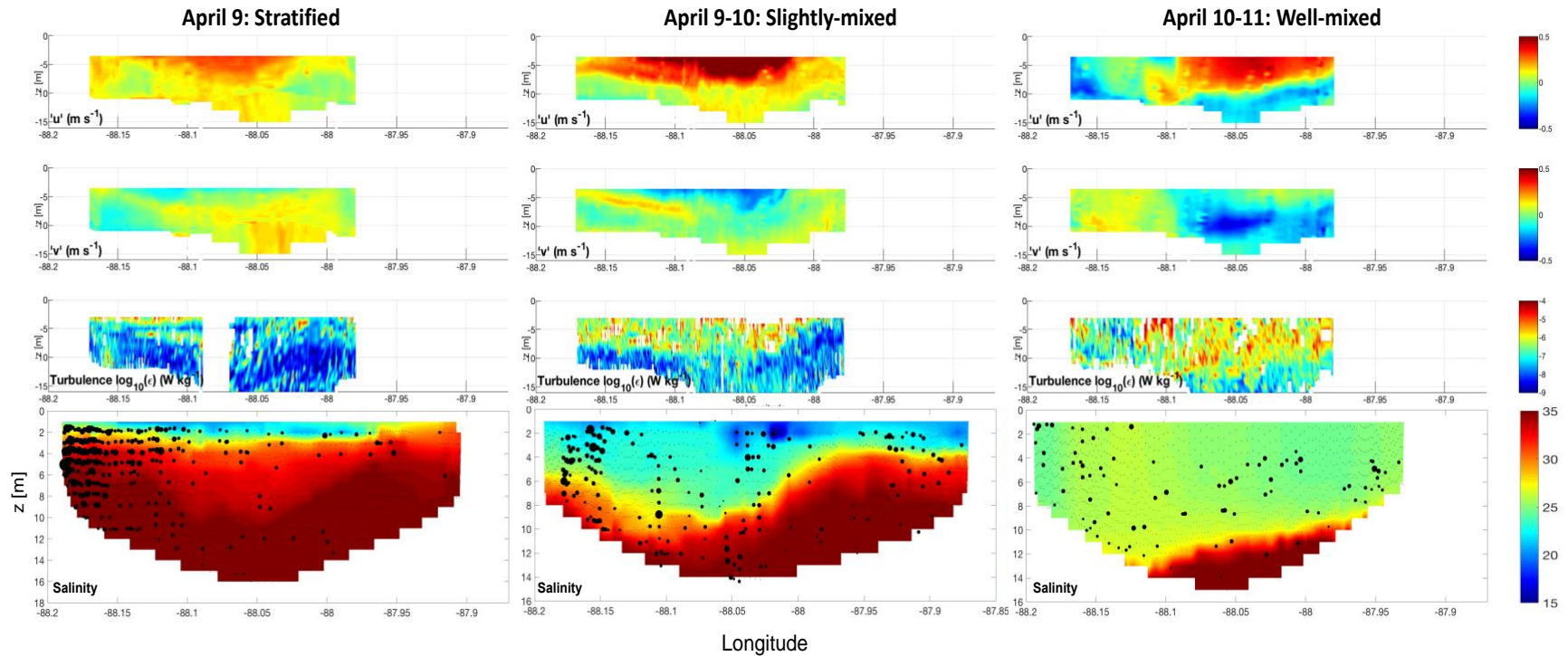


Fig. 2.8. Current velocities and turbulence structure of the Mobile Bay plume (top three rows) and distributions of fish larvae (black dots in lowest panels) superimposed on salinity structure across different water column plume regimes: Stratified (April 9), slightly-mixed (April 9-10), and well-mixed (April 10-11). The Chameleon microstructure profiler sampled currents and turbulence during the approximate time and location (~ 3 km inshore) as the In Situ Ichthyoplankton Imaging System (ISIIS).

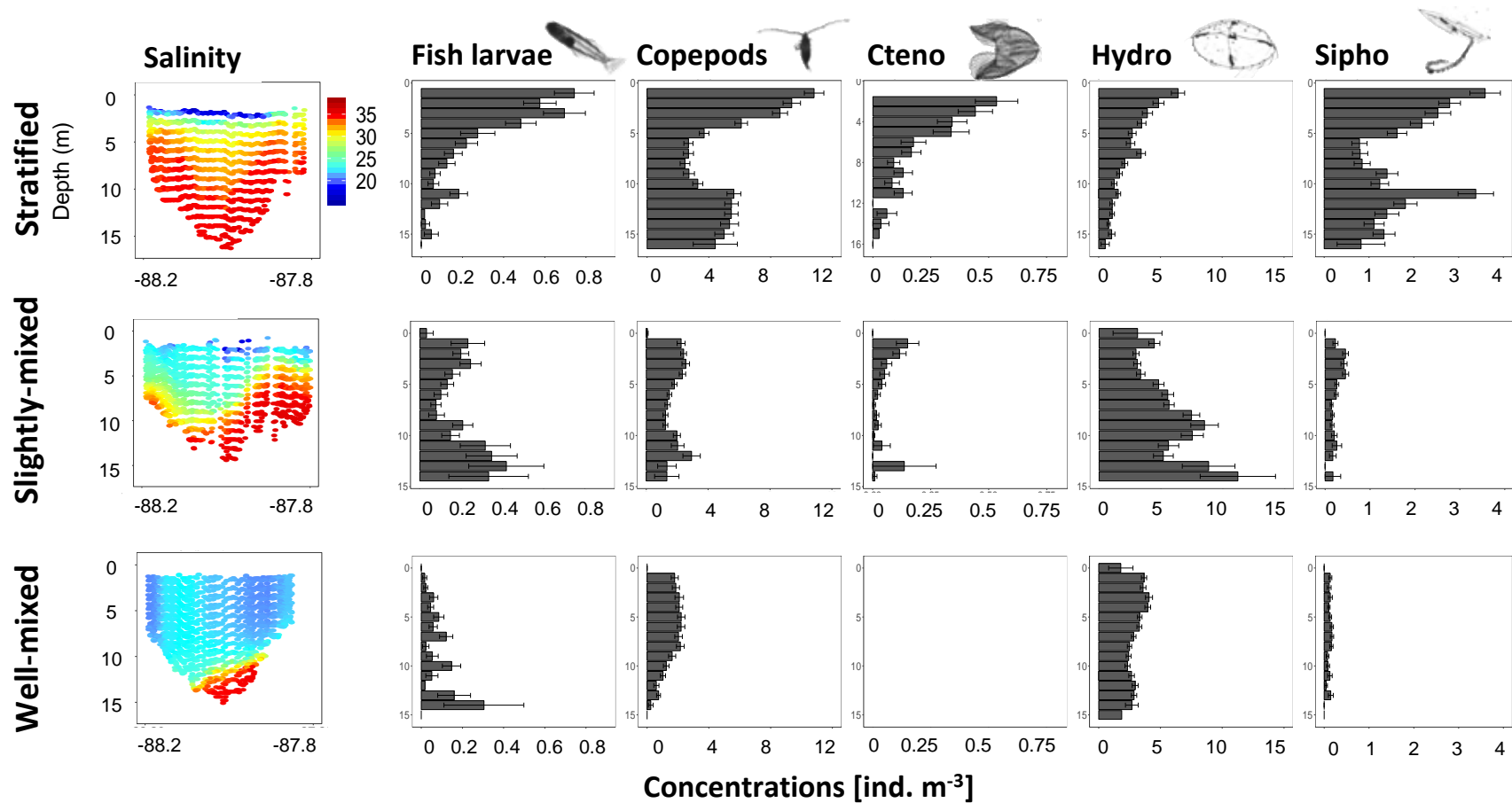
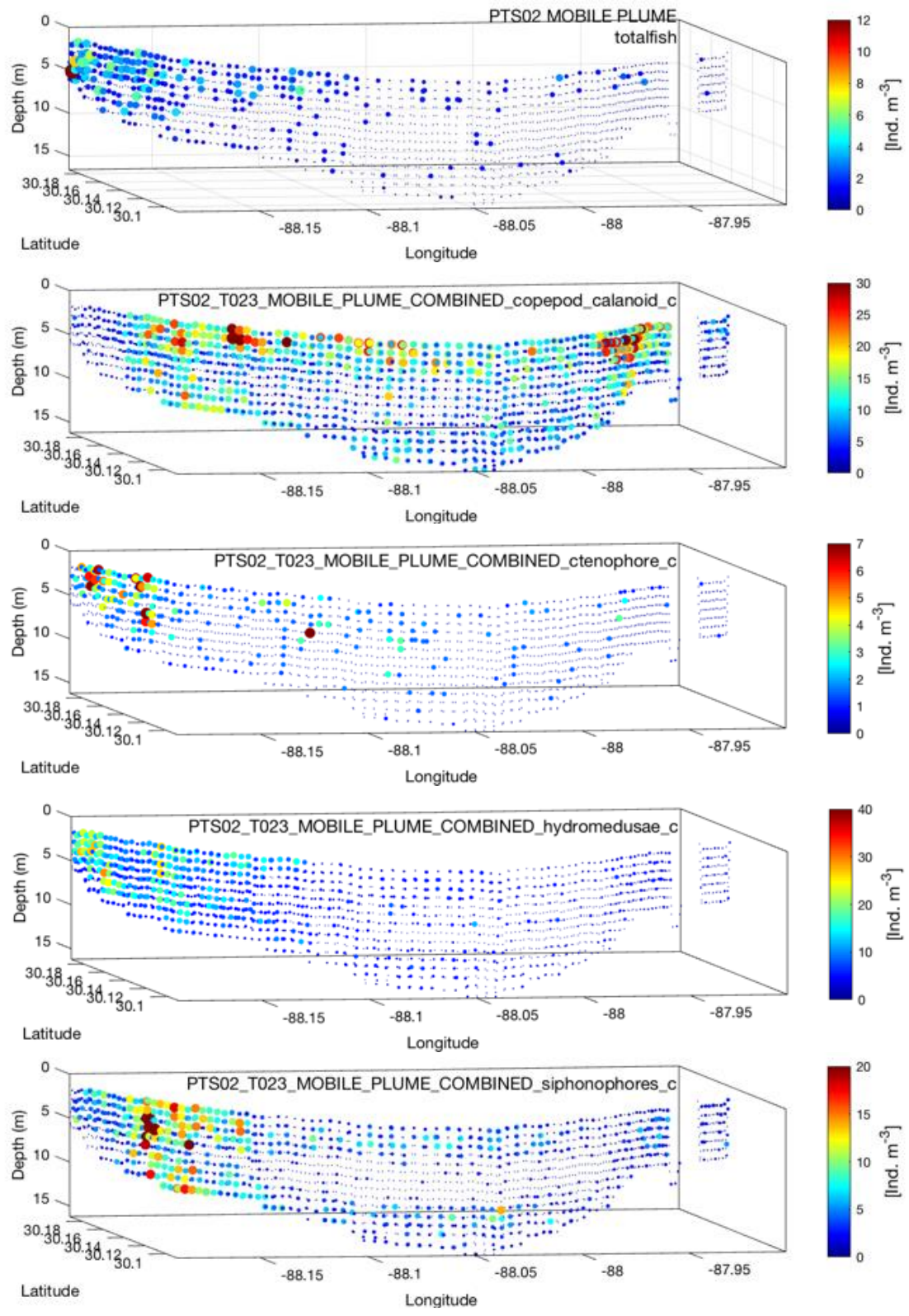
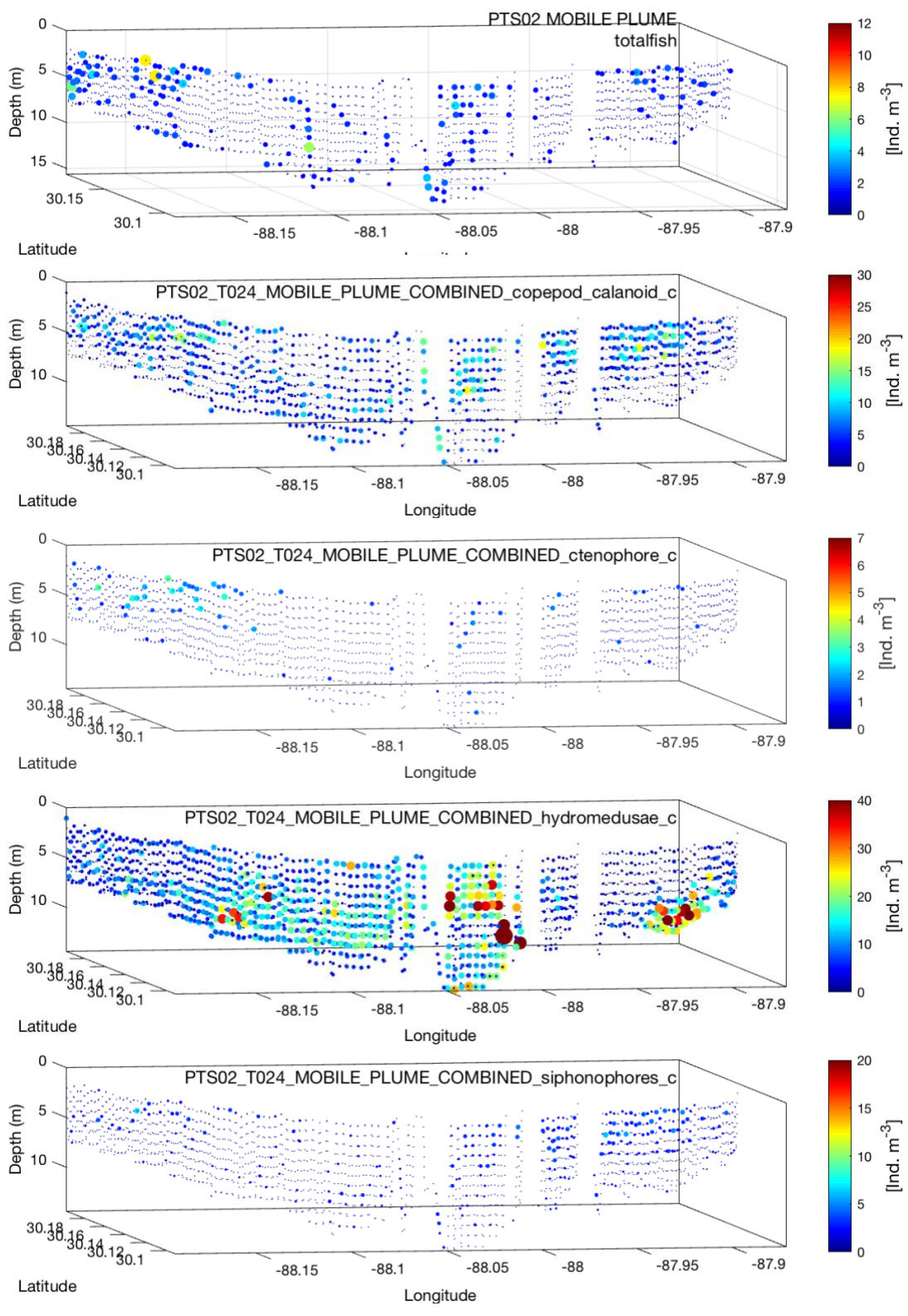


Fig. 2.9. Vertical distributions of larval fishes, calanoid copepods, and gelatinous zooplankton groups across different plume regimes of the Mobile Bay plume. Bars are stacked to give the total concentration (ind. m⁻³) of organisms in each 1 m³ depth bin. Note the changing x-axis scale among the different taxa. All physical and biological data were collected with the In Situ Ichthyoplankton Imaging system between April 9-11, 201

a) 9-Apr 10:13-13:52 p.m.



b) 9-Apr to 10-Apr 21:27-02:11 a.m.



c) 10-Apr to 11-Apr 21:04-00:42 a.m.

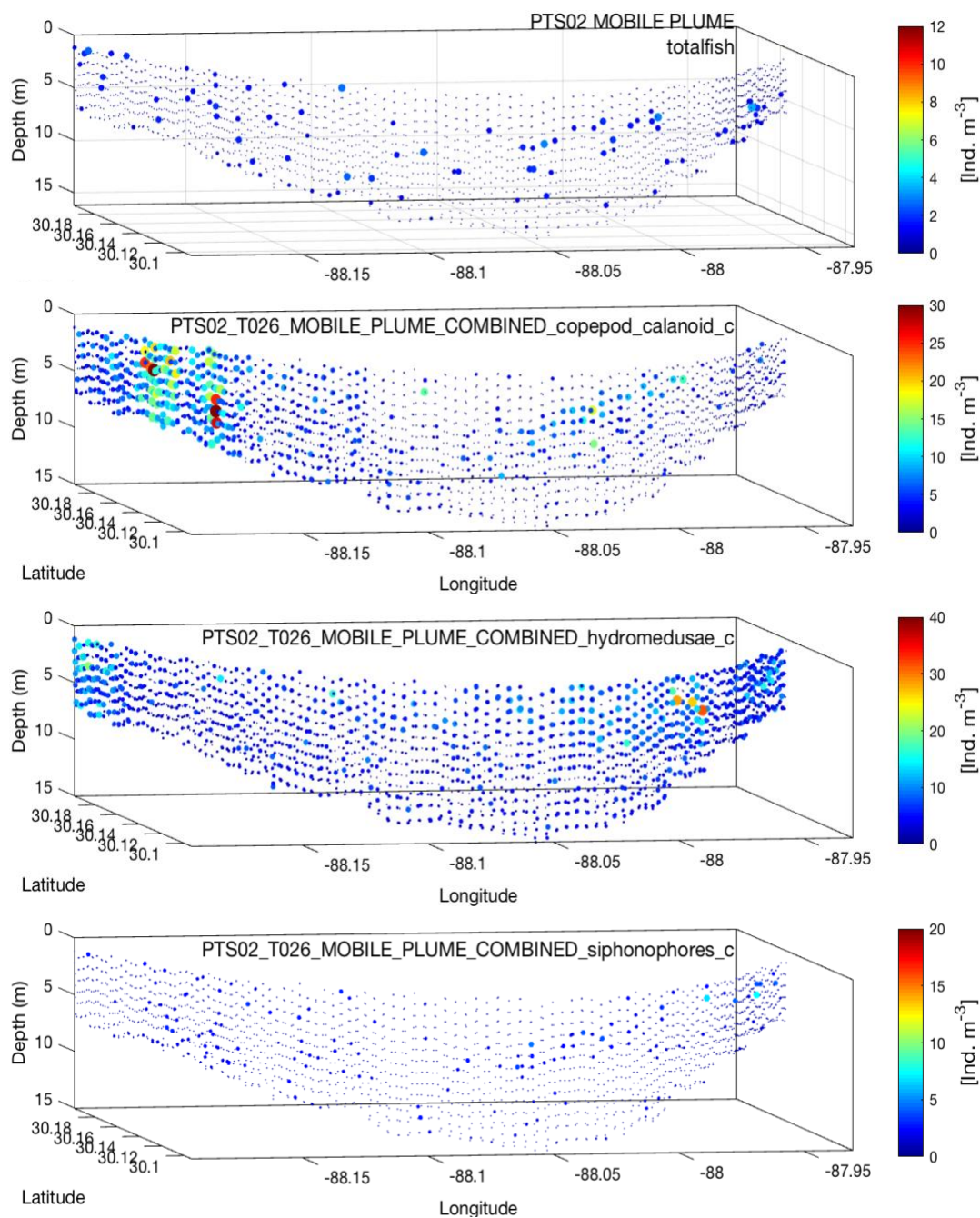


Fig. 2.10. Fine-scale concentrations (ind. m⁻³) of larval fishes, calanoid copepods, and gelatinous zooplankton throughout each transect on: a) April 9, b) April 9-10, and c) April 10-11, 2016. Larval fish and zooplankton were sampled using an In Situ Ichthyoplankton Imaging system to capture fine-scale distributions across varying plume regimes. Note: No ctenophores were sampled on April 10-11, 2016.

c) 10-Apr to 11-Apr 21:04-00:42 a.m.

T026 Entire Transect

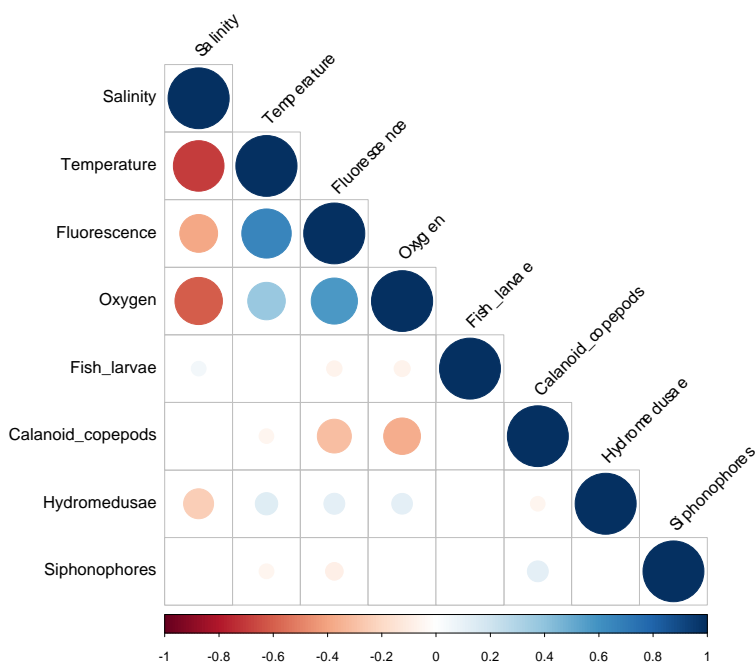


Fig. 2.11. Spearman correlation matrices for 1 m³ binned organism concentrations (ind. m⁻³) and physical variables detected along full water column transects for (a) April 9, (b) April 9-10, and (c) April 10-11. Positive correlations are displayed in blue and negative correlations in red. Color intensity and the size of the circle are proportional to the correlation coefficients. In the right side of the correlogram, the legend color shows the correlation coefficients and the corresponding colors. Correlations with a p-value > 0.01 are considered insignificant and left blank.

CHAPTER 3: THE IMPACT OF RIVER PLUMES AND COASTAL PROCESSES ON LARVAL FISH FITNESS AND SURVIVAL IN THE NORTHERN GULF OF MEXICO

3.1 Introduction

Survival of the early life stages of marine fishes is tightly linked to the physical and biological oceanographic conditions they encounter (Houde 2009). Several key factors regulate survival of the planktonic larval phase, including the ability of fish larvae to successfully capture prey, grow fast, and evade predators. All of these factors are highly influenced by physical oceanographic conditions, which are capable of structuring larval fish and zooplankton spatial distributions and therefore trophic interactions (Grimes & Finucane 1991). River discharge into coastal shelf ecosystems can profoundly impact fisheries production depending on river water characteristics such as nutrient content, sediment load, discharge rate, and its associated physical gradients (e.g., density, temperature, salinity) and hydrodynamic processes (Grimes & Finucane 1991; Le Pape et al. 2003). Therefore, for coastal marine fishes, river plumes likely have a major, though variable, effect on the number of fish that survive to recruitment (Sabatés & Masó 1990). Many studies have determined that nearshore and estuarine-dependent fish larvae, either by biological or physical processes, aggregate near river plumes in the northern Gulf of Mexico (Govoni et al. 1989; Grimes & Finucane 1991; Govoni & Grimes 1992; Chapter 2), yet the ecological consequences (e.g., feeding, growth, condition, survival) of such aggregations are inconsistent likely due to variability in the biotic and abiotic conditions that these fish larvae experience.

Feeding success is a major determinant in the success or failure of a given cohort of fishes (Grimes & Finucane 1991), thus riverine influence on the abundance and distribution of prey is a key process. Previous studies have shown that strong density stratification generated by low salinity plume waters overlying high salinity shelf waters can stabilize the water column and biological concentrations of larval fishes and their zooplankton prey (e.g., copepods and nauplii) have been observed along river plume fronts (e.g., Grimes & Kingsford 1996; Cowan et al. 2008). The influx of nutrient-rich plume waters into the coastal ocean often results in phytoplankton blooms (Lohrenz et al. 1997), which can enhance secondary production and

ultimately benefit fish larvae. As a result of these plume front aggregations, the encounter rate of larval fishes with their prey may increase and several studies have shown elevated feeding success and growth in plume-associated larvae in comparison with their shelf conspecifics (Grimes & Lang 1992; Lang, Grimes & Shaw 1994; Rissik & Suthers 1996; Govoni 1997). There are advantages for fish larvae that encounter a habitat that facilitates enhanced foraging success, as it is well-established that the fate of year classes hinges on the ability of larvae to find sufficient quantities of prey to support foraging and growth (Hjort 1914; Cushing 1969). For instance, enhanced feeding conditions support fast growth, rapid development, and higher condition in fish larvae, which can improve swimming capabilities (Fisher & Bellwood 2001) and potentially counter high predation mortality by reducing the duration of the vulnerable early life stages (Houde 1987, 2009; Anderson 1988).

Whether or not this enhanced foraging environment conveys a survival advantage to the larval stages has been contested, with some studies finding slower growth rates and no trophic, condition, or survival advantages for plume-associated larvae (Govoni & Chester 1990; Powell et al. 1990; Lochmann et al. 1997; Allman & Grimes 1998). Fish larvae with lower nutritional condition are typically smaller, weaker, and more poorly developed with regard to sensory and behavioral capacities than well-fed larvae of the same age. Other studies have found wind-induced mixing and intense upwelling to be detrimental to fish larvae due to the dispersal of aggregated prey that normally persist under non-turbulent conditions (e.g., 'stable ocean hypothesis'; Lasker 1975, 1978). Furthermore, the same physical factors that concentrate larval fishes and their prey items within near-surface frontal zones also aggregate known larval fish predators, such as gelatinous zooplankton (e.g., scyphomedusae, hydromedusae, ctenophores, and salps (Purcell & Arai 2001). These buoyant organisms have been found to aggregate across frontal boundaries in a variety of systems (MacGregor & Houde 1996; Graham et al. 2001; Bakun 2006; McClatchie et al. 2012; Luo et al. 2014). Heightened predator abundances within river plumes could increase the mortality rates of plume-associated larvae and offset any trophic advantages.

Constraints to larval foraging can be imposed by certain abiotic features in the local environment. For instance, key factors regulating the rates of larval feeding and growth include

turbulence and light intensity (Peck et al. 2012). Both factors can alter the distribution of larvae with respect to their prey and, in some systems, will be intimately linked to turbidity and suspended sediment loads. For instance, turbidity can limit light and thus reduce visibility of food organisms. Vision is a relatively well-developed sense in fish larvae, as eyes develop at a very early developmental stage (Lecchini et al. 2005) and many fish larvae are known to be visual predators (Checkley 1982). Therefore, turbidity can negatively affect larval feeding success by reducing reactive distance and prey contrast (Barrett et al. 1992; Gregory & Northcote 1993; Salonen et al. 2009). However, the turbid plume environment may serve as refuge if visual predators are unable to find fish larvae (Reichert et al. 2010), thereby alleviating predation pressure and potentially increasing larval survivorship (De Robertis et al. 2003; Pangle et al. 2012; Carreon-Martinez et al. 2014). It is unclear if these plume-associated benefits apply to systems with an abundance of tactile (non-visual) predators (i.e., gelatinous zooplankton).

While many studies have been conducted on the shelf in the northwestern Gulf of Mexico, relatively few have focused on larval fish assemblages on the northcentral shelf region under direct impact of Mobile Bay and even fewer have examined larval fitness and survival in response to environmental variability in this system (but see Hernandez et al. 2010; Carassou et al. 2012). Fronts associated with the outflow plume of Mobile Bay can persist over time scales of several tidal cycles (hours) to several days, depending on shelf circulation, magnitude of river discharge, and local wind-stress and mixing conditions (Dinnel et al. 1990). These temporal scales, though brief, are long enough to affect larval fish growth and condition if feeding conditions are favorable, but short enough to disperse aggregations of prey. Because larval fishes grow faster in response to higher concentrations of food, measuring the persistence and influence of these plume features on time scales relevant to the feeding, growth, and development of fish larvae is critical to understanding their role in supporting higher fish production (McManus & Foster 1998). To examine how fish larvae respond to variable salinity gradients, wind-stress, and discharge regimes around the Mobile Bay outflow, we compared variations in larval fish growth and morphometric condition in plume (i.e., regions where Mobile Bay outflow and coastal shelf waters mix) to nearshore Gulf of Mexico shelf waters (i.e.,

regions outside of the direct flow of the plume). In addition to measuring environmental variables associated with each water mass (temperature, salinity, prey supply), we conducted a diet analysis to evaluate the potential for food limitation across the salinity gradient.

3.2 Methods

3.2.1 Study region & river plume sampling

Mobile Bay is a shallow, river-dominated estuary in the northern Gulf of Mexico that emits pulses of freshwater that vary in size and seasonal flow and drive a salinity gradient between the bay mouth and coastal waters. It is the largest local system delivering freshwater to the Mississippi Bight (Greer et al. 2018) and the fourth largest river system in the continental United States (Schroeder & Lysinger 1979). To capture the biological effects of entrainment within a plume at the scale of an individual fish larva, we sampled the Mobile Bay plume during a peak annual discharge period (April 10, 2016; Table 2.1). Distinctive Mobile Bay plume signatures were located by a suite of oceanographic equipment (see Chapter 2.2 [Methods]). Because salinity gradients were consistent with other plume characteristics (e.g., fluorescence and turbulence, Chapter 2) in delineating the general boundaries of each plume water mass, low salinity (≤ 25) was used as an indicator of Mobile Bay's plume location and movement.

3.2.2 Ichthyo- and zooplankton collection

The Mobile Bay plume outflow was targeted for repeated sampling with a multinet BIONESS sampler (Bedford Institute of Oceanography Net Environmental Sampling System; Open Seas Instrumentation, Inc., Musquodoboit Harbor, Nova Scotia) that was towed behind the *R/V Point Sur*. Fish larvae and zooplankton were collected at stations immediately preceding and following three-dimensional water column imaging for zooplankton (In Situ Ichthyoplankton Imaging System, ISIS, deployments; see Chapter 2). The 0.25-m² mouth opening of the BIONESS was fitted with six 333- μ m-mesh and three 202- μ m-mesh plankton nets to better target larval fishes and zooplankton, respectively. Tows were conducted during both daylight and nighttime hours. The BIONESS was outfitted with a conductivity-temperature-depth probe (CTD; SBE19, Sea-Bird Electronics, Inc., Bellevue, Washington) to provide

temperature ($^{\circ}\text{C}$), salinity (unitless), and depth (m) profiles for each tow. Mean temperature and salinity observations (average of values measured at the opening and closing time of the nets for each depth bin) were examined at each station to determine the real-time environmental conditions in which larval fishes were collected. A flowmeter (General Oceanics, Inc., Miami, FL, USA) calculated the volume filtered for each sample.

Five nearshore stations (within 15 km of the Gulf coastline) around the Mobile Bay outflow were sampled for fish larvae and zooplankton. Although the plume outflow tended to fluctuate in magnitude and direction, four of the stations were located within the well-mixed, low salinity waters (≤ 25) leftover from the passage of an outwelling plume front into the ambient northern Gulf shelf water. These stations were clustered at the mouth of Mobile Bay approximately 7-13 km south of Main Pass (Fig. 3.1) and were sampled on April 8-10, 2016. Another station was located nearshore and outside of the direct flow of the plume approximately 15 km to the west of Main Pass (Fig. 3.1) and was sampled on April 9, 2016. At the time this station was sampled, a very shallow (< 2 m) surface lens of turbid, low-salinity water overlaid the much denser, saline water (> 32) indicative of ambient northern Gulf shelf water. The result of this thin lens was a highly stratified water column. Due to these characteristics of high salinity and water column stratification, this station was considered to be a “shelf” station and selected for comparison with the four well-mixed, low salinity “plume” stations (salinity ≤ 25). Only net samples < 10 m depth were analyzed to standardize depth between plume and shelf stations. Based on the designated salinity and depth criteria, 10 plume net samples and 9 shelf net samples were selected for analysis (Table S.3.1). These samples were used to provide specimens for growth, condition, and diet analyses, verification of ISIIS image classifications, and development of the ISIIS image library.

Plankton net contents were rinsed with seawater, sieved, fixed in 95% ethanol, and stored in 85% ethanol. All fish larvae and zooplankton collected by the BIONESS nets were sorted and identified to the lowest possible taxonomic level. Concentrations of each species or taxon (individuals m^{-3}) were calculated by dividing counts from each net by the volume of water filtered through the net. Larval fish and zooplankton concentrations were log-transformed and compared between plume and shelf net stations using Welch’s t-tests or non-parametric Mann

Whitney *U*-tests, which make no assumptions about the distribution of the data. Also because they make no assumptions about the normality or variability in the data, non-parametric Spearman rank correlation coefficients were used to compare larval fish concentrations with those of their copepod prey and gelatinous predators using ISIS-collected imagery data for higher spatial resolution. The ISIS-imagery was grouped by plume (≤ 25) or shelf (> 25) salinities and fish and zooplankton correlations compared across each transect. The significance levels of these correlations were assessed using an approximation of the Student's *t* distribution in the 'Hmisc' package of R (Harrell et al. 2016).

Although the BIONESS net mesh was too large ($> 200 \mu\text{m}$) to comprehensively sample phytoplankton abundances, environmental concentrations of dinoflagellates were calculated from separate CTD cast stations in the same region and during the same time period as the net tows. BIONESS tows were aligned with their closest (spatially and temporally) CTD cast to estimate average dinoflagellate concentrations at each plume and shelf net station. Microplankton ($20\text{--}200 \mu\text{m}$) assemblage composition, size distribution, and abundances were described by imaging water samples with a FlowCAM® Benchtop B3 Series.

3.2.3 Focal species

Engraulidae and Sciaenidae are two of the most abundant species in the northern Gulf of Mexico and were likewise the most abundant larval families in both plume and shelf net samples during the study period. We therefore confined our growth, condition, and diet analyses to one species of engraulid and one sciaenid: striped anchovy (*Anchoa hepsetus*) and sand seatrout (*Cynoscion arenarius*), both of which are common nearshore species in the northern Gulf of Mexico. Members of the family Sciaenidae are some of the most prominent inshore fishes in the United States coastline of the northern Gulf of Mexico and are important sport and commercial fishery resources (Cowan & Shaw 1988). Striped anchovy, while not of direct commercial importance, serve as an important food staple for large commercial piscivorous fishes due to their abundance and small size (Franks et al. 1996). Both striped anchovy and sand seatrout primarily spawn from March to April in shallow Gulf of Mexico waters and some larvae enter estuarine-lagoon systems which provide critical nursery habitat

for postlarval and juvenile life stages (Barger & Williams 1980; Robinette 1985; Cowan & Shaw 1988). As larvae, striped anchovy and sand seatrout primarily feed on copepods, particularly calanoid copepods (McNeil & Grimes 1995; Holt & Holt 2000).

3.2.4 Size and growth analysis

Larval body lengths were measured to the nearest 0.01 mm (either notochord length [NL] if preflexion or standard length if post-flexion [SL]) for a subset of larvae of each species using a Leica MZ16 dissecting microscope. All imaging was conducted using a QImaging digital camera and Image-Pro Premier 9.1 software (Media Cybernetics, Inc., Rockville, Maryland). Sagittal otoliths were dissected from each individual and stored in immersion oil on a glass slide for a week to “clear” and facilitate reading (Sponaugle et al. 2009). All otoliths from both species were analyzed by a single reader. Otoliths were read along the longest axis at 1000× magnification through a Zeiss Axio Scope.A1 compound microscope using a QImaging digital camera and Image-Pro Plus software. All otoliths were read twice, and if the reads differed by ≤5%, one read was randomly chosen for analysis. If reads differed by >5%, a third read was conducted and compared with the first two reads. If any comparison differed by ≤5%, one read from that comparison was randomly chosen for analysis. Otoliths where all reads differed by >5% were removed from any further analyses (Sponaugle et al. 2009).

Two separate otolith microstructure analyses were used to compare the variation in larval growth of the focal species captured in plume and shelf water masses: 1) recent growth and 2) daily otolith growth (individual increment widths) as a proxy for growth at specific ages during larval life. Because the exact timing of larval entrainment within a plume could not be determined, we examined recent growth during the last few complete days prior to capture for all larvae to minimize the potential effect of differential spatial and environmental conditions on early larval growth. Otolith increment width increases with the age of the individual fish, so we corrected for this by detrending for age (e.g., Baumann et al. 2003; Robert et al. 2009). Detrending for age enabled us to compare recent growth of differently aged larvae. A detrended growth index was computed using:

$$DG_{ij} = (G_{ij} - G_j) SD_j^{-1}$$

where DG_{ij} is the detrended growth of the individual i at age j , G_{ij} is the otolith growth (increment width) for individual i at age j , G_j is the mean of otolith growth of all individuals at age j , and SD is the standard deviation of G (Robert et al. 2009). The detrended growth index was computed for the last 3 full days of life (i.e., width of the last 3 complete otolith increments). We then compared the detrended recent growth (DRG) for each species from the two water mass types using analysis of covariance (ANCOVA) with age as a covariate. The oldest (>14 d) and youngest (<7 d) *C. arenarius* ($n=42$) were removed from analyses due to uneven sample sizes between water masses. The effect of temperature on recent growth in different water masses was also assessed using simple linear regression. For the comparison of daily growth at specific ages throughout life for each species, mean otolith increment widths (MIW) for each day of larval life were compared by region using separate one-way ANOVAs. Mean increment width (MIW) values were truncated when sample sizes of fishes were $n < 4$.

3.2.5 Morphometric condition analysis

To examine differences in larval fish body condition between plume and shelf water masses, we analyzed larval morphology using five linear body dimensions (six for seatrout larvae) that have been shown in other fishes to vary with larval feeding success, and hence are related to body condition (body depth at pectoral fin, DPF; body depth at anus, DA; head length, HL; head depth, HD; eye diameter, ED; and in the case of the seatrouts, lower jaw length, LJJ; Lochmann & Ludwig 2003; Gisbert et al. 2004; Hernandez et al. 2016; Ransom et al. 2016). Only specimens with the full suite of morphometric measurements were used in the analysis of body condition. In general, deeper-bodied and heavier larvae at a given length are in better body condition than their skinnier counterparts (Ransom et al. 2016). The residual of each body measurement (e.g., head depth) was computed from its linear correlation with notochord length to standardize and account for size variation among larvae (Hernandez et al. 2016). We did not correct for ethanol shrinkage because of the relatively narrow size range of collected specimens (8-18 mm for *A. hepsetus* and 2-7 mm for *C. arenarius*); however to be conservative, we conducted two NMS analyses: 1) on all fish larvae and 2) on a size-truncated portion of the collected specimens of both species. The size-truncated analyses were conducted

to account for the larval size differences between water masses as well as the potential influence of allometric and ontogenetic changes in body morphology that occur during the transition from pre- to post-flexion larval stages (Suthers 1998). Flexion occurs at ~8-9 mm in striped anchovy (Richards 2005) and therefore larvae <10 mm and >16 mm (n = 24) were removed from the size-truncated analysis to examine the morphometrics of a narrower size range of post-flexion larvae. Similarly, flexion occurs at ~4.2-5.2 mm in sand seatrout (Richards 2005), thus larvae >4 mm (n = 11) were removed from the corresponding size-truncated analysis to examine only pre-flexion larvae.

Nonmetric multidimensional scaling (NMS) was used to ordinate larvae according to body shape to investigate changes in morphometric condition between water masses (Kruskal 1964; Mather 1976). NMS ordination was chosen for the morphometric analyses because it accounts for the high degree of correlations among the different body dimensions and also because it has the least restrictive assumptions and can represent the structure of data sets in their original dimensions (McCune et al. 2002). All NMS ordinations were performed in PC-ORD version 7 software (McCune et al. 2002, MjM Software Design, Gleneden Beach, Oregon). The final NMS ordination was performed using the “slow and thorough” autopilot setting in conjunction with the Sorensen Bray-Curtis distance measured on the residual body dimensions. A nominal value of 1 was added to all residuals because the Bray-Curtis distance measure can only calculate distances for positive integers. Outliers were identified as those larvae with an average distance of >3 standard deviations above the grand mean of distances and removed from the analysis (n=3 striped anchovy larvae and n=5 sand seatrout larvae). Once the NMS axes were derived, each axis was correlated with the original body dimension residuals to identify which dimensions were more closely related to variation among larvae in body shape (Hernandez et al. 2016). NMS axes can be independently analyzed to compare differences in larval body shape because they are orthogonal (Rettig et al. 2006).

3.2.6 Diet analysis

To determine whether river plumes create enhanced feeding conditions for larval fishes, the short-term feeding success of fish larvae collected from plume waters was compared to

those captured in shelf waters. Gut contents were examined under a Leica MZ16 stereomicroscope by excising the alimentary canal with minuten pins and, after transferring to 4% solution of glycerol, teasing out prey items. Prey items were counted, identified to the lowest possible taxon, categorized to major groups, and measured for length using Image-Pro Premier software (copepod prosome length and longest dimension in all other prey). To compare prey composition between the different water masses, the numerical percentage (%N; proportion of each prey type from all prey extracted) and frequency of occurrence of prey types (%FO; proportion of larvae with the prey type present in gut or else percent frequency of occurrence among larvae containing food) were calculated. A total of 166 anchovies were dissected for gut contents and ranged 8-14 mm in length from plumes and 8-18 mm in length from shelf waters. Of 172 larval seatrouts dissected for gut contents, 165 were 2-4 mm in length and six were 4-6 mm in length. To compare sizes of consumed prey between fishes captured from different water masses, the residual lengths for each prey item (e.g., calanoid copepod prosome length) were calculated from their linear correlation with the fish's body length to standardize and account for trends in larval fish size and consumed prey lengths.

Schoener's diet overlap index (Schoener 1970) was calculated to measure the dietary similarity between fish larvae captured in different water masses. The index was calculated as follows:

$$\alpha = 100[1 - 0.5 \sum_{i=1}^n (P_{xi} - P_{yi})]$$

where P_{xi} is the proportion of prey items in category i to total prey items for fish larvae in a water mass x , while P_{yi} represents the same proportion in a water mass y . The value of α ranges from 0 (no dietary overlap) to 100 (complete dietary overlap). According to Wallace and Ramsey (1983), overlap values >60 can be considered biologically significant.

Prey availability estimates were calculated by subsampling a known volume of plankton with a Hensen-Stempel pipette and enumerating all zooplankton from the same samples as the larval fish specimens. Subsampling continued until at least 200 copepods and 200 of all other organisms combined had been recorded. Dinoflagellate concentrations were calculated from water samples collected throughout the nearshore Mobile Bay outflow during the same study

period (Boyette, unpubl. data). Prey selectivity in plume water masses was analyzed by following the methods of Manly et al. (2002) and Llopiz & Cowen (2008). Consumed prey were compared with the prey available in the environment such that:

$$w_i = o_i/\pi_i$$

where o_i is the proportion of prey type i consumed and π_i is the proportion in the environment. Values >1 indicate selection for a prey type while values <1 indicate selection against a prey type. Selection ratios are near 1 when consumed proportions reflect those of the environment. Confidence intervals (Bonferroni-adjusted) used:

$$SE(w_i) = \sqrt{\left[\frac{o_i(1 - o_i)}{u_+ \pi_i^2}\right]}$$

where u_+ is the total number of consumed prey items. Significant selection for or against a prey type was shown by the confidence intervals not overlapping with 1. Analyses were performed for the dominant prey of sand seatrout larvae (i.e., calanoid, harpacticoid, cyclopoid, and poecilostomatoid copepods, nauplii, and dinoflagellates). Selectivity analysis was not conducted on striped anchovy larvae because too few prey items were found in their guts (see Results). Selectivity values were calculated for individual samples by pooling consumed prey by all seatrout larvae from each sample. This selection ratio was used because of its simplistic statistical design; however, it should be noted that confidence intervals can be questionable when ingested prey are $n < 5$ in any category (Manly et al. 2002).

3.3 Results

3.3.1 Ichthyoplankton concentrations and community composition

A total of 2,903 fish larvae captured over the study period could be identified to family. The total concentrations of fish larvae (individuals m^{-3}) did not vary statistically between plume (0.489 ind. m^{-3}) and shelf water (0.701 ind. m^{-3}) masses within the study region (Mann-Whitney U -test, $p=0.1266$). Although larvae of 14 different families were collected, most occurred in

very low densities or were patchy in their distributions throughout our study region (Fig. 3.2). However, the families Engraulidae and Sciaenidae comprised 74.4% and 23.9% of the total fish larvae, respectively, with striped anchovy (*Anchoa hepsetus*) and sand seatrout (*Cynoscion arenarius*) dominating their respective families. In total, 372 striped anchovy and 475 sand seatrout were collected during the study (Table S.3.2). Larval concentrations as sampled by BIONESS net tows did not differ significantly between water masses for either species (Mann-Whitney *U*-tests: $p > 0.05$).

3.3.2 Zooplankton concentrations and community composition

The total density of zooplankton (log-transformed Welch's *t*-test: $p = 0.052$) as well as the most common prey (copepods) did not differ between plume and shelf stations (log-transformed Welch's *t*-test: $p = 0.431$). The zooplankton community consisted of 18 taxa at plume stations and 23 taxa at shelf stations (Fig. 3.3). In the plume stations, calanoid copepods, chaetognaths, cyclopoid copepods, and appendicularians dominated the zooplankton community, while calanoid copepods, mysids, and known larval fish predators such as chaetognaths, siphonophores, polychaetes, salps, and doliolids were most abundant at the shelf station. The microplankton (20-200 μm) community throughout the Mobile Bay nearshore region was comprised primarily of diatoms, ciliates, and dinoflagellates (e.g., proroctroid, dinophysoid, and gymnodinoid functional groups (Boyette, unpubl. data).

3.3.3 Predator-prey relationships

Spearman correlation coefficients were used to calculate the spatial overlap of potential prey (e.g., copepods) and predator (e.g., gelatinous zooplankton) groups using *in situ* ISIS-imagery from three different transects sampled between April 9-11, 2016 (see Chapter 2). The first ISIS transect sampled a highly stratified water column, the majority of which was not subjected to the direct flow of the plume. During these stratified conditions, fish larvae were positively correlated with their copepod prey in shelf waters (Spearman rank correlation coefficient = 0.146, $p < 0.001$) but not in plume waters. On the night of April 9-10, when conditions were still stratified but the plume extended deeper into the water column, fish

larvae were positively correlated with calanoid copepods in both plume and shelf water masses (Spearman rank correlation coefficient = 0.222, $p < 0.001$; 0.165, $p < 0.001$, respectively). During the highly mixed transect (night of April 10-11), however, fish larvae were not significantly correlated with their copepod prey.

Co-occurrence of fish larvae with potential gelatinous predators in each water mass was also inversely related to river discharge. Fish larvae overlapped spatially with ctenophores, hydromedusae, and siphonophores in the shelf portion of the highly stratified region on April 9 (Spearman rank correlation coefficient = 0.255, $p < 0.001$; 0.376, $p < 0.001$; 0.276, $p < 0.001$, respectively), but only co-occurred with ctenophores and hydromedusae in the plume portion (Spearman rank correlation coefficient = 0.314, $p < 0.001$; 0.355, $p < 0.001$, respectively). As the plume peaked at its highest discharge rate of the whole year, fish larvae did not significantly spatially overlap with any of their gelatinous zooplankton predators in either plume or shelf water masses ($p > 0.01$).

3.3.4 Size and growth analysis

Both striped anchovy and sand seatrout showed variable size and age distributions between water masses. Striped anchovy larvae ranged in size from 7 to 21 mm SL and were 15 to 47 d old. Sand seatrout larvae were 1 - 7 mm, SL and were 4 - 21 d old. Size and age frequency distributions revealed that relatively larger (>15 mm) and older (>37 d) anchovy larvae and seatrout larvae (>3.5 mm and >16 d) larvae were present in shelf waters but absent from plume waters (Fig. 3.4). Recent growth was used to analyze the potential effects of residence in different environmental conditions on growth rate over the last few days prior to collection. Detrended recent growth (DRG) during the last three full days of life of both striped anchovy and sand seatrout was significantly lower (ANCOVA: $p = 0.033$ and $p = 0.017$, respectively) in plume waters than in shelf water masses (Fig. 3.5). Temperature was not significantly correlated with recent growth for either fish species ($p = 0.416$ and $p = 0.158$, respectively).

Daily growth as measured by mean otolith increment width (MIW) varied between water masses for both species of fish (Fig. 3.6). MIW for striped anchovy during the first 3

weeks of larval life did not vary between water masses but began diverging at day 25 and were significantly higher on day 27 (One-way ANOVA: $p = 0.045$) in fish captured from shelf waters. Small sample sizes of older plume fish precluded testing the continuation of this trend. Similarly, MIW in sand seatrout did not vary significantly during the first 5 days of larval life but diverged at days 6-10 (One-way ANOVA: $p < 0.020$), with larvae captured in shelf waters exhibiting significantly faster daily growth than those from plume waters. Based on these data, significantly different growth trajectories began at ~6 days of life of seatrout larvae and ~25 days of life in anchovy larvae.

3.3.5 Morphometric condition analysis

Among the focal specimens collected, 106 striped anchovy and 182 sand seatrout met the criteria for morphometric condition analyses (Table S.3.2). The NMS ordination performed on the residuals of the five linear body dimensions of striped anchovy resulted in a 2-dimensional solution that explained 91.2% of the variation in the larval morphometric measurements (final stress = 13.70948 and instability < 0.000001 after 107 iterations of real data). Axis 1 explained 71.8% of the variation in larval body shape while Axis 2 explained an additional 19.4%. A similar NMS ordination on the residuals of six body dimensions of sand seatrout larvae settled on a 2-dimensional solution that explained 96.2% of the variation in the larval morphometric measurements (final stress = 9.98360 and instability < 0.000001 after 65 iterations of real data). Axis 1 explained 88.3% and Axis 2 explained 7.8% of the data.

For both species of fish, Axis 1 explained most of the variation in body shape. Axis 1 scores were strongly and positively correlated with all body dimensions (Table 3.1) and therefore served as a suitable proxy for larval body condition. Axis 1 scores differed based on the type of water mass in which larvae were collected (Fig. 3.7): scores were significantly lower for larvae from plume water masses than for those from shelf waters (anchovy: Mann-Whitney U -tests, $p = 1.278e-10$; seatrout: Mann-Whitney U -test, $p = 3.017e-16$). When the size-truncated (10-16 mm SL) striped anchovy larvae ($n=82$) and size-truncated (2-4 mm SL) sand seatrout larvae were analyzed ($n=171$), results were the same (Mann-Whitney U -test, $p = 4.167e-10$; $p < 2.2 e-16$, respectively).

3.3.6 Diet analysis

Striped anchovy:

A total of 166 striped anchovy larvae were dissected for diet analyses yet the vast majority (~93%) had empty guts (only 13 total prey items were found). This is not surprising since larval fishes are widely assumed to do the majority of their feeding during daylight hours, and our shelf station was sampled only at night. Thus the following results are included only for completion. The most common prey of striped anchovy were calanoid copepods (n=6), poecilostomatoid copepods (n=2), and unidentified eggs (n=2; Table 3.2). Striped anchovy diets (Fig. 3.8) and feeding incidences (prey items/fish) did not differ significantly between water masses (mean \pm SE: Plume 1.4 ± 0.40 ; Shelf 1.4 ± 0.245 , Welch's test: $p = 1$). Schoener's index showed a low degree of dietary overlap between anchovy larvae captured at plume and shelf stations (SI=28.6); however, it is important to note the small sample sizes. Calanoid copepods were the most abundant prey item in the stomachs of anchovy larvae in both plumes (n=2) and shelf waters (n=4), however the %FO and %N of calanoids were greatest in shelf waters, comprising 66.7% of prey items found (Table 3.2). No selectivity analyses were performed due to few feeding incidences.

Sand seatrout:

A total of 201 different prey items were found in the stomachs of 172 larval sand seatrout. Consistent identification to lower taxonomic levels proved to be difficult due to the small size of the seatrout larvae (~2-3 mm in length), so prey were grouped at higher levels for analyses. The most common prey items were dinoflagellates (n=50) followed by unidentified copepods (n=45), unidentified zooplankton (n=26), calanoid copepods (n=24), and nauplii (n=22; Table 3.3). Schoener's index showed a slight dietary overlap between the diets of seatrout larvae captured from the two water masses (SI=43.6), despite shelf larvae consuming much less prey overall (due to nighttime sampling). Significantly higher feeding incidences (prey items/fish) were observed in larvae captured at plume stations (mean \pm SE: Plume 3.48 ± 0.427 ; Shelf 1.5 ± 0.267 , Welch's test: $p = 6.697e-05$); however, this could be a product of reduced

larval feeding at night rather than a product of different prey fields. Copepods ($n=87$, $\%N=47.3\%$) and dinoflagellates ($n=47$, $\%N=25.5\%$) were the dominant prey items in the stomachs of seatrout larvae in plume waters (Table 3.3). Calanoid copepods, of which *Acartia* spp. was the main taxa, were the dominant prey item in shelf waters ($n=7$), comprising 41.2% of prey items found. While the sizes of ingested calanoid copepods and dinoflagellates did not differ significantly between water masses (Mann-Whitney U -tests: $p = 0.622$ and 0.386 , respectively), all ingested copepods combined were 0.15 mm longer on average in shelf seatrouts than those consumed by plume seatrouts (Welch's test: $p = 0.008$). Although larval seatrout diets appeared relatively similar between plume and shelf stations, it should be noted that immediately prior to their collection plume seatrouts were generally eating smaller prey items (e.g., dinoflagellates, nauplii, and small copepods) than their shelf counterparts (Fig. 3.9). Of the prey consumed, calanoid copepods and nauplii appear to have been consumed by seatrout in greater proportions than were available in the plankton, while dinoflagellates were selected against and consumed in far smaller proportions than what was environmentally available (Table 3.4).

3.4 Discussion

Larval fishes must capture sufficient prey and avoid predation to grow, survive, and successfully recruit to juvenile and adult populations. Here we demonstrate that larval fish encounter with dynamic, turbulent, and low salinity plumes exiting the mouth of Mobile Bay negatively impacts two important indicators of larval fitness; growth and condition. Otolith microstructure analyses revealed that recent growth during the last few days of life of both larval striped anchovies and larval sand seatrout was significantly lower in low salinity, turbulent plume waters than the highly-stratified shelf waters. Daily growth analyses offered insights into the timing of larval entrainment in water masses, with plume-resident seatrouts showing a slower growth rate than their shelf counterparts early on in their lifespans, while plume-resident anchovies began growing slower much later on in their lifespans than their shelf conspecifics. These diverging growth trajectories may be indicative of early entrainment within a plume water mass. Based on these data, it is possible that once entrained within a plume,

larvae are retained within that water mass. If regular exchange between the two physical environments was occurring, daily growth trajectories would likely have been more similar throughout the lifespan of the larvae. Even if there is some larval movement between water masses in this dynamic area, these data indicate that growth is reduced in plume-captured fish. In other words, fish larvae that spent more time in well-mixed, low salinity water grew significantly slower than fish that spent more time in highly-stratified, high salinity conditions. Furthermore, both species captured from plume waters were in poorer morphometric condition (e.g., skinnier at length) than their shelf counterparts. Together these results suggest that larval survival is affected by plume dynamics and that there are biological consequences to these encounters. In general, fast-growing fish larvae are of higher condition, accumulating more lipids and reaching a minimum condition necessary for metamorphosis sooner than their slower growing counterparts (Searcy & Sponaugle 2000). Slower-growing, lower condition larvae in low salinity plume waters are likely more vulnerable to predation and must also remain in this stage for a longer period, further increasing their vulnerability to predation and hence, suffering a higher mortality rate (stage duration hypothesis; (Anderson 1988; Cushing 1990). By lengthening the duration of the small and vulnerable larval stage, encounter with low salinity plume waters likely confers a survival disadvantage.

These findings are inconsistent with a few studies on the nearby Mississippi River plume indicating that plume-associated larval fishes had fitness and growth-rate advantages over those from nearby shelf waters (Grimes & Lang 1992; Lang et al. 1994; Rissik & Suthers 1996; Govoni 1997). However, other studies found either no difference in growth rates or decreased growth of some larval and juvenile fish species in relation to high river discharge (e.g., DeVries et al. 1990). Growth and survival of juvenile gulf menhaden in an estuarine nursery area west of the Mississippi Delta was found to be inversely related to river discharge (Deegan 1990). Similarly, after the opening of the Bonnet Carré Spillway (a flood control structure in the Mississippi River) diverted freshwater into the Mississippi Bight, larval gulf menhaden from the from higher turbidity, lower salinity water masses in the highly freshwater-influenced Chandeleur Sound region had significantly lower recent growth and poorer condition than larvae captured in the eastern Mississippi Bight (Hoover 2018). Hernandez et al. (2016) found

that high river discharge was strongly and negatively correlated with poorer body condition and slower growth. Plume-resident striped anchovy (Day 1993), little tunny (Allman & Grimes 1998), Spanish and king mackerel (Grimes and DeVries, unpubl. data) all displayed instantaneous mortality rates that were higher in the vicinity of the Mississippi river plume. The authors attribute this higher mortality to greater abundances of larval predators within the plume region.

Environmental drivers of larval fish fitness

Exposure to unfavorable environmental conditions could account for these growth and condition differences between plume and shelf larval fishes. The four net-sampled plume stations were all either within the direct flow of the plume or in the path of its associated currents as it was advected offshore and to the east on April 8-10. Therefore, plume-entrained fish larvae were not only exposed to low salinities but were also subjected to elevated currents and turbulence. In an open ocean system, reef fish larvae that encountered low salinity North Brazil Current rings for at least 7 d experienced slower growth rates than those that did not encounter these features (Sponaugle & Pinkard 2004). The significant negative relationship between salinity and larval growth and condition in the present study is noteworthy but given the eurythermal and euryhaline nature of both striped anchovy and sand seatrout, it is likely that other physical and biological factors are more directly associated with reduced larval fitness. For instance, an 8 unit drop in salinity signaled the influx of plume water onto the Alabama continental shelf, yet field studies in the northern Gulf of Mexico have observed larvae of both species of larvae to inhabit a wide range of salinities (sand seatrout: 0-30 salinity; Warren & Sutter 1982 and striped anchovy: 0.3-44 salinity; Roessler 1970; Tarver & Savoie 1976). Temperature has been shown to heavily impact growth rates of fish larvae (Houde 1989), however the higher growth observed in shelf-captured larvae was likely not temperature-related as there was no significant difference between the mean temperature of the plume (20.2°C) and shelf stations (20.4°C). Striped anchovy larvae have previously been collected from waters ranging from 15.0° to 34.9°C (Perret 1971; Tarver & Savoie 1976) and

sand seatrout larvae have been found to be abundant in water temperatures between 20-30°C (Warren & Sutter 1982).

Environmental drivers of zooplankton concentrations

Instead it is more likely that the ensuing regimes of wind-stress, turbulent mixing, advection processes, and physical convergence that occur with the passage of freshwater pulses out of Mobile Bay alters or disrupts access to the prey field, resulting in a poorer feeding environment for fish larvae (Chapter 2). Zooplankton concentrations from the BIONESS samples did not differ significantly between water masses, suggesting that larval fitness was unrelated to prey supply. However, the temporal mismatch of net sampling (shelf stations at night and plume stations during daylight) and the fact that only zooplankton net samples collected within the upper 10 m of the water column were analyzed (to standardize for depth), indicate that these data may not be representative of the actual prey supply. For instance, any observed differences between the water masses could be in part due to diel vertical migration (DVM) out of the sampling range and cannot be solely attributed to forcing by the physical environment. The much higher-resolution ISIS imagery (Chapter 2) synoptically sampled the prey and predator field throughout the entire water column in roughly the same locations and over the same time period as our net stations. This overlapping sampling design, in conjunction with diet composition data of our focal species, provides a more accurate comparison of prey availability and feeding success between plume and shelf waters.

Mobile Bay plume discharge is highly influenced by ambient circulation and wind-stress, and over the 3-d flood event caused major shifts in the physical structuring of the water column, nutrient input, and planktonic distributions (Chapter 2). It has been hypothesized that fish larvae in the vicinity of a discharge plume can prey on potentially rich food resources and consume a superior diet, grow faster, and thus experience a shorter stage duration, likely leading to higher rates of survival (McNeil & Grimes 1995). On April 9, we sampled the shelf station for larval fishes and zooplankton with BIONESS nets ~7 hrs before towing ISIS through the same region, allowing for comparisons between the net-collected larval fishes and the ISIS-imaged copepod prey and predator data. While this shelf station was nearshore and clearly

“plume-influenced” as indicated by a very shallow (<2 m deep) low-salinity lens, it was not subjected to the direct flow, currents, and turbulence of the Mobile Bay plume and thus fish larvae were considered “shelf.” Low wind-stress and a highly stratified water column acted in conjunction with plume-edge effects (e.g., hydrodynamic convergence and upwelling) to facilitate dense aggregations of larval fishes, their copepod prey, and gelatinous predators (e.g., ctenophores, hydromedusae, and siphonophores) at this shelf station. The high biological production in this region, which was located ~15 km west of Main Pass and out of the direct flow and low salinities of the Mobile Bay plume, suggests that the observed faster larval fish growth and higher condition could be attributed to this greater prey supply. For instance, calanoid copepods, a major prey item of both anchovy and seatrout larvae in this study, were observed in the ISIS data to be highly concentrated throughout the study region during the same time period (April 9) that the shelf station was sampled by BIONESS. Zooplankton in the central and east side of the transect (where the plume stations were sampled) were exposed to both turbulent mixing and advective processes, which likely contributed to dispersive losses.

As the magnitude of river discharge increased over the next 2 d and wind-forced downwelling pushed the halocline deeper and mixed the water column, calanoid copepods greatly decreased in overall density and became patchier in their distributions. Small, poor-swimming zooplankton were likely dispersed offshore and out of our sample transect as the plume velocity and discharge rate (m^3s^{-1}) increased to its peak flow of the entire year ($\sim 6,000 \text{ m}^3\text{s}^{-1}$) on the night of April 10, 2016, rivaling the much larger Columbia River system in average flow rate ($5,890 \text{ m}^3\text{s}^{-1}$; Lutz et al. 1975). Additionally, fish larvae, which were positively correlated with their copepod prey during stratified conditions, were no longer correlated with copepods when the plume was at its peak flow. Therefore, the effect of changing oceanographic conditions on larval prey supply could be partly responsible for the observed differences in growth and condition.

Access to prey access in plume-influenced environments

In addition to potentially reduced prey supply in turbulent plume waters, plume-entrained larvae may experience diminished prey-capture abilities due to the reduction in

visibility that occurs where higher levels of primary and secondary production, suspended sediments, and turbulence exist. Mobile Bay plume water is heavily laden with suspended solids and chlorophyll (Zhao et al. 2011), two properties that scatter and absorb light, reducing larval fish vision and prey capture abilities (Chesney 1989). The high turbulence and turbidity measured at the stations directly within the flow of the plume likely impaired the ability of fish larvae there to effectively capture prey, similar to what has been observed in experimental studies (Barrett et al. 1992; Salonen et al. 2009). Small-scale turbulence induced by wind-mixing may enhance encounter rates between fish larvae and their prey, especially at low prey concentrations (Rothschild & Osborn 1988; MacKenzie & Leggett 1991; Kristiansen et al. 2014). However, very high turbulence levels could be detrimental for prey capture success if larval reaction times are too slow to respond to fast-moving prey passing through their visual fields (Kjørboe & Saiz 1995). Experimental studies predict that herring larvae (Munk & Kjørboe 1985) and cod larvae (MacKenzie et al. 1994) experience declines in capture success at very high turbulence intensities ($\epsilon > 10^{-1} \text{ cm}^2 \text{ s}^{-3}$). During our study, fish larvae in proximity to the Mobile Bay river plume experienced turbulent intensities that consistently exceeded this threshold, reaching $\epsilon = 10^1 \text{ cm}^2 \text{ s}^{-3}$ during the high-discharge plume regime sampled on April 10-11. Such high levels of turbulence accompanying strong river pulses into the Mississippi Bight have detrimental implications for capture efficiency and feeding success of fish larvae in this region, which could easily account for the reduced growth and condition of our plume fish larvae.

Feeding success in plume-influenced environments

Diet analyses of plume-collected larvae provided further insights into the observed growth and condition patterns. However, due to inconsistent BIONESS net sampling times among stations wherein the shelf station was sampled at night while the plume stations were all sampled during daylight and the observation that 93% of anchovy guts were empty, no useful diet data are available for anchovy larvae and data are inconclusive for striped anchovies. Most larval fishes are known to feed in daylight hours, then cease or greatly reduce feeding during the hours of darkness (Canino & Bailey 1995; Conway et al. 1998) and some species, including anchovies, are known to rapidly evacuate their gut contents (Theilacker

1987). While a robust comparison of larval diets between water masses is not possible for anchovies, diets of the few anchovy larvae that contained prey were similar between plume and shelf stations. For example, fish from both water masses fed primarily on copepods (85.7% of total prey items in plumes and 66.7% in shelf waters; mostly calanoids and poecilostomatoids). Similarly, McNeil and Grimes (1995) found that striped anchovy captured from the Mississippi River plume region were primarily eating diatoms and copepods (60.4, 69.5, and 81.2% of total prey items in plume, front, and shelf samples, respectively). Striped anchovy larvae captured from within Mississippi River plume waters were also found to be feeding more frequently on dinoflagellates than their shelf conspecifics (7.14% and 3.13 %FO, respectively; McNeil & Grimes 1995).

Approximately 63% of the sand seatrout guts contained prey. The diets of sand seatrout collected during the day from plume stations were similar overall in prey composition to their night-collected shelf counterparts with copepods (e.g., calanoids, cyclopoids, poecilostomatoids, and harpacticoids) comprising 47.3% of total ingested prey items in plume-collected fish and 47.1% of prey in shelf-collected fish. However, the stomachs of plume residents contained significantly smaller prey items, such as dinoflagellates (56.0% frequency of occurrence [FO] among larvae containing food), nauplii (26.2% FO), and invertebrate eggs (3.6% FO). In comparison, only a few dinoflagellates (3.4% FO) and no nauplii nor invertebrate eggs but significantly larger copepods were found in shelf fish guts. These differential prey sizes echo the findings of Govoni and Chester (1990) who found that larval spot (*Leiostomus xanthurus*), another sciaenid, ate twice as many prey items in Mississippi River plume water than adjacent Gulf of Mexico shelf waters but the prey were smaller (e.g., tintinnids, copepod nauplii, invertebrate eggs vs. copepodites and adult copepods). Thus, while the volume and nutritional quality of prey were roughly equivalent between plume and shelf waters, suggesting no trophic advantage in either water mass, capturing greater numbers of small, lower quality prey likely entailed higher energy expenditure (Govoni & Chester 1990; Powell et al. 1990).

Selectivity analyses indicated that seatrout larvae in plume waters selected for calanoid copepods and nauplii and against dinoflagellates. Preferential feeding on calanoids and nauplii by seatrout larvae is consistent with previous literature demonstrating that calanoid copepods

are the main prey, and copepod nauplii secondary prey, of larval spotted seatrout larvae (*Cynoscion nebulosus*) in the Gulf of Mexico (Houde & Lovdal 1984; Holt & Holt 2000). However, our results indicating that dinoflagellates comprised a significant portion (56.0 %FO of stomach contents) of seatrout diets are surprising. Previous studies detected no phytoplankton in the guts of larval seatrout leading the authors to classify them as carnivorous (Flores-Coto et al. 1998; Ocana-Luna & Sanchez-Ramirez 1998). Despite this frequency, our selectivity analyses indicated that larvae selected against dinoflagellates. It is possible that the seatrout larvae in our study appeared to select against dinoflagellates because dinoflagellates are the most abundant prey taxa in the environment by five to eight orders of magnitude. Whether or not seatrout larvae are selecting dinoflagellates, they are still likely expending more energy foraging for smaller, less nutritious prey (Govoni & Chester 1990). So although the food quantity is high, net food quality is relatively low. It is also possible that the seatrout larvae were selecting for their preferred prey (e.g., copepods and nauplii), and were only incidentally ingesting the small (~0.07 mm) dinoflagellates due to their sheer abundance in plume waters. Substituting microplankton in place of larger, more nutritious copepods could potentially explain the reduced growth and condition exhibited by plume-resident larvae.

Larval fish survivorship in plume environments

There were clear differences in the size structure of fish larvae in this study, with populations of plume-collected fish showing a truncated distribution that lacked larger individuals. Size and age frequency distributions revealed that relatively larger (>15 mm) and older (>37 d) anchovy larvae and seatrout larvae (>3.5 mm and >16 d) present in shelf waters were absent from plume waters. One potential explanation for this difference in size and age structure could be higher predation and mortality within the plume. Research on striped anchovies across the Mississippi River outflow has suggested that natural mortality in the front (0.13 d^{-1}) and plume (0.23 d^{-1}) may be higher than that experienced in shelf waters (0.09 d^{-1}) (Day 1993). In our study, slower growth in plume waters may also make fish larvae more susceptible to starvation and predation mortality, and explain the absence of larger, older larvae in plume waters. However, ISIS imagery detected substantially more larval predators

(e.g., ctenophores, hydromedusae, and siphonophores) at the highly-stratified shelf station, potentially indicating that starvation mortality in plume waters is more important than losses due to predation. We note that net-collected larval fish concentrations were similar between water masses despite the fact that the composition (e.g., growth and condition) of individuals was different.

Ontogenetic vertical or horizontal migration could also explain the observed differences in larval fish size and age structure between plume and shelf waters. As an alternative hypothesis to reduced survivorship, the absence of larger and older larvae from plume waters may instead indicate that at a certain size and age (~16 mm for anchovies and 4 mm for seatrout), fish larvae may be developed enough (post-flexion) to actively avoid these unfavorable habitats. In this case, successful avoidance would entail overcoming the strong currents and turbulence inherent of plume habitats and swimming either horizontally or vertically out of or away from the unfavorable water mass, potentially by taking advantage of favorable ambient currents that reduce dispersive losses (Paris & Cowen 2004). The fact that no relatively older/larger fish larvae were captured from plume stations and that plume-entrained fish larvae were smaller and in poorer condition suggests that these larvae (many preflexion) may have been too small or poorly swimming to avoid or escape from the offshore-moving plume currents.

Published swimming speeds of striped anchovy and sand seatrout larvae are unavailable; however, swimming speeds of closely related species suggest avoidance of high discharge plume regimes by preflexion larvae is unlikely. For instance, temperate and tropical sciaenid larvae have been recorded to swim critical speeds (U_{crit}) of 1.1-20.5 cm s^{-1} (e.g., *Sciaenops ocellatus*, 3.0-23.4 mm in length; Fuiman et al. 1999) and *in situ* speeds of 2.5-8.4 cm s^{-1} (e.g., *Argyrosomus japonicus*, 3.5-14.0 mm in length; Clark et al. 2005). Temperate engraulids have routine swimming speeds of 1.0-20.0 cm s^{-1} (e.g., *Engraulis mordax*, 4.0-25.1 mm in length; Hunter 1972). In comparison, shipboard ADCP equipment during our study period recorded current velocities within the plume that exceeded 50 cm s^{-1} during peak flows. Therefore, it is unlikely that preflexion sand seatrout (<4 mm) or preflexion striped anchovies (<10 mm) would have been able to overcome the swift currents within these peak discharge

flows once entrained within the water mass. However, outside of the direct plume flow the ambient current speeds were 10-25 cm s⁻¹ and moving shoreward, which is more typical of the coastal region and could enhance retention of fish larvae in these nearshore regions so long as they were able to avoid the direct plume flow and advection offshore. In summary, it is likely that a combination of ontogenetic swimming behavior and physical forcing facilitate transport and retention of fish larvae in these river-dominated ecosystems. Fish larvae distributed near a river plume-influenced region may respond variably depending on ontogeny such that the early stages (preflexion) are entrained and advected offshore while larger larvae are able to avoid the direct plume flow yet maintain their position near highly productive estuaries by taking advantage of ambient shoreward currents (Epifanio 1988; Teodósio et al. 2016). While the underlying mechanisms (higher mortality or ontogenetic avoidance or a combination of both) remain unclear, these data indicate that high discharge river plume regimes are unfavorable habitats for larval fishes with measurable consequences for survival.

Conclusions

Definitive evidence of the link between freshwater discharge and recruitment has been elusive and no study has yet demonstrated a direct relationship between plume dynamics and year-class success (Fuiman & Werner 2002). This is in large part due to the dynamic physical and biological properties inherent of riverine plumes. We provide evidence that high-magnitude river plumes can cause environmental variability that creates an unfavorable habitat and negatively impacts the fitness and likely survival of two species of marine fish larvae. The reduced growth, condition, and trophodynamic environment we measured for fish larvae in plume waters has important implications beyond the larval stage. The magnitude of mesoscale freshwater plumes discharging onto the continental shelf in the northern Gulf of Mexico likely influences the survivorship of a large number of recruits, thereby contributing to the population dynamics of the adult populations. Thus, an improved understanding of variable coastal oceanographic conditions influencing population replenishment should inform population management. Further, shifts in the distributions and structuring of marine communities are anticipated to occur as more extreme environmental disturbances such as rising global temperatures and greater precipitation become increasingly widespread. Thus, documenting

variability in larval fish habitat use and fitness in response to dynamic river-estuarine processes is a critical first step toward understanding how future climate scenarios will affect fisheries production in river-dominated coastal ecosystems worldwide.

References

- Allman RJ & Grimes CB (1998) Growth and mortality of little tunny (*Euthynnus alletferatus*) larvae off the Mississippi River plume and Panama City, Florida. *Bull Mar Sci* 62:189–197.
- Anderson JT (1988) A review of size dependent survival during pre-recruit stages of fishes in relation to recruitment. *J Northw Atl Fish Sci* 8:55–66.
- Bakun A (2006) Fronts and eddies as key structures in the habitat of marine fish larvae: opportunity, adaptive response and competitive advantage. *Sci Mar* 70S2:105–122.
- Barger LE & Williams ML (1980) A summarization and discussion of age and growth of spot, *Leiostomus xanthurus* (Lacépède), sand seatrout, *Cynoscion arenarius* (Ginsburg), and silver seatrout, *Cynoscion nothus* (Holbrook), based on a literature review. NOAA Technical Memorandum. NMFS-SEFC-14. U.S. Department of Commerce.
- Barrett JC, Grossman GD & Rosenfeld J (1992) Turbidity-induced changes in reactive distance of rainbow trout. *Trans Am Fish Soc* 121:437–443.
- Baumann H, Pepin P, Davidson FJ., Mowbray F, Schnack D & Dower JF (2003) Reconstruction of environmental histories to investigate patterns of larval radiated shanny (*Ulvaria subbifurcata*) growth and selective survival in a large bay of Newfoundland. *ICES J Mar Sci* 60:243–258.
- Canino M & Bailey K (1995) Gut evacuation of walleye pollock larvae in response to feeding conditions. *J Fish Biol* 46:389–403.
- Carassou L, Hernandez FJ, Powers SP & Graham WM (2012) Cross-shore, seasonal, and depth-related structure of ichthyoplankton assemblages in coastal Alabama. *Trans Am Fish Soc* 141:1137–1150.
- Carreon-Martinez LB, Wellband KW, Johnson TB, Ludsin SA & Heath DD (2014) Novel molecular approach demonstrates that turbid river plumes reduce predation mortality on larval fish. *Mol Ecol* 23:5366–5377.
- Checkley, Jr. DM (1982) Selective feeding by Atlantic herring (*Clupea harengus*) larvae on zooplankton in natural assemblages. *Mar Ecol Prog Ser* 9:245–253.
- Chesney Jr EJ (1989) Estimating the food requirements of striped bass larvae *Morone saxatilis*: effects of light, turbidity and turbulence. *Mar Ecol Prog Ser* 53:191–200.

- Clark DL, Leis JM, Hay AC & Trnski T (2005) Swimming ontogeny of larvae of four temperate marine fishes. *Mar Ecol Prog Ser* 292:287–300.
- Conway DVP, Coombs SH & Smith C (1998) Feeding of anchovy *Engraulis encrasicolus* larvae in the northwestern Adriatic Sea in response to changing hydrobiological conditions. *Mar Ecol Prog Ser* 17:35–49.
- Cowan JH, Grimes CB & Shaw RF (2008) Life history, history, hysteresis, and habitat changes in Louisiana's coastal ecosystem. *Bull Mar Sci* 83:197–215.
- Cowan JH & Shaw RF (1988) The distribution, abundance, and transport of larval sciaenids collected during winter and early spring from the continental shelf waters off west Louisiana. *Fish Bull* 86:129–142.
- Cushing DH (1990) Plankton production and year-class strength in fish populations: an update of the match/mismatch hypothesis. *Adv Mar Biol* 26:249–293.
- Cushing DH (1969) The regularity of the spawning season of some fishes. *ICES J Mar Sci* 33:81–92.
- Day GR (1993) Distribution, abundance, growth and mortality of striped anchovy, *Anchoa hepsetus*, about the discharge plume of the Mississippi River. M.S. Thesis, University of West Florida, Pensacola, FL.
- Deegan L (1990) Effects of estuarine environmental conditions on population dynamics of young-of-the-year Gulf menhaden. *Mar Ecol Prog Ser* 68:195–205.
- De Robertis A, Ryer CH, Veloza A & Brodeur RD (2003) Differential effects of turbidity on prey consumption of piscivorous and planktivorous fish. *Can J Fish Aquat Sci* 60:1517–1526.
- DeVries DA, Grimes CB, Lang KL & White DB (1990) Age and growth of king and Spanish mackerel larvae and juveniles from the Gulf of Mexico and U.S. South Atlantic Bight. *Environ Biol Fishes* 29:135–143.
- Dinnel SP, Schroeder WW & Wiseman Jr. WJ (1990) Estuarine-shelf exchange using Landsat images of discharge plumes. *J Coast Res* 6:789–799.
- Epifanio CE (1988) Transport of crab larvae between estuaries and the continental shelf. In: *Coastal-Offshore Ecosystem Interactions*. Springer, Berlin, Heidelberg. pp. 291–305.
- Fisher R & Bellwood DR (2001) Effects of feeding on the sustained swimming abilities of late-

- stage larval *Amphiprion melanopus*. *Coral Reefs* 20:151–154.
- Flores-Coto C, Sánchez-Iturbe A, Zavala-García F & Warlen S (1998) Age, growth, mortality and food habits of larval *Stellifer lanceolatus*, *Cynoscion arenarius* and *Cynoscion nothus* (Pisces: Sciaenidae), from the southern Gulf of Mexico. *Estuar Coast Shelf Sci* 47:593–602.
- Franks J, Garber N & Warren J (1996) Stomach contents of juvenile cobia, *Rachycentron canadum*, from the northern Gulf of Mexico. *Fish Bull* 94:374–380.
- Fuiman LA, Smith ME & Malley VN (1999) Ontogeny of routine swimming speed and startle responses in red drum, with a comparison of responses to acoustic and visual stimuli. *J Fish Biol* 55:215–226.
- Fuiman LA & Werner RG (2002) *Fishery science: the unique contributions of early life stages*. Blackwell Scientific Publications: Oxford, UK.
- Gisbert E, Conklin D & Piedrahita R (2004) Effects of delayed first feeding on the nutritional condition and mortality of California halibut. *J Fish Biol* 64:116–132.
- Govoni JJ, Hoss DE & Colby DR (1989) The spatial distribution of larval fishes about the Mississippi River plume. *Limnol Oceanogr* 34:178–187.
- Govoni JJ & Chester AJ (1990) Diet composition of larval *Leiostomus xanthurus* in and about the Mississippi River plume. *J Plankton Res* 12:819–830.
- Govoni JJ & Grimes CB (1992) The surface accumulation of larval fishes by hydrodynamic convergence within the Mississippi River plume front. *Cont Shelf Res* 12:1265–1276.
- Govoni JJ (1997) The association of the population recruitment of gulf menhaden, *Brevoortia patronus*, with Mississippi River discharge. *J Mar Syst* 12:101–108.
- Graham WM, Pagès F & Hamner WM (2001) A physical context for gelatinous zooplankton aggregations: A review. *Hydrobiologia*. 155:199–212.
- Greer C, Shiller A, Hofmann E, Wiggert J, Warner S, Parra S, Pan C, Book J, Joung D, Dykstra S, Krause J, Dzwonkowski B, Soto I, Cambazoglu M, Deary A, Briseño-Avena C, Boyette A, Kastler J, Sanial V, Hode L, Nwankwo U, Chiaverano L, Fitzpatrick P, Lau Y, Dinniman M, Martin K, Ho P, Mojzis A, Howden S, Hernandez F, Church I, Miles T, Sponaugle S, Moum J, Arnone R, Cowen R, Jacobs G, Schofield O & Graham W (2018) Functioning of coastal river-dominated ecosystems and implications for oil spill response. *Oceanography* 31:90–103.

- Gregory RS & Northcote TG (1993) Surface, planktonic, and benthic foraging by juvenile chinook salmon (*Oncorhynchus tshawytscha*) in turbid laboratory conditions. *Can J Fish Aquat Sci* 50:223–240.
- Grimes CB & Finucane JH (1991) Spatial distribution and abundance of larval and juvenile fish, chlorophyll and macrozooplankton around the Mississippi River discharge plume, and the role of the plume in fish recruitment. *Mar Ecol Prog Ser* 75:109–119.
- Grimes CB & Kingsford MJ (1996) How do riverine plumes of different sizes influence fish larvae: Do they enhance recruitment? *Mar Freshw Res* 47:191–208.
- Grimes CB & Lang KL (1992) Distribution, abundance, growth, mortality, and spawning dates of yellowfin tuna, *Thunnus albacares*, larvae around the Mississippi River discharge plume. *Collect Vol Sci Pap ICCAT Recl Doc Sci* 38:177–194.
- Harrell, Jr, FE, with contributions from C. Dupont and many others. 2016. Hmisc: Harrell Miscellaneous. R package version 3.17-4. <http://CRAN.R-project.org/package=Hmisc>.
- Hernandez FJ, Powers SP & Graham WM (2010) Seasonal variability in ichthyoplankton abundance and assemblage composition in the northern Gulf of Mexico off Alabama. *Fish Bull* 108:193–207.
- Hernandez FJ, Filbrun JE, Fang J & Ransom JT (2016) Condition of larval red snapper (*Lutjanus campechanus*) relative to environmental variability and the Deepwater Horizon oil spill. *Environ Res Lett* 11.
- Hjort J (1914) Fluctuations in the great fisheries of northern Europe viewed in the light of biological research. *Rapp Process Réunions Cons Perm Intern Explor Mer* 20:1–228.
- Holt GJ & Holt SA (2000) Vertical distribution and the role of physical processes in the feeding dynamics of two larval sciaenids *Sciaenops ocellatus* and *Cynoscion nebulosus*. *Mar Ecol Prog Ser* 193:181–190.
- Hoover AM (2018) Influence of natural and anthropogenic environmental variability on larval fish diet, growth, and condition in the northcentral Gulf of Mexico. M.S. Thesis, University of Southern Mississippi, Hattiesburg, MS.
- Houde ED & Lovdal J (1984) Seasonality of occurrence, foods and food preferences of ichthyoplankton in Biscayne Bay, Florida. *Estuar Coast Shelf Sci* 18:403–419.

- Houde ED (1987) Fish Early Life Dynamics and Recruitment Variability. In: *American Fisheries Society Symposium*. p. 17-29.
- Houde ED (1989) Subtleties and episodes in the early life of fishes. *J Fish Biol* 35:29–38.
- Houde ED (2009) Recruitment variability. In: T. Jakobsen, B.A. Fogarty, B.A. Megrey & E. Moksness (eds). *Fish Reproductive Biology: Implications for assessment and management*. Wiley-Blackwell: West Sussex, UK. pp. 91–171.
- Hunter J (1972) Swimming and feeding behavior of larval anchovy *Engraulis mordax*. *Fish Bull* 70:821–838.
- Kjørboe T & Saiz E (1995) Planktivorous feeding in calm and turbulent environments, with emphasis on copepods. *Mar Ecol Prog Ser* 122:135–146.
- Kristiansen T, Vollset KW, Sundby S & Vikebø F (2014) Turbulence enhances feeding of larval cod at low prey densities. *ICES J Mar Sci* 71:2515–2529.
- Kruskal JB (1964) Nonmetric multidimensional scaling: A numerical method. *Psychometrika* 29:115–129.
- Lang KL, Grimes CB & Shaw RF (1994) Variations in the age and growth of yellowfin tuna larvae, *Thunnus albacares*, collected about the Mississippi River plume. *Environ Biol Fishes* 39:259–270.
- Lasker R (1975) Field criteria for survival of anchovy larvae: The relation between inshore chlorophyll maximum layers and successful first feeding. *Fish Bull* 73:453–462.
- Lasker R (1981) The role of a stable ocean in larval fish survival and subsequent recruitment. Pages 80–87 in R. Lasker, ed. *Marine fish larvae: morphology, ecology and relation to fisheries*. University of Washington Press, Seattle.
- Lecchini D, Shima J, Banaigs B & Galzin R (2005) Larval sensory abilities and mechanisms of habitat selection of a coral reef fish during settlement. *Oecologia* 143:326–334.
- Le Pape O, Chauvet F, Désaunay Y & Guérault D (2003) Relationship between interannual variations of the river plume and the extent of nursery grounds for the common sole (*Solea solea*, L.) in Vilaine Bay. Effects on recruitment variability. *J Sea Res* 50:177–185.
- Llopiz JK & Cowen RK (2008) Precocious, selective and successful feeding of larval billfishes in the oceanic Straits of Florida. *Mar Ecol Prog Ser* 358:231–244.

- Lochmann S & Ludwig G (2003) Relative triacylglycerol and morphometric measures of condition in sunshine bass fry. *North Am J Aquat* 65:191–202.
- Lochmann SE, Taggart CT, Griffin DA, Thompson KR & Maillet GL (1997) Abundance and condition of larval cod (*Gadus morhua*) at a convergent front on Western Bank, Scotian Shelf. *Can J Fish Aquat Sci* 54:1461–1479.
- Lohrenz SE, Fahnenstiel GL, Redalje DG, Lang GA, Chen X & Dagg MJ (1997) Variations in primary production of northern Gulf of Mexico continental shelf waters linked to nutrient inputs from the Mississippi river. *Mar Ecol Prog Ser* 155:45–54.
- Luo JY, Grassian B, Tang D, Irisson JO, Greer AT, Guigand CM, McClatchie S & Cowen RK (2014) Environmental drivers of the fine-scale distribution of a gelatinous zooplankton community across a mesoscale front. *Mar Ecol Prog Ser* 510:129–149.
- Lutz G, Hubbell D & Stevens H (1975) Discharge and flow distribution, Columbia River Estuary.
- MacGregor J & Houde E (1996) Onshore-offshore pattern and variability in distribution and abundance of bay anchovy *Anchoa mitchilli* eggs and larvae in Chesapeake Bay. *Mar Ecol Prog Ser* 138:15–25.
- MacKenzie BR & Leggett WC (1991) Quantifying the contribution of small-scale turbulence to the encounter rates between larval fish and their zooplankton prey: effects of wind and tide. *Mar Ecol Prog Ser* 73: 149-160.
- MacKenzie BR, Miller TJ, Cyr S & Leggett WC (1994) Evidence for a dome-shaped relationship between turbulence and larval fish ingestion rates. *Limnol Oceanogr* 39:1790–1799.
- Manly B, McDonald L, Thomas D, McDonald T & Erickson W (2002) Resource selection by animals: statistical design and analysis for field studies, 2nd edn. Kluwer Academic Publishers, Dordrecht.
- Mather PM (1976) *Computational Methods of Multivariate Analysis in Physical Geography*. 532 pp. Wiley; New York.
- McClatchie S, Cowen R, Nieto K, Greer A, Luo JY, Guigand C, Demer D, Griffith D & Rudnick D (2012) Resolution of fine biological structure including small narcomedusae across a front in the Southern California Bight. *J Geophys Res* 117:C04020.
- McCune B, Grace JB & Urban DL (2002) *Analysis of ecological communities*, Vol 28. MjM

software design, Gleneden Beach, OR.

- McManus GB & Foster CA (1998) Seasonal and fine-scale spatial variations in egg production and triacylglycerol content of the copepod *Acartia tonsa* in a river-dominated estuary and its coastal plume. *J Plankton Res* 20(4):767-785.
- McNeil CS & Grimes CB (1995) Diet and feeding ecology of striped anchovy, *Anchoa hepsetus*, along environmental gradients associated with the Mississippi River discharge plume. In: D.K. Atwood, W.F. Graham & C.B. Grimes (eds). *Nutrient-enhanced Coastal Ocean Productivity*. pp. 81–89.
- Munk P & Kiørboe T (1985) Feeding behaviour and swimming activity of larval herring (*Clupea harengus*) in relation to density of copepod nauplii. *Mar Ecol Prog Ser* 24:15-21.
- Ocana-Luna A & Sanchez-Ramirez M (1998) Feeding of sciaenid (Pisces: Sciaenidae) larvae in two coastal lagoons of the Gulf of Mexico. *Gulf Res Rep* 10:1–9.
- Pangle KL, Malinich TD, Bunnell DB, DeVries DR & Ludsin SA (2012) Context-dependent planktivory: interacting effects of turbidity and predation risk on adaptive foraging. *Ecosphere* 3:114.
- Paris CB & Cowen RK (2004) Direct evidence of a biophysical retention mechanism for coral reef fish larvae. *Limnol Oceanogr* 49:1964–1979.
- Peck MA, Huebert KB & Llopiz JK (2012) Intrinsic and extrinsic factors driving match-mismatch dynamics during the early life history of marine fishes. *Adv Ecol Res* 47:177–302.
- Perret WS (1971) Cooperative Gulf of Mexico estuarine inventory and study, Louisiana - Phase IV, Biology. Louisiana Wildlife and Fisheries Commission. pp. 31-69.
- Powell AB, Chester AJ, Govoni JJ & Warlen SM (1990) Nutritional condition of spot larvae associated with the Mississippi River plume. *Trans Am Fish Soc* 119:957–965.
- Purcell JE & Arai MN (2001) Interactions of pelagic cnidarians and ctenophores with fish: A review. *Hydrobiologia* 451:27–44.
- Ransom JT, Filbrun JE & Hernandez Jr. FJ (2016) Condition of larval Spanish mackerel *Scomberomorus maculatus* in relation to the Deepwater Horizon oil spill. *Mar Ecol Prog Ser* 558:143–152.
- Rettig J, Shuman L & McCloskey J (2006) Seasonal patterns of abundance: Do zooplankton in

- small ponds do the same thing every spring–summer? *Hydrobiologia* 556:193–207.
- Richards WJ (2005) Early stages of Atlantic fishes. CRS Press: Boca Raton, FL.
- Rissik D & Suthers IM (1996) Feeding in a larval fish assemblage: the nutritional significance of an estuarine plume front. *Mar Biol* 125:233–240.
- Robert D, Castonguay M & Fortier L (2009) Effects of preferred prey density and temperature on feeding success and recent growth in larval mackerel of the southern Gulf of St. Lawrence. *Mar Ecol Prog Ser* 377:227–237.
- Robinette HR (1985) Species profiles: Life histories and environmental requirements of coastal fishes and invertebrates (Gulf of Mexico) -- bay anchovy and striped anchovy. U.S. Fish and Wildlife Service, Division of Biological Services. FWS/OBS-82/11.14.
- Roessler MA (1970) Checklist of fishes in Buttonwood Canal, Everglades National Park, Florida, and observations on the seasonal occurrence and life histories of selected species. *Bull Mar Sci* 20:860–890.
- Rothschild BJ & Osborn TR (1988) Small-scale turbulence and plankton contact rates. *J Plankton Res* 10:465–474.
- Sabatés A & Masó M (1990) Effect of a shelf-slope front on the spatial distribution of mesopelagic fish larvae in the western Mediterranean. *Deep Sea Res Part A Oceanogr Res Pap* 37:1085–1098.
- Salonen M, Urho L & Engström-Öst J (2009) Effects of turbidity and zooplankton availability on the condition and prey selection of pike larvae. *Boreal Environ Res* 14:981–989.
- Schoener TW (1970) Nonsynchronous spatial overlap of lizards in patchy habitats. *Ecology* 5:408–418.
- Schroeder WW & Lysinger WR (1979) Hydrography and circulation in Mobile Bay. In: H.A. Loyacano & J.P. Smith (eds). *Symposium on the Natural Resources of the Mobile Bay Estuary*. U.S. Army Corps of Eng.: Mobile, AL. pp. 75–94.
- Searcy S & Sponaugle S (2000) Variable larval growth in a coral reef fish. *Mar Ecol Prog Ser* 206:213–226.
- Sponaugle S, Llopiz JK, Havel LN & Rankin TL (2009) Spatial variation in larval growth and gut fullness in a coral reef fish. *Mar Ecol Prog Ser* 383:239–249.

- Sponaugle S & Pinkard DR (2004) Impact of variable pelagic environments on natural larval growth and recruitment of the reef fish *Thalassoma bifasciatum*. *J Fish Biol* 64:34–54.
- Suthers IM (1998) Bigger? Fatter? Or is faster growth better? Considerations on condition in larval and juvenile coral-reef fish. *Austral Ecol* 23:265–273.
- Tarver JW & Savoie LR (1976) An inventory and study of the Lake Pontchartrain-Lake Maurepas estuarine complex - Phase 11, Biology. Louisiana Wildlife and Fisheries Commission, Oysters, Water Bottoms, and Seafoods Division, Tech. Bull. 19:7-99.
- Teodósio MA, Paris CB, Wolanski E & Morais P (2016) Biophysical processes leading to the ingress of temperate fish larvae into estuarine nursery areas: A review. *Estuar Coast Sci* 183:187-202.
- Theilacker GH (1987) Feeding ecology and growth energetics of larval northern anchovy, *Engraulis mordax*. *Fish Bull* 85:213–228.
- Wallace RK & Ramsey JS (1983) Reliability in measuring diet overlap. *Can J Fish Aquat Sci* 40:347–351.
- Warren JR & Sutter FC (1982) Industrial bottomfish-monitoring and assessment, p. 43-69. In: *Fishery Monitoring and Assessment Completion Report*, 1 January 1977 to 31 December 1981, Ch. II, Sec. I, Proj. No. 2-296-R, Gulf Coast Res. Lab., Ocean Springs, Mississippi.
- Zhao H, Chen Q, Walker ND, Zheng Q & Macintyre HL (2011) A study of sediment transport in a shallow estuary using MODIS imagery and particle tracking simulation. *Int J Remote Sens* 32:6653–6671.

Table 3.1. Correlations between nonmetric multidimensional scaling (NMS) axes and the five striped anchovy morphometric residuals and six sand seatrout morphometric residuals. Axes 1 and 2 explained 71.8% and 19.4% of the variation in body size among anchovy larvae, respectively, while Axes 1 and 2 explained 88.3% and 7.8% of the variation in body size among seatrout larvae, respectively.

| Striped anchovy (All fish larvae) | Axis 1 | | Axis 2 | |
|--|----------|----------|----------|-----------|
| Larval body measurement | <i>r</i> | <i>P</i> | <i>r</i> | <i>P</i> |
| Eye diameter (ED) | 0.354 | 0.000197 | -0.032 | 0.744699 |
| Head depth (HD) | 0.691 | <0.00001 | 0.471 | <0.00001 |
| Head length (HL) | 0.742 | <0.00001 | -0.607 | <0.00001 |
| Depth at pelvic fin (DPF) | 0.737 | <0.00001 | 0.427 | <0.004069 |
| Dorsal depth (DD) | 0.807 | <0.00001 | 0.145 | 0.13807 |

| Sand seatrout (All fish larvae) | Axis 1 | | Axis 2 | |
|--|----------|----------|----------|----------|
| Larval body measurement | <i>r</i> | <i>P</i> | <i>r</i> | <i>P</i> |
| Eye diameter (ED) | 0.598 | <0.00001 | -0.192 | 0.009416 |
| Lower jaw length (LJL) | 0.784 | <0.00001 | -0.224 | 0.002367 |
| Head depth (HD) | 0.885 | <0.00001 | 0.157 | 0.034294 |
| Head length (HL) | 0.846 | <0.00001 | -0.359 | <0.00001 |
| Depth at pectoral fin (DPF) | 0.801 | <0.00001 | 0.526 | <0.00001 |
| Depth at anus (DA) | 0.843 | <0.00001 | -0.152 | 0.040523 |

Table 3.2. Gut content analysis of 166 larval striped anchovy collected in April 2016 around the outflow of Mobile Bay, Alabama. %N = percent of the total prey items (n) found in that water mass; FO = frequency of occurrence; %FO = percent frequency of occurrence among larvae containing food; and n = the total number in each category.

| Prey Item | Water Masses | | | | | | | |
|-----------------------------------|--------------|-------------|----------|------------|----------|-------------|----------|------------|
| | Plume | | | | Shelf | | | |
| | n | %N | FO | %FO | n | %N | FO | %FO |
| Copepods | 6 | 85.7 | 4 | 4.3 | 4 | 66.7 | 3 | 4.1 |
| Calanoid | 2 | 28.6 | 2 | 2.2 | 4 | 66.7 | 2 | 2.7 |
| <i>Acartia spp.</i> | | | | | 1 | 16.7 | 1 | 1.4 |
| <i>Parvocalanus crassirostris</i> | 1 | 14.3 | 1 | 1.1 | | | | |
| Unidentified calanoid | 1 | 14.3 | 1 | 1.1 | 3 | 50.0 | 1 | 1.4 |
| Harpacticoid | 1 | 14.3 | 1 | 1.1 | | | | |
| <i>Euterpina acutifrons</i> | 1 | 14.3 | 1 | 1.1 | | | | |
| Poecilostomatoid | 2 | 28.6 | 1 | 1.1 | | | | |
| <i>Oncaea spp.</i> | 2 | 28.6 | 1 | 1.1 | | | | |
| Unidentified copepod | 1 | 14.3 | 1 | 1.1 | | | | |
| Unidentified zooplankton | 1 | 14.3 | 1 | 1.1 | | | | |
| Invertebrate egg | | | | | 2 | 33.3 | 2 | 2.7 |
| Total Prey | 7 | | | | 6 | | | |
| No. of Fish | 93 | | | | 73 | | | |
| No. of Empty Guts | 88 | | | | 67 | | | |

Table 3.3. Gut content analysis of 172 larval sand seatrout collected in April 2016 near the outflow of Mobile Bay, Alabama. %N = percent of the total prey items (n) found in that water mass; FO = frequency of occurrence; %FO = percent frequency of occurrence among larvae containing food; n = the total number in each category.

| Prey Item | Water Masses | | | | | | | |
|---|--------------|-------------|-----------|-------------|----------|-------------|----------|------------|
| | Plume | | | | Shelf | | | |
| | n | %N | FO | %FO | n | %N | FO | %FO |
| Appendicularian | | | | | 1 | 5.9 | 1 | 1.1 |
| Bivalve larva | | | | | 1 | 5.9 | 1 | 1.1 |
| Copepod | 87 | 47.3 | 36 | 42.9 | 8 | 47.1 | 4 | 4.5 |
| Calanoid | 15 | 9.1 | 9 | 10.7 | 7 | 41.2 | 3 | 3.4 |
| <i>Acartia</i> spp. | | | | | 5 | 29.4 | 2 | 2.3 |
| <i>Centropages</i> spp. | 2 | 1.1 | 1 | 1.2 | | | | |
| <i>Parvocalanus</i> <i>crassirostris</i> | 1 | 0.5 | 1 | 1.2 | 1 | 5.9 | 1 | 1.1 |
| Unidentified calanoid | 12 | 6.5 | 8 | 9.5 | 1 | 5.9 | 1 | 1.1 |
| Cyclopoid | 8 | 4.3 | 7 | 8.3 | | | | |
| <i>Oithona</i> spp. | 8 | 4.3 | 3 | 3.6 | | | | |
| Harpacticoid | 4 | 2.2 | 1 | 1.2 | | | | |
| <i>Euterpina acutifrons</i> | 3 | 1.6 | 3 | 3.6 | | | | |
| Unidentified harpacticoid | 1 | 0.5 | 1 | 1.2 | | | | |
| Poecilostomatoid | 8 | 4.3 | 7 | 8.3 | | | | |
| <i>Oncaea</i> spp. | 4 | 2.2 | 4 | 4.8 | | | | |
| <i>Sapphirinidae</i> spp. | 4 | 2.2 | 3 | 3.6 | | | | |
| Unidentified copepod | 45 | 24.2 | 24 | 28.6 | 1 | 5.9 | 1 | 1.1 |
| Copepod pieces | 7 | 3.8 | 1 | 1.2 | | | | |
| Dinoflagellate | 47 | 25.3 | 21 | 25.0 | 3 | 17.6 | 3 | 3.4 |
| <i>Protoperidinium</i> spp. | 8 | 4.3 | 8 | 9.5 | | | | |
| <i>Gyrodinium</i> spp. | 1 | 0.5 | 1 | 1.2 | | | | |
| <i>Prorocentrum</i> spp. | 1 | 0.5 | 1 | 1.2 | | | | |
| Unidentified dinoflagellate | 37 | 19.9 | 16 | 44.0 | 3 | 17.6 | 3 | 3.4 |
| Protist | 3 | 1.6 | 2 | 3.6 | | | | |
| Unidentified zooplankton | 22 | 11.8 | 16 | 26.2 | 4 | 23.5 | 3 | 3.4 |
| Invertebrate egg | 3 | 1.6 | 3 | 3.6 | | | | |
| Unidentified nauplii | 22 | 11.8 | 19 | 22.6 | | | | |
| Total Prey | 184 | | | | 17 | | | |
| No. of Fish | 84 | | | | 88 | | | |
| No. of Empty Guts | 31 | | | | 77 | | | |

Table 3.4. Prey selectivity analysis and environmental prey concentrations for 4 plume samples collected in April 2016. Numbers of copepods (Ca=Calanoid, Cy=Cyclopoid, P=Poecilostomatoid, and H=Harpacticoid), nauplii (N), and dinoflagellates (D) excised from larval anchovies are indicated by u_+ for each prey type. Significant selection for ($w_i > 1$) or against ($w_i < 1$) (see Eq. 1) a prey type is denoted by asterisks, all at $p < 0.05$. Calanoid copepods and nauplii were significantly selected for, while dinoflagellates were selected against.

| Sand seatrout | | Total # of prey items consumed (u_+) | | | | | | Prey selection (w_i) | | | | | | Env. Conc. (ind. m^{-3}) | | | | | |
|---------------|-----|--|-----|----|----|----|----|--------------------------|----|-------|-------|---------------|--------------|-----------------------------|----|-------|------|------|-------|
| Day | Net | uCa | uCy | uP | uH | uN | uD | Ca | Cy | P | H | N | D | Ca | Cy | P | H | N | D* |
| 4/8 | 365 | 1 | | | | 1 | 3 | 4.2e3 | | | | 3.5e5 | 0.11* | 2329.7 | 7 | 870.1 | 14.0 | 28.1 | 1.9e8 |
| 4/9 | 403 | | | 2 | | 3 | 1 | 0 | | 2.7e5 | | 3.3e6 | 0.05* | 417.6 | | 64.1 | | 7.77 | 2.7e8 |
| 4/9 | 408 | 4 | 8 | | 2 | 8 | 15 | 1.9e4 | 0 | 0 | 0 | 3.3e6* | 0.23* | 596.3 | 0 | 22.1 | 0 | 6.90 | 2.7e8 |
| 4/9 | 409 | 10 | | 6 | 2 | 10 | 28 | 1.6e4* | | 1.8e5 | 1.1e5 | 3.5e5* | 0.30* | 1295.9 | | 67.5 | 37.9 | 59.1 | 2.7e8 |

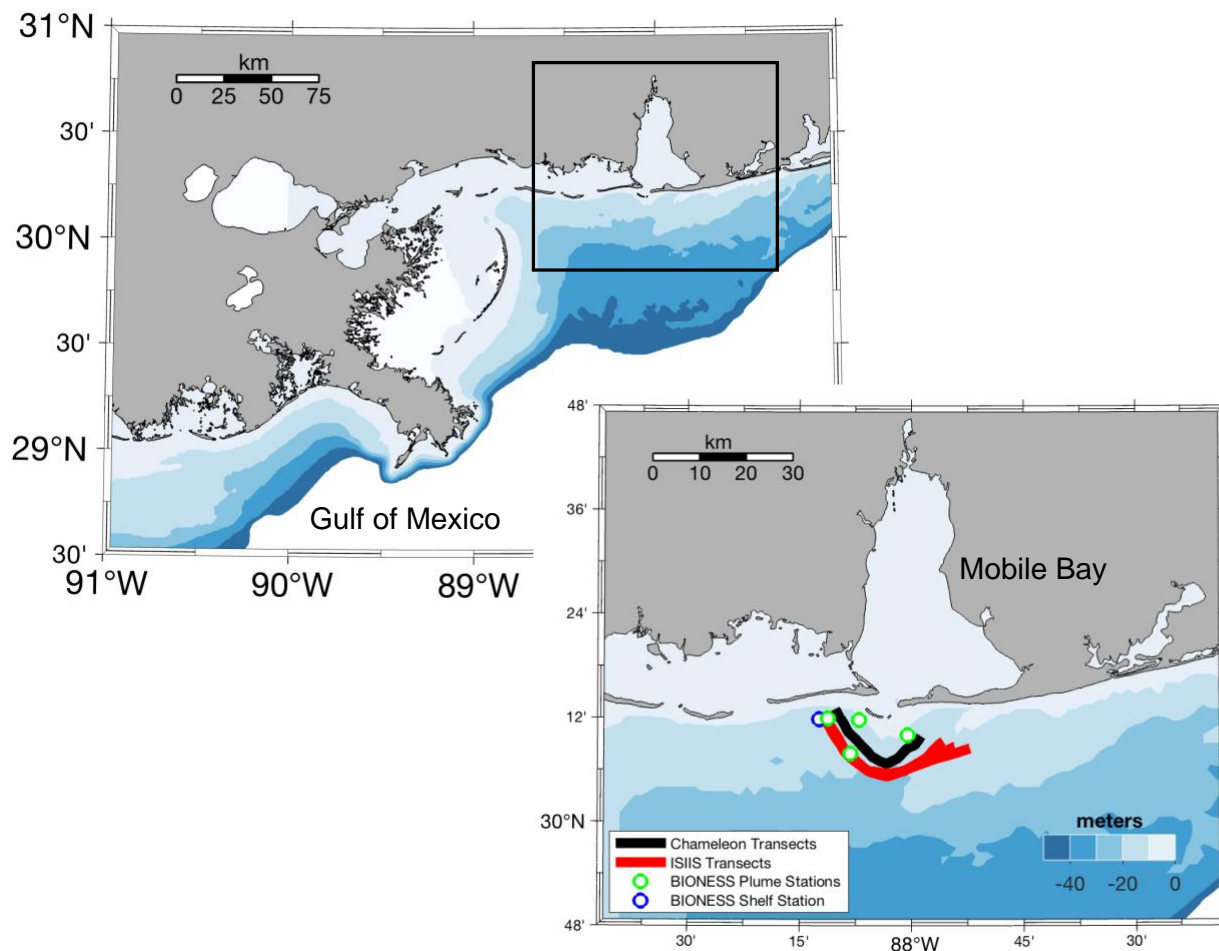


Fig. 3.1. The Mobile Bay plume outflow in the northern Gulf of Mexico was sampled for larval fishes and zooplankton during the peak flood event on April 8-11, 2016. Ichthyoplankton and zooplankton were sampled using a Chameleon microstructure profiler, an In Situ Ichthyoplankton Imaging System (ISiIS) and a Bedford Institute of Oceanography Net Environmental Sampling System (BIONESS). The ISiIS was towed in three, 20-km long arcs (red lines) through the Mobile Bay plume outflow to sample the fine-scale distributions of larval fishes and zooplankton across varying plume regimes, while the Chameleon was towed in a parallel arc ~3 km inshore to characterize the *in situ* physical properties of each plume (black lines). The BIONESS was deployed to capture fish larvae from plume (green circles; n=10 nets at 4 stations) and shelf (blue circle; n=9 nets at 1 station) water masses.

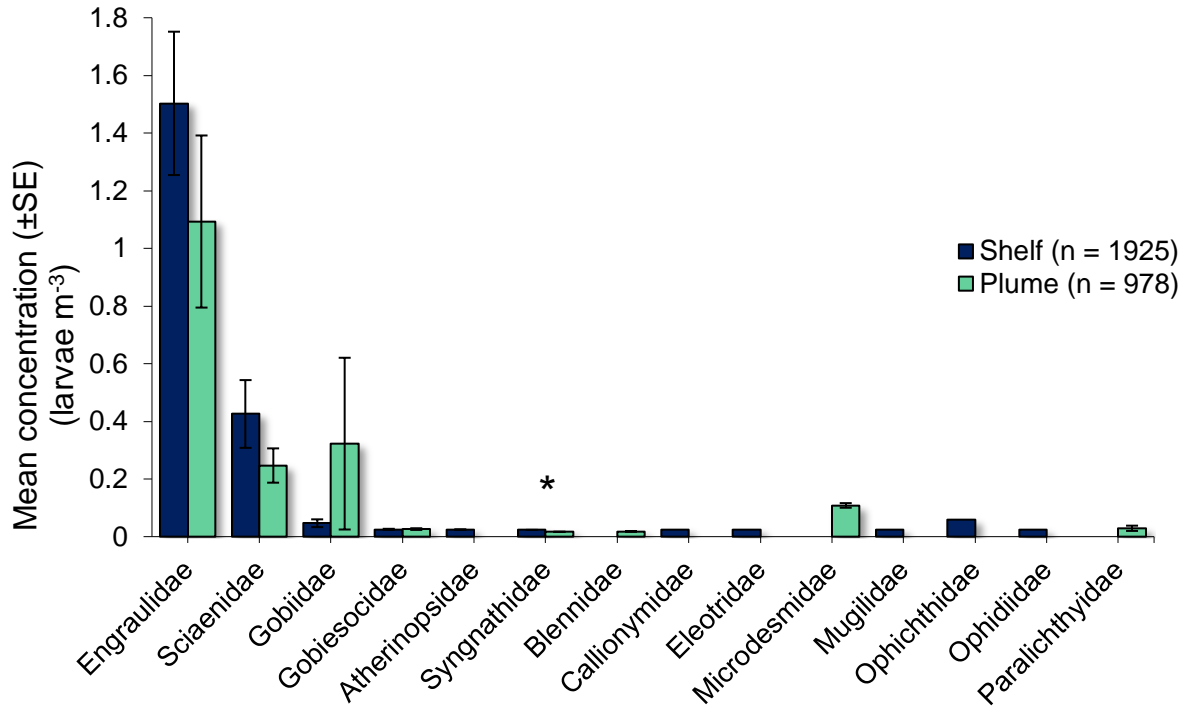


Fig. 3.2. Larval fish family concentrations (mean \pm SE) and community compositions in plume and shelf stations around the mouth of Mobile Bay, Alabama on April 8-10, 2016. A total of 8 plume and 11 shelf families were represented in the net samples. The asterisk (*) denotes families that differed significantly between water masses (Mann-Whitney U -test: $p < 0.05$).

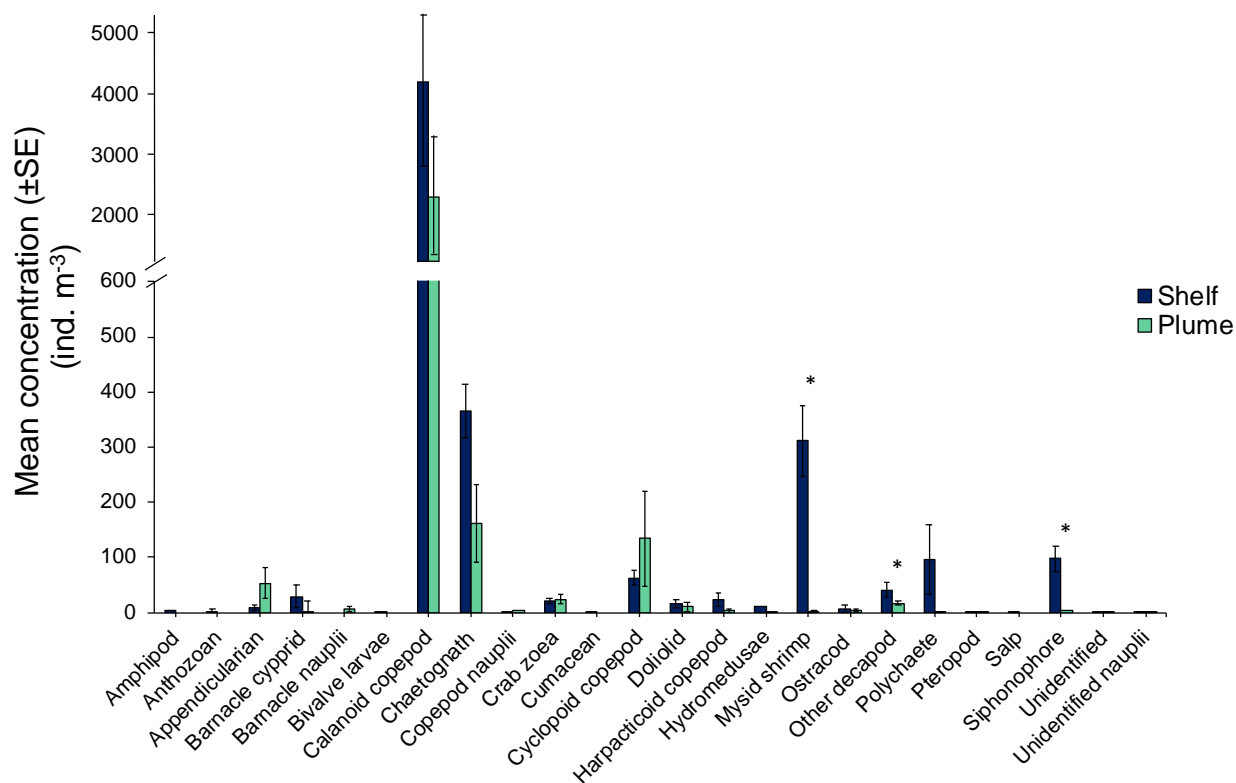


Fig. 3.3. Zooplankton concentrations (mean \pm S.E.) and community composition at plume (green) and shelf (blue) stations sampled on April 8-10, 2016 by the BIONESS in the northern Gulf of Mexico. Error bars are standard errors. Asterisks indicate significant differences (log-transformed Welch's t-test: $p < 0.05$).

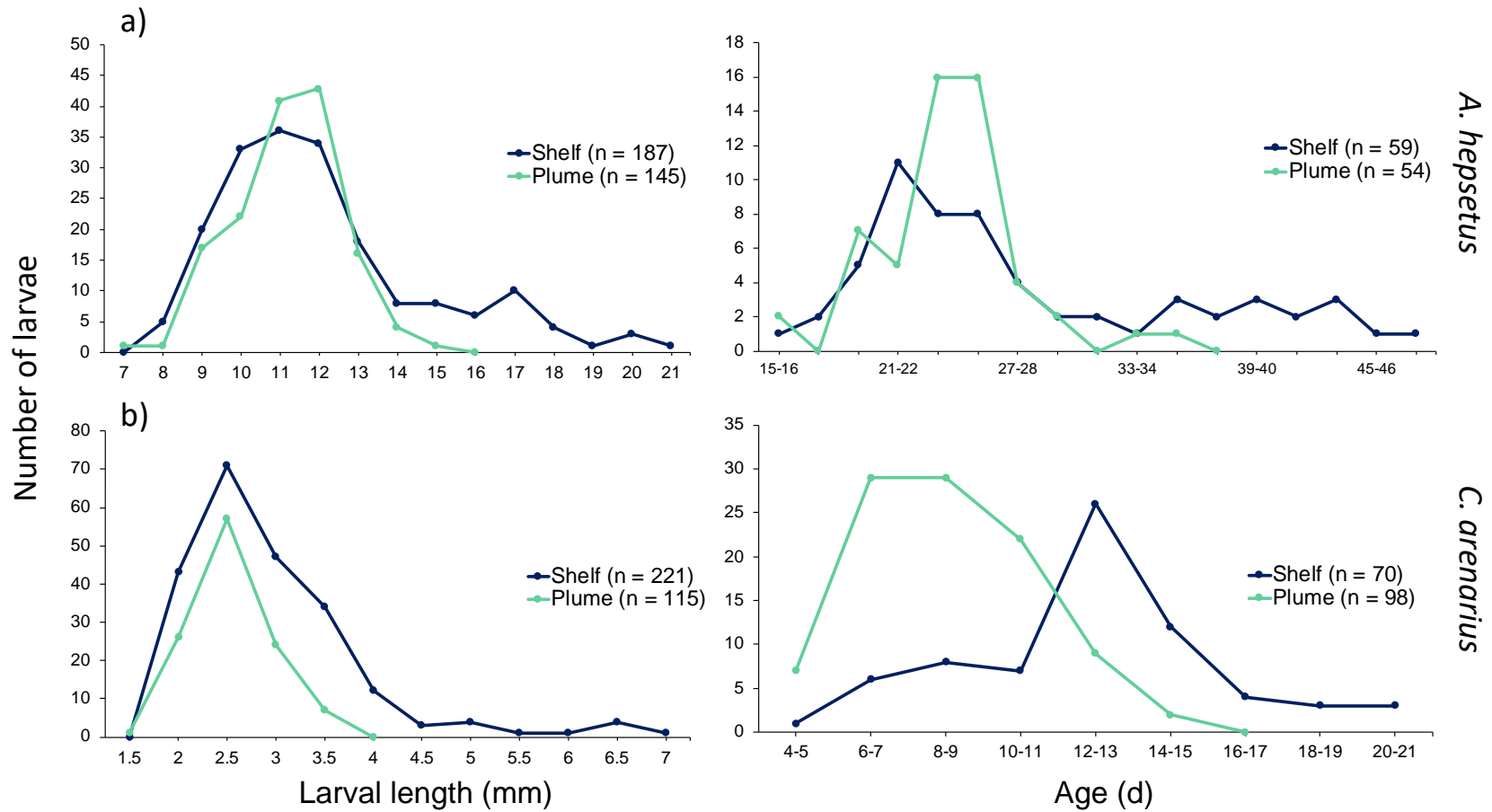


Fig. 4. Comparisons of size and age distributions between plume (green) and shelf (blue) individuals for a) striped anchovy (*Anchoa hepsetus*) and b) sand seatrout (*Cynoscion arenarius*). Note that the axes are different for each species.

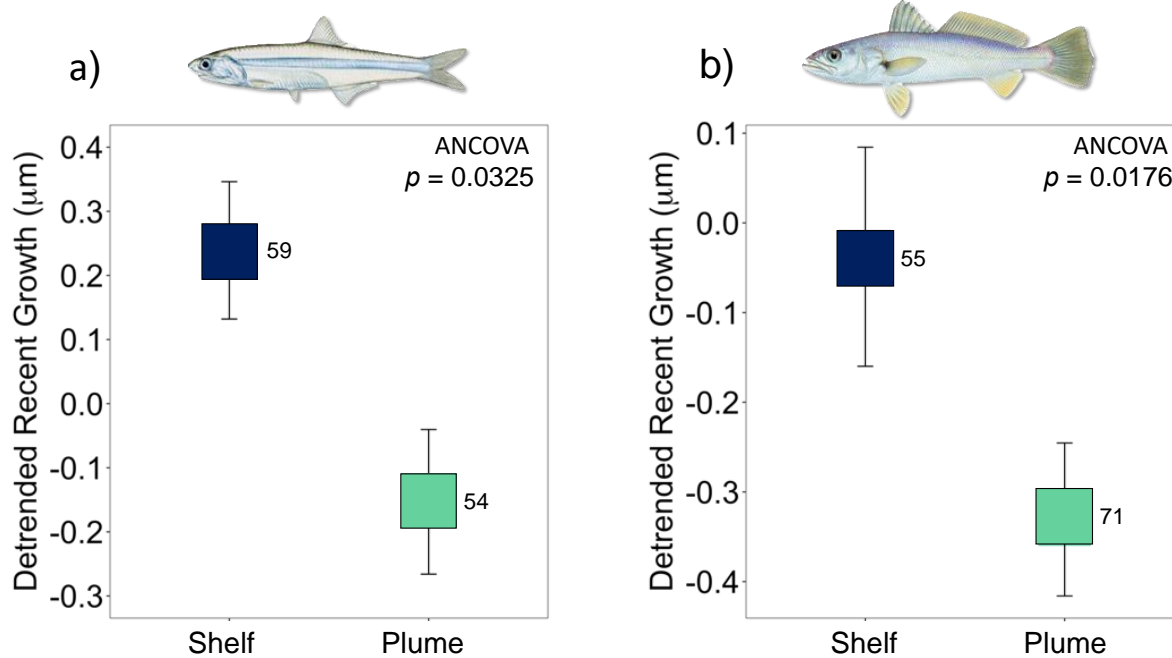


Fig. 3.5. Detrended recent growth (DRG) of the last three complete days of life prior to collection were analyzed for a) striped anchovy and b) sand seatrout larvae captured from either plume or shelf water masses. Analysis of covariance (ANCOVA) with age as a covariate was used to compare recent growth between plume and shelf habitats. Sample sizes of fish larvae are denoted next to each square. Note that y-axes differ between species.

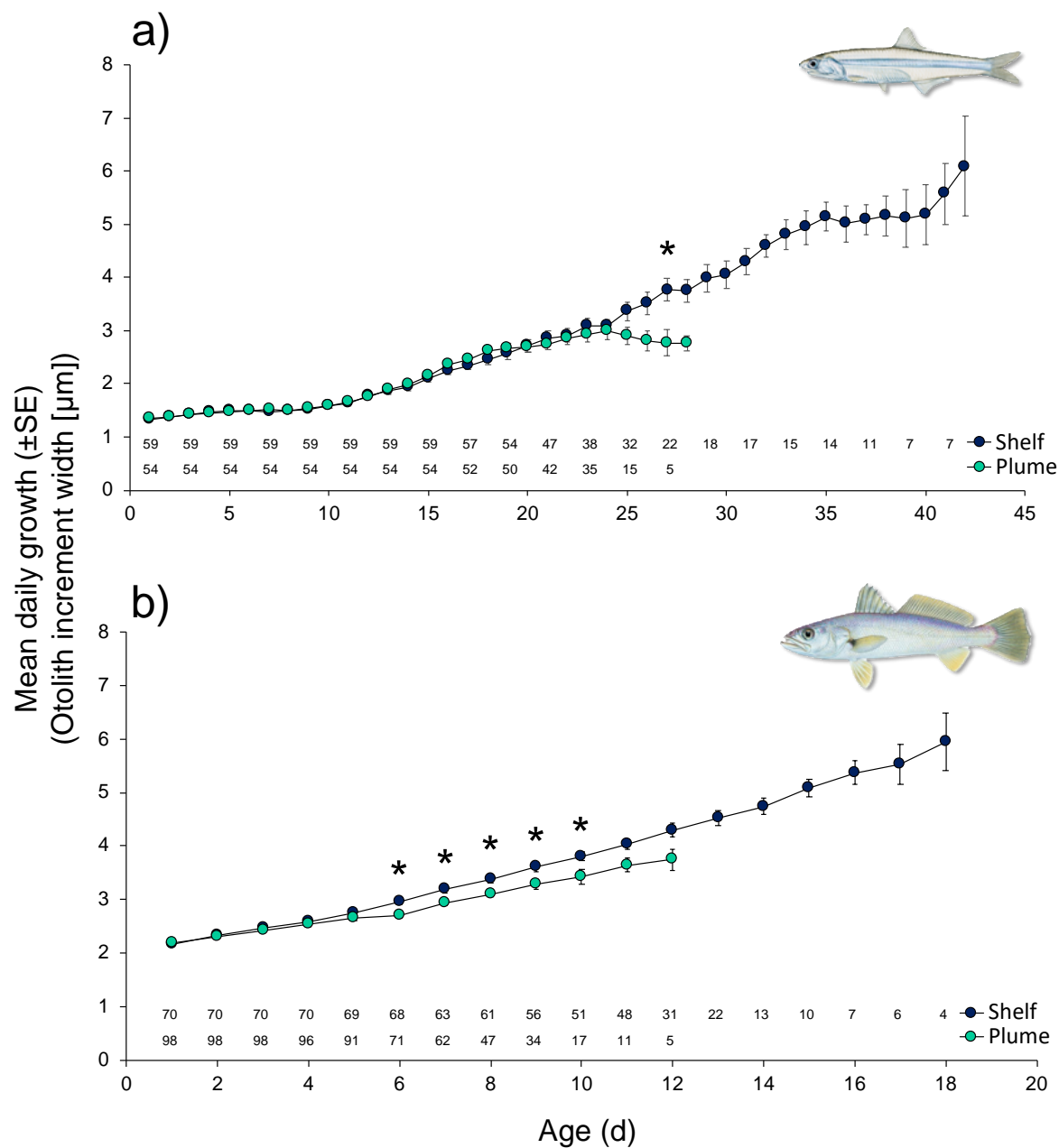


Fig. 3.6. Mean daily growth for a) striped anchovy and b) sand seatrout larvae collected from plume and shelf water masses. Mean otolith increment width (MIW) values were truncated when $n < 4$. Separate one-way ANOVA comparisons of MIW between water masses were made for each day of larval life. All days of growth tested were non-significant (ANOVA: $p > 0.05$) between water masses, except where indicated (asterisk; *A. hepsetus*: day 27, $p = 0.045$; *C. arenarius*: day 6 - 10, $p < 0.02$). Error bars are ± 1 SE. Sample sizes (n) for every other increment are indicated at the bottom of each plot

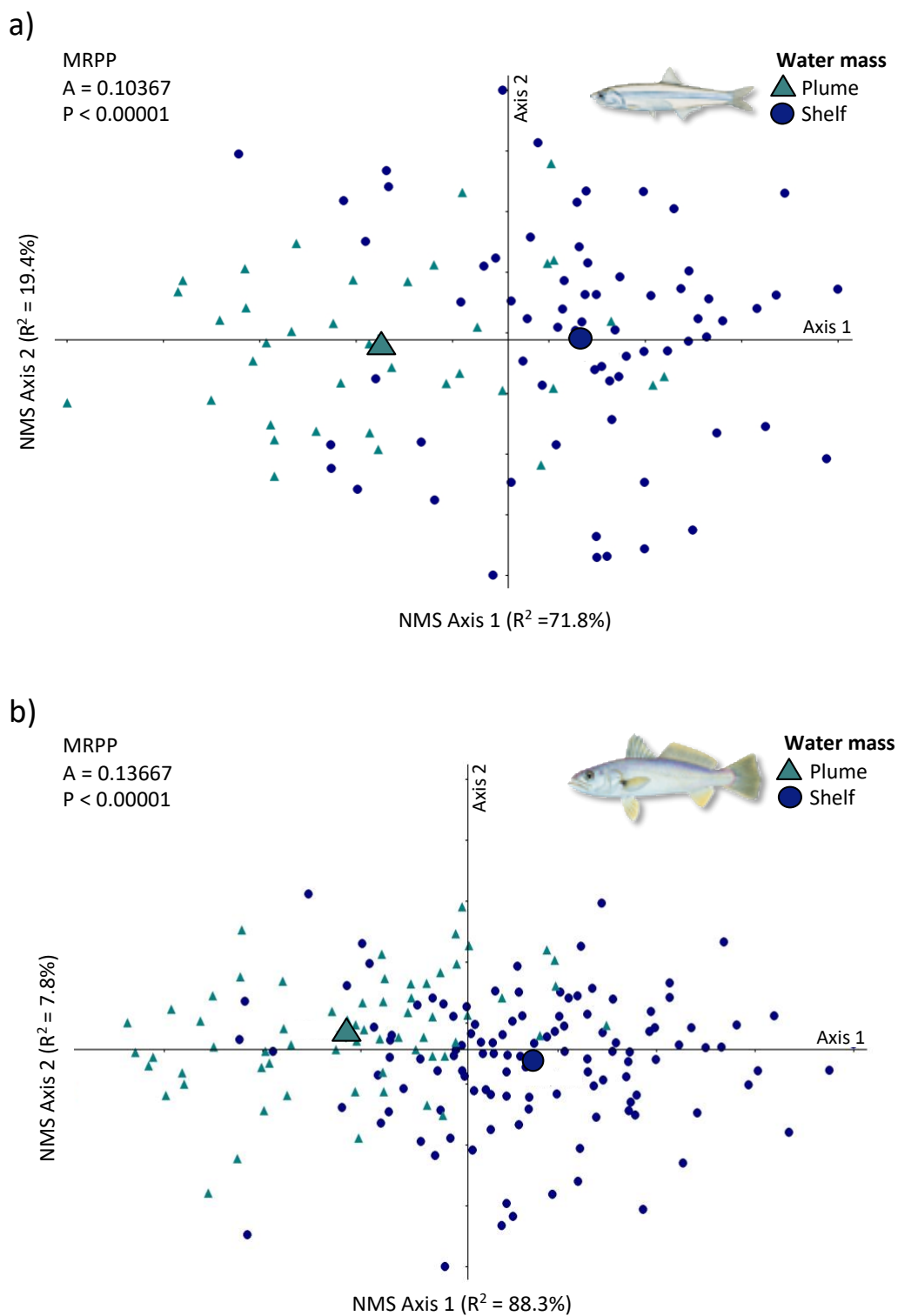


Fig. 3.7. Nonmetric multidimensional scaling (NMS) scores of a) striped anchovy and b) sand seatrout larvae grouped by the type of water mass they were collected from. Smaller shapes represent individual larvae and larger shapes represent mean values of larvae collected in plume (triangles) and shelf (circles) water masses.

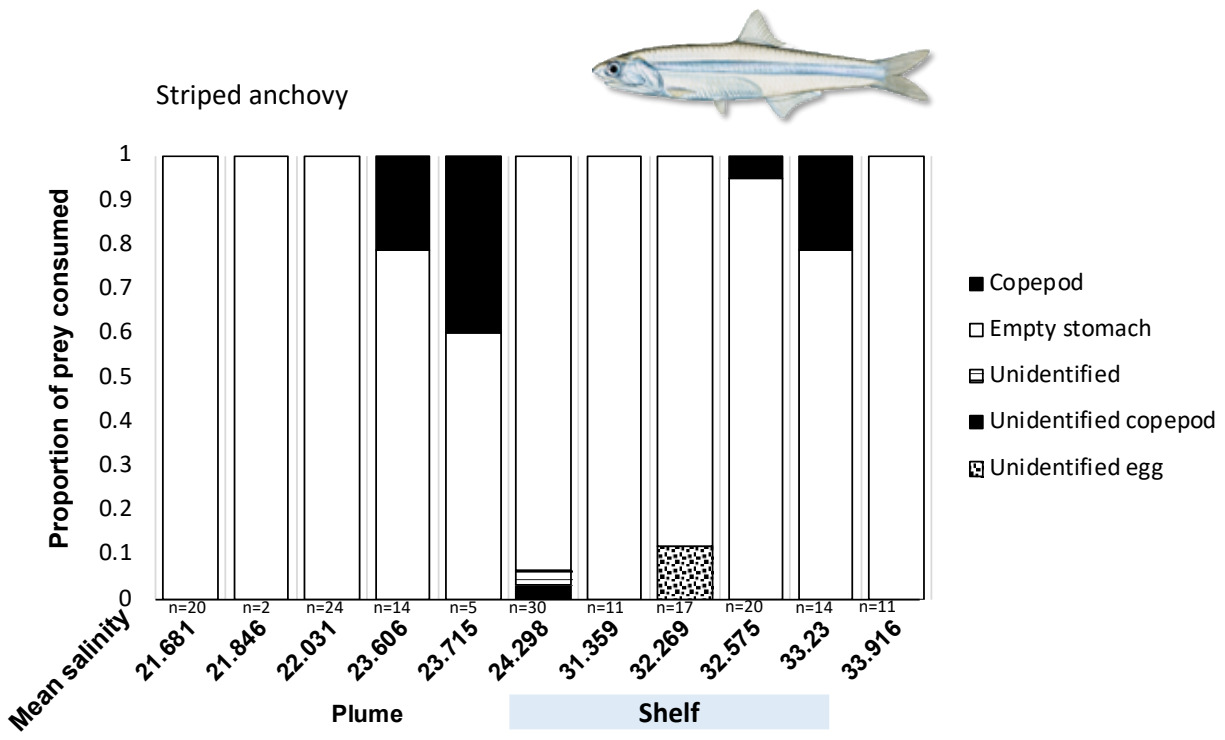


Fig. 3.8. Numerical proportions of ingested prey by water mass and the average salinity of each net tow for striped anchovy larvae. Sample sizes of dissected individuals from each net tow are listed below the corresponding bar.

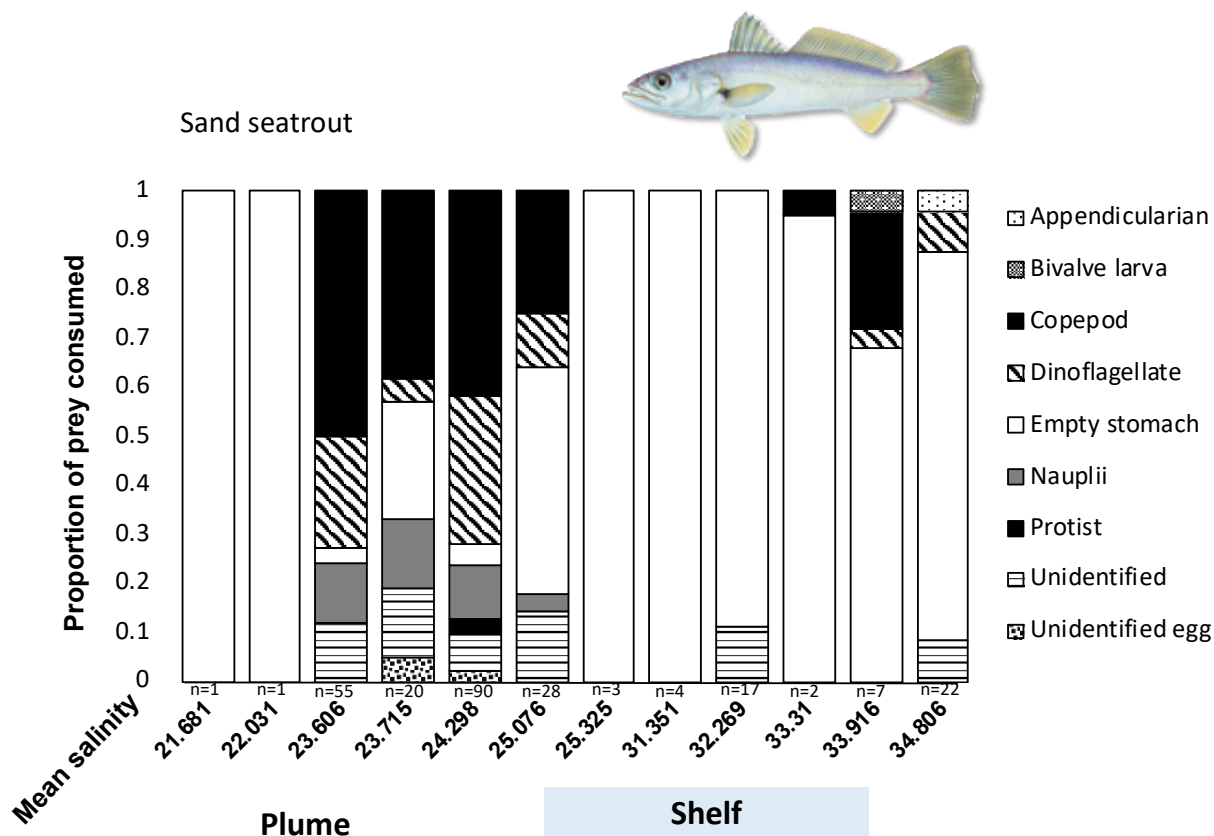


Fig. 3.9. Numerical proportions of ingested prey by water mass and the average salinity of each net tow for sand seatrout larvae. Sample sizes of dissected individuals from each net tow are listed below the corresponding bar.

CHAPTER 4: GENERAL CONCLUSIONS

River plumes and associated hydrodynamic processes are primary determinants of survival and recruitment of the early life stages of coastal and estuarine fishes, but few studies have been able to characterize the plume environment at sufficiently fine scales. There are many dynamic processes in the northern Gulf of Mexico (nGOM) that influence the distribution, transport, and overall fitness of larval fishes. To better understand how physical processes structure biological assemblages on fine scales, we towed an *in situ* plankton imaging system through the plume outflow of Mobile Bay in the nGOM during the high-flow month of April 2016. Chapter 2 examined how variable river discharge and mixing processes can structure the distributions and predator-prey relationships of larval fishes. As the magnitude of plume water and turbulence increased in the water column, we observed the dissipation of a multi-taxa biological aggregation coupled with a diminishing co-occurrence of larval fishes with their prey and predators. Additionally, the vertical distributions of organisms became less associated with the upper water column as plume and mixing processes strengthened. Chapter 3 examined the biological consequences of these altered distributions on larval fish fitness (e.g., growth, condition, and diet) and found fish larvae collected from plume water masses to be growing more slowly and be of lower condition (skinnier-at-length) than larvae from shelf waters. Taken together, these data demonstrate that strong, turbulent plumes exiting Mobile Bay are capable of disrupting the larval prey field by dispersing planktonic aggregations, with detrimental consequences to larval fish fitness (Table S.3.3).

These data fit into CONCORDE's primary objective of describing the dynamic nearshore ecosystem and further provide insights into how plankton can be forced by coastal physics and processes. Coupling traditional net samples with *in situ* imagery allowed for a fine-scale biophysical characterization of the study region and provided a comprehensive analysis of factors that can influence larval fish distributions, predator-prey relationships, and fitness within a plume-driven ecosystem. These data contribute significantly to our understanding of how coastal river plumes influence larval fish survival and can be used to better model population replenishment of regionally important marine fishes exposed to regions of exposed to seasonally variable freshwater influence.

This research would benefit from further study in a few key areas: 1) Temporal alignment of net sampling such that larvae in both water masses are sampled during daylight hours. Due to sampling constraints of this collaborative study, the shelf station was sampled at night while the plume stations were largely sampled during the day, making direct comparison of the plume and shelf environments limited. As a result, we were unable to use the BIONESS data to determine if larval fish diets and overall plankton abundances varied between plume and shelf waters. However, ISIS data enabled direct comparisons of plankton distributions and abundances because the towed vehicle samples full water column profiles (within ~1 m of the surface and bottom). 2) Further comparisons of larval fish and zooplankton assemblages and distributions between the nearshore eutrophic plume-environment and the more oligotrophic, offshore environment. BIONESS and ISIS were both towed in the inner shelf region within 10 km of the Mobile Bay Main Pass and therefore only characterized the nearshore plume environment. It would be interesting to compare the nearshore, freshwater-influenced larval fish and zooplankton community to those from an offshore, oligotrophic region. 3) Additional high-resolution sampling from the mouth of Mobile Bay on an ebb tide across the plume boundary and frontal region (as indicated by haloclines, pycnoclines, and thermoclines) to oceanic shelf waters. Although we sampled plankton distributions and abundances across a vertical plume front (the convergent zone that separates fresher plume waters from the denser shelf waters), it is unclear if our arcing transects captured a horizontal plume “front” in the typical sense of the word. Perpendicular sampling of ichthyo- and zooplankton across the plume-shelf convergent front would enable testing of some of the hypotheses suggested by our results. In general, future studies should utilize high-resolution *in situ* imaging over longer time scales and reoccurring flow regimes to enable a more complete characterization and generate baseline data on the impact of different river plume regimes on larval fish and zooplankton distributions. Further research into the basic ecology of the early life stages of nearshore and estuarine-dependent fishes will support these objectives and inform predictions of changes in larval fish population dynamics under different scenarios of sea level rise, increased precipitation and flooding due to climate change, and direct anthropogenic modifications (e.g., levees, dredging, dams) that need to be anticipated by fisheries management.

APPENDIX A – CHAPTER 3 SUPPLEMENTARY TABLES AND FIGURES

Table S.3.1. Summary of plankton samples collected at plume and shelf stations off the coast of Alabama during April 8-10, 2016.

| Station No. | Tow No. | Date (2016) | Water Column Depth (m) | Time | Water Mass | No. Samples (Sample Bin Depth) | Larval Fish Concentration no./m ³ (SE) |
|-------------|---------|-------------|------------------------|-------|------------|--------------------------------|---|
| 1 | 42 | April 8 | 17.3 | Day | Plume | n=2 (1-4 m) | 0.261 (0.108) |
| 2 | 44 | April 9 | 13.9 | Night | Shelf | n=9 (1-10 m) | 0.701 (0.122) |
| 3 | 47 | April 9 | 14.1 | Day | Plume | n=3 (1-3 m) | 0.667 (0.288) |
| 4 | 48 | April 10 | 11.0 | Night | Plume | n=3 (1-3 m) | 0.674 (0.228) |
| 5 | 49 | April 10 | 11.2 | Day | Plume | n=2 (1-3 m) | 0.249 (0.203) |

Table S.3.2. Number of focal specimens (*Anchoa hepsetus* and *Cynoscion arenarius*) by type of water mass used for otolith, morphometric, and diet analyses between the plume and shelf waters immediately south of Mobile Bay, Alabama.

| | Water mass type | | Total |
|--|-----------------|-------|------------|
| | Plume | Shelf | |
| Total focal species captured in study | | | |
| <i>A. hepsetus</i> | 145 | 227 | 372 |
| <i>C. arenarius</i> | 115 | 360 | 475 |
| Size frequency analysis | | | |
| <i>A. hepsetus</i> | 145 | 187 | 332 |
| <i>C. arenarius</i> | 115 | 221 | 336 |
| Otolith analysis | | | |
| <i>A. hepsetus</i> | 54 | 59 | 113 |
| <i>C. arenarius</i> | 55 | 71 | 126 |
| Morphometric analysis | | | |
| All <i>A. hepsetus</i> | 40 | 66 | 106 |
| Post-flexion <i>A. hepsetus</i> | 40 | 42 | 82 |
| All <i>C. arenarius</i> | 64* | 118 | 182 |
| Pre-flexion <i>C. arenarius</i> | 67 | 104 | 171 |
| *A few individual larvae were removed from the analysis as outliers. | | | |
| Diet analysis | | | |
| <i>A. hepsetus</i> | 93 | 73 | 166 |
| <i>C. arenarius</i> | 84 | 88 | 172 |

Table S.3.3. Summary of biotic and abiotic variables used in this study to examine patterns of larval fish fitness in striped anchovy and sand seatrout collected from plume and shelf stations.

| <i>Striped anchovy</i> | Relationship | | |
|--|--------------|---|-------|
| Larval Fish Fitness Factors | | | |
| Growth | Plume | < | Shelf |
| Morphometric condition | Plume | < | Shelf |
| Biological Explanatory Variables | | | |
| Copepod concentration (BIONESS)* | Plume | = | Shelf |
| Predator concentration (BIONESS)* | Plume | < | Shelf |
| No. Prey per Larva* | Plume | = | Shelf |
| Consumed copepod length* | Plume | = | Shelf |
| % Empty Guts* | Plume | < | Shelf |
| Copepod concentration (Ch 2: ISIIS) | Plume | < | Shelf |
| Predator concentration (Ch 2: ISIIS) | Plume | < | Shelf |
| Physical Explanatory Variables | | | |
| Temperature | Plume | = | Shelf |
| Salinity | Plume | < | Shelf |
| Turbidity (Ch 2: Particle Scattering) | Plume | > | Shelf |
| Turbulence (Ch 2: Dissipation Rate) | Plume | > | Shelf |
| Current velocity (Ch 2: ADCP U and V Plots) | Plume | > | Shelf |
| *Note: Shelf ichthyo- and zooplankton were only captured at night, when larvae typically do not feed | | | |

| <i>Sand seatrout</i> | Relationship | | |
|--|--------------|---|-------|
| Larval Fish Fitness Factors | | | |
| Growth | Plume | < | Shelf |
| Morphometric condition | Plume | < | Shelf |
| Biological Explanatory Variables | | | |
| Copepod concentration (BIONESS)* | Plume | = | Shelf |
| Predator concentration (BIONESS)* | Plume | < | Shelf |
| No. Prey per Larva* | Plume | > | Shelf |
| Consumed copepod length* | Plume | < | Shelf |
| % Empty Guts* | Plume | < | Shelf |
| Copepod concentration (Ch 2: ISIIS) | Plume | < | Shelf |
| Predator concentration (Ch 2: ISIIS) | Plume | < | Shelf |
| Physical Explanatory Variables | | | |
| Temperature | Plume | = | Shelf |
| Salinity | Plume | < | Shelf |
| Turbidity (Ch 2: Chameleon Scattering) | Plume | > | Shelf |
| Turbulence (Ch 2: Chameleon Dissipation Rate) | Plume | > | Shelf |
| Current velocity (Ch 2: ADCP U and V Plots) | Plume | > | Shelf |
| *Note: Shelf ichthyo- and zooplankton were only captured at night, when larvae typically do not feed | | | |
